1. Information on the study

Data point:	KCA 7.1.3.1.1
Report author	Dollinger, J., et al.
Report year	2018
Report title	Contrasting soil property patterns between ditch bed and neighbouring field profiles evidence the need of specific approaches when assessing water and pesticide fate in farmed landscapes
Document No	Geoderma 309 (2018) 50–59
Guidelines followed in study	OECD 106
Deviations from current test guideline	study not sufficiently described to check validity of the results
GLP/Officially recognised testing facilities	No, not conducted under GLP/Officially recognised testing facilities
Acceptability/Reliability:	Reliable with restrictions (study not sufficiently described to check validity of the results)

2. Full summary of the study according to OECD format

The authors' aim was to evaluate the specificity of ditch material properties to determine whether ditches require an approach that differs from that of field soils when studying water and pesticide fate in farmed landscapes. The authors thus analysed the variations in the pedological, herbicide sorption and flow properties of soil materials along a 2D cross-section of an intermittently flooded ditch in the Roujan catchment of southern France. They found that the upper part of the ditch bed soil profile is composed of 3 horizons that formed after the original creation of the ditch, most likely via the deposition of field-eroded particles and the accumulation of organic matter. These specific horizons have greater porosity, mostly due to their dense root systems, and contain up to 2 times more organic carbon than the neighbouring banks or field soils. Consequently, the hydraulic conductivity is greater, and the sorption of hydrophobic herbicides is up to 2 times greater in ditch bed materials than it is in soils located farther away from the ditch surface. Moreover, significant macroporal flow was evidenced in both profiles but with different contribution to the global flow. The contrasts in the hydrodynamic and sorption properties between both the ditch bed and banks materials likely results in significantly different water and pesticide infiltration patterns in ditches compared to crop fields. Given these differences, they recommend investigating the specific properties of ditch beds when studying and modelling water and pesticide fate in croplands.

Materials and methods

Study site

The studied ditch is located near the outlet of the Roujan catchment (Herault, France). This 91 ha catchment (Figure 1 and Table 1) is cultivated mainly by vineyards and a dense network of ditches, 11 km total length, was implemented between the vine fields. Except on the plateau, the soils are directly developed over the Miocene loose sandstone and are organized along a toposequence. The soils depth increase and soil texture evolve consistently with the colluvial accumulations of clay and gravels in the glacis. Nearby the study site the soil is classified as a gleyic cambisol (IUSS Working Group WRB, 2014). A perennial groundwater has developed on the bottom part of the catchment (Figure 1) and >5 km of ditches (47 % of the total length of ditches) drain this area.

The catchment is subjected to semi-arid Mediterranean climate characterized by scarce high-intensity rainfall events. This specific precipitation pattern results in the periodic flooding of ditches and the rapid fluctuation of the shallow water table in the bottom part of the catchment. The high reactivity of the water table leads to the alternation of downward and upward fluxes in ditch beds during storm events. The studied ditch is chosen near the catchment outlet in order to: i) represent the typical functions of ditch in a perennial groundwater environment (Figure 1) and ii) be representative of the soil type and ditch characteristics combination that prevail in the 33 ha of the bottom part of the catchment.

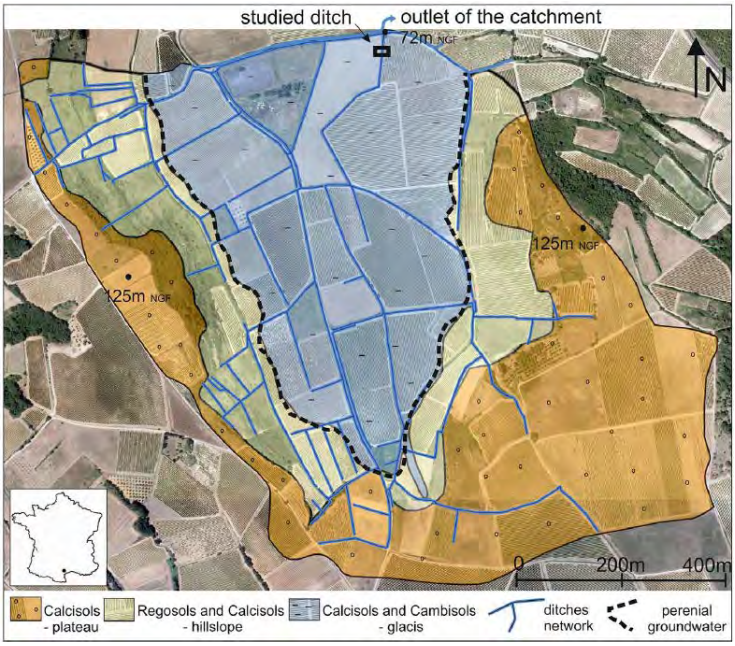

Figure 1. **The ditch network over the Roujan catchment in relation with the soils and the perennial groundwater.**

Table 1 **The spatial variability of ditches network over the catchment.**

Topographic position	Dominant soil types (WRB 2014)	Soil depth	Surface area	Total length of ditch in the network
		m	ha	km
Plateau	Calcisols	0.4–2	36	1.49
Hillslope	Regosols and calcisols	0.2–1.5	22	4.78
Glacis	Calcisols and cambisols	1–4	33	5.48
Catchment			*91*	*11.75*

Experimental design

Characterization of soil properties and core sampling along the cross section

For characterizing and sampling soil heterogeneity of the ditch soil and its vicinity, a 1.50-m-wide, 1.50-m-deep trench was excavated across the ditch in February 2014. The studied ditch is densely vegetated, and roots are present along the entire soil profile to a depth of 1.5 m (Figure 2A).

A series of morphological parameters, including texture, structure, colour, stone and root abundances, were observed in the field. Soil horizons were determined based on these observations. Bulk densities (ρ_b) were measured by core sampling with 100-cm^3 cylinders, using 6 replicates per horizon. The ρ_b was determined as the ratio between the dry soil mass and the total core sampling volume. Samples of over 500 g were collected from each horizon for further laboratory characterization. Particle size distribution, pH, cation exchange capacity (CEC), organic carbon content (OC), and calcium carbonate ($CaCO_3$) content were measured at the INRA-ARRAS Laboratory (France) (see Table 2).

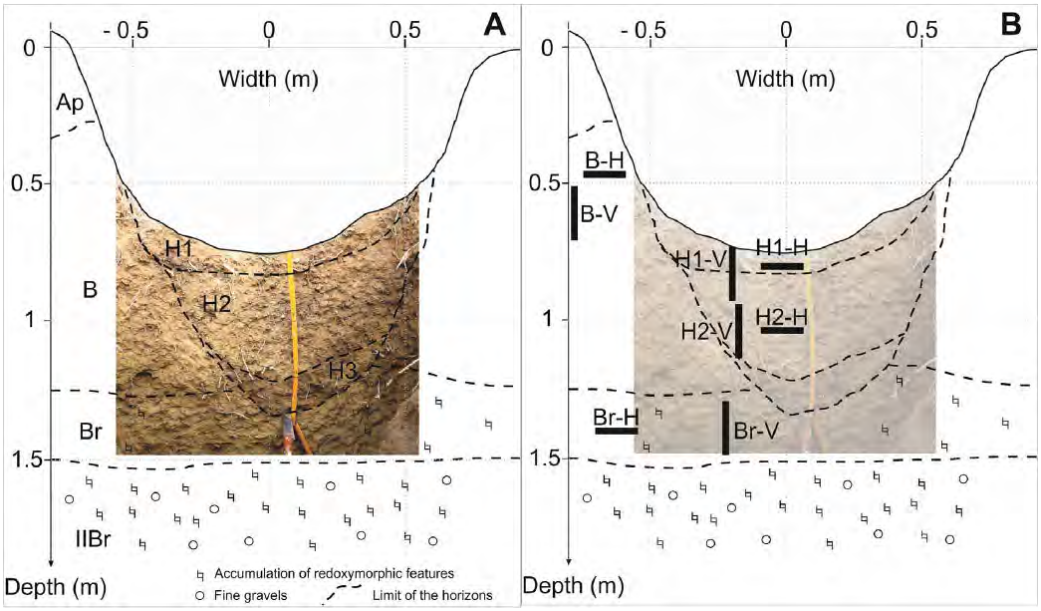

Figure 2. **Morphology of the ditch cross-section soil profile. A) Description of the soil profile, B) core sampling scheme. The black lines represent core sampling locations within the soil profile. V and H represent the cores sampling axis direction being, respectively, vertical and horizontal.**

Table 2 **Physico-chemical properties of ditch-bed and banks soils.**

Horizon	Depth from field topsoil	Structure	Sand	Silt	Clay	OC	CEC	pH	$CaCO_3$	ρ_b
	m		%	%	%	%	cmol kg^{-1}		g kg^{-1}	g cm^{-3}
B	0.4–1.30	Polyhedral subangular blocky – hydromorphic features	7.7	57.2	35.1	0.96	14.2	8.71	247.0	1.36 ± 0.01
H1	0.75–0.82	Stratified	35.9	39.1	25.0	1.58	12.5	8.44	150.0	1.25 ± 0.06
H2	0.82–1.15	Granular	40.3	33.1	26.6	1.56	12.1	8.54	160.0	1.26 ± 0.04
H3	1.15–1.35	Stratified and subangular blocky – hydromorphic features	10.4	56.7	32.9	1.17	14.0	8.59	248.0	1.21 ± 0.05
Br	1.30–1.50	Polyhedral blocky – hydromorphic and redoximorphic features	4.7	58.5	36.8	0.73	14.4	8.63	285.0	1.48 ± 0.03

Four undisturbed soil cores were sampled from each horizon except in the Ap horizon of the bank profile that has no counterpart in the ditch soil profile. These cores were collected by gently pushing stainless-steel cylinders with internal diameters of 15 cm and heights of 20 cm in the soil until the soil surface was approximately 5 cm from the top of the cylinder. The soil around the cylinders was then excavated to facilitate the undisturbed extraction of the monoliths. To characterize the anisotropy of downward vs. lateral water and solute flow, a series of monoliths was sampled vertically and a second series was sampled horizontally (Figure 2B). Due to the length of the sampled cores, the core sampled in the first horizon below the ditch also included the top of the second horizon; because the third horizon below the ditch was too narrow, it could not be sampled. After extraction, cores were stored at 4°C until undergoing tracer experiments.

Tracer displacement experiments

Tracer displacement experiments were performed on soil cores sampled vertically and horizontally in the ditch bed and bank profiles (Figure 2B) in order to characterize the water flow patterns of these materials. Because bromide is only present at trace concentrations in the environment and rarely sorbs to soil particles, it was selected as a conservative tracer of water flow for these displacement experiments.

Stainless-steel grids with 6-mm-diameter holes were sealed at the bottom of the columns to prevent soil loss occurring during the infiltration experiments without disturbing the water flux in the columns. Prior to tracer injections, the columns were gradually saturated via capillarity for 48 h to prevent the trapping of gas bubbles in soil pores.

The tracer solutions used for the displacement experiments contained 800 mg/L of bromide (Br^-). At the beginning of the displacement experiments, the saturated columns were manually ponded with a

30-mm water height of the tracer solution. This water height was chosen to mimic the infiltration conditions in the Roujan catchment during intermittent flooding and corresponds to the water level commonly monitored in ditches during flood events with a 1-month return period. The water height was kept constant during the infiltration by adjusting the supply of the tracer solution. A total of 85 mm of solution was supplied to the columns. Among the 16 columns, the pore volumes ranged from 63 to 82 mm. Therefore, the volume of tracer solution supplied during the displacement experiment was always higher than the pore volume of the columns. When the solution supply stopped, the decrease in water head was monitored during the remaining period of ponded water infiltration. Just after all the ponded solution had infiltrated, the columns were ponded again with a constant head of 30 mm, and the columns were flushed with 85 mm of tap water, following the same procedure. During the infiltration and flushing periods, 50 ml fractions of the percolates were collected in glass containers at the outlets of the columns. The sampling frequency varied from 15 s to about 6 min, depending on the columns drainage fluxes. The outlet flowrates were monitored using the timing of sample collection and their precise weights. The inlet flowrates were monitored by weighing the injection tank at 1-s intervals.

The concentrations of bromide in the percolate samples were measured using an ion-specific electrode (Hanna Instruments, HI4002, Lingolsheim). These concentration values were cross-validated with ion chromatography measurements of randomly selected samples. A good fit was found between the ion-specific electrode and the ion chromatograph results (data not shown). The electrical conductivity and pH were also measured in the percolate samples.

Dye tracing of the active macroporosity

Following the displacement experiments, dye tracing was performed on the columns to visualize and quantify the active macroporosity. The dye tracing experiments were also used to visualize the presence or absence of sidewall flow. The displacement experiments were validated when sidewall flow was absent or weak and discontinuous along the sides of the columns. In contrast, when continuous sidewall flow was detected along the sides of the columns, the corresponding displacement experiments were dismissed. A total of 8 columns, containing one sample per horizon and one sample per direction (vertical/lateral) were validated based on dye staining experiments.

The infiltration conditions of dye tracing were identical to those of the displacement experiments, as the fraction of active porosity mobilized for percolation in structured soils likely varies with initial moisture and water head conditions. The columns were thus saturated again via capillarity for 48 h; then, 57 mm of the fluorescent dye sulforhodamine B at a concentration 1 g/L was percolated through the columns with a constant water head of 30 mm. At a concentration of 1 g/L, the sorption sites of sulforhodamine B on soils in contact from all horizons were saturated, which guaranteed homogeneous staining among the columns. After percolation, the columns were sliced into cross-sections approximately 2 cm in height. A marker was placed on the sides of the slices to determine the orientation and superposition of the 7 slices within a given column. The slices were then imaged in a dark chamber with homogeneous LED lighting (3800 K) using a digital camera that was equipped with a 28-mm lens and was positioned 65 cm above the slice. The image resolution was 300 dpi, which corresponds to a pixel size of 71 µm. The illumination and hue saturation of the raw images were corrected using Nikon Capture NX2 software based on the grey and colour scales positioned next to the column slices during imaging. The RGB channels were split, and the colour thresholds were adjusted in each of the channels. The minimum/maximum thresholds applied to all images were 9/255, 118/253 and 4/255 for the R, G and B channels, respectively. The RGB channels were then merged, and the image was binarized. Both bright and dark isolated pixels were removed using the 'Noise' function of the ImageJ software, with a radius of 10 pixels, for white and black pixels, successively. The respective areas of both bright and dark pixels relative to the total area of the column cross-section were then calculated with ImageJ. The dark areas correspond to the stained areas on the cross-sections of the columns.

The volume of macroporosity mobilized during percolation relative to the total porosity (ω) was estimated from the dye coverage area. As dye diffusion in the matrix is limited, due to its short infiltration time, ω_i was calculated for each column cross-section (i) by multiplying the average dye coverage area per column slice (i.e., top and bottom coverage) by the slice height and dividing it by the

total porosity (i.e., the total volume of soil in the slice multiplied by the soil porosity). The average ω per column was also calculated as a geometric mean of the respective ω_i values of the 7 column slices (i).

Inverse modelling of transport properties

Water flow and transport equations

Inverse modelling was performed with the HYDRUS-1D model that solves the Richards and convection-dispersion equations. Four modelling approaches were compared in the first place: single porosity, dual porosity, dual porosity + mobile-immobile (DP + MIM) and dual permeability (see Šimůnek et al., 2003 for a detailed description of these approaches). Only the dual-permeability model provided satisfactory fits of the tracer displacement experiments for most of the columns and is thereby considered in this paper. The column H2-H was the only exception for which the model DP + MIM was better adapted than the dual permeability model. DP + MIM was used to simulate the bromide breakthrough curve of H2-H but is not described in this paper (for the description of the model please refer to Šimůnek et al., 2003). Equations of the dual permeability model are briefly reviewed below.

The dual permeability model assumes that flow and solute transport occur within and between two distinct compartments, namely the macropore compartment, consisting in inter-aggregate or fracture porosities, and the micropore or matrix compartment, consisting in intra-aggregate porosity. The water flow equations in the macroporal and matrix compartments are assumed similar by HYDRUS 1D and given by:

$$\frac{\partial \theta_f(h_f)}{\partial t} = \frac{\partial}{\partial z}\left[K_f(h_f)\left(\frac{\partial h_f}{\partial z} + 1\right)\right] - S_f(h_f) - \frac{\Gamma_w}{\omega} \qquad (1a)$$

$$\frac{\partial \theta_s(h_s)}{\partial t} = \frac{\partial}{\partial z}\left[K_s(h_s)\left(\frac{\partial h_s}{\partial z} + 1\right)\right] - S_s(h_s) - \frac{\Gamma_w}{1-\omega} \qquad (1b)$$

where subscript *f* and *s* respectively refers to the fast macroporal compartment and the slow matrix compartment, θ is the water content [L^3/L^3], *h* is the pressure head [L], *K(h)* is the unsaturated hydraulic conductivity function, *S* is a sink or source term [T^{-1}], ω is the ratio of the macroporal volume of fast to the total poral volume of the soil (dimensionless) and Γ_w is the transfer rate between the two compartments [T^{-1}]. The water retention curve $\theta(h)$ and the unsaturated hydraulic function *K(h)* are defined for both compartments using the van Genuchten model. *K(h)* is described as the product of the relative hydraulic conductivity function *Kr* (dimensionless) and the saturated hydraulic conductivity *Ks* [L/T].

The transport equations associated with the dual-permeability formulation for water flow are based on the classical convection-dispersion equation for both the fast macroporal compartment and the slow matrix compartment with an exchange term between the two compartments:

$$\frac{\partial \theta_f c_f}{\partial t} + \rho\frac{\partial s_f}{\partial t} = \frac{\partial}{\partial z}\left(\theta_f D_f \frac{\partial c_f}{\partial z}\right) - \frac{\partial q_f c_f}{\partial z} - \phi_f - \frac{\Gamma_s}{\omega} \qquad (2a)$$

$$\frac{\partial \theta_s c_s}{\partial t} + \rho\frac{\partial s_s}{\partial t} = \frac{\partial}{\partial z}\left(\theta_s D_s \frac{\partial c_s}{\partial z}\right) - \frac{\partial q_s c_s}{\partial z} - \phi_s + \frac{\Gamma_s}{1-\omega} \qquad (2b)$$

$$\Gamma_s = \omega_{dp}(1-\omega)\theta_s(c_f - c_s) + \Gamma_w c^* \qquad (2c)$$

where *c* is the solute concentration [M/L^3], *s* is the sorbed solute concentration [M/M], ρ is the bulk density [M/L^3], *D* is the dispersion coefficient accounting for both molecular diffusion and hydrodynamic dispersion [L^2/T], *q* is the Darcian flux [L/T] ϕ is a sink-source term [$M/(L^3\ T)$], Γs is the mass transfer term for solute between the macroporal and the matrix compartments [$M/(L^3\ T)$] and c^* is equal to c_f. for $\Gamma_w > 0$ c_m for $\Gamma_w < 0$.

Inverse modelling design

The 0.15 m-soil profiles were densely discretized with 101 nodes to facilitate numerical convergence. An initial hydrostatic equilibrium with a zero-pressure at the top of the soil columns was considered. A variable head was imposed at the upper boundary condition. It was fixed at the ponding head value (3 cm) during the injection and rinsing phases and varied between both phases to correspond to the ponding height decreases monitored during the experiments (see Section *Tracer displacement experiments*). The eight following parameters were fitted against the cumulative water outflows heights and bromide concentrations at the outlet of the soil column: θs_s, θs_f, Ks_s, Ks_f, ω, $Disp_s$, $Disp_f$, ω_{dp} with θs and θr respectively the saturated and residual soil water content and *Disp*, the dispersion coefficient [L]. To avoid local minimum, the stability of the fitted parameter set estimated was evaluated using different sets of initial parameters, including the estimated sets themselves. The other hydrodynamic parameters were set according to the textural composition and bulk density of the soils using Rosetta, except θr_f that was set to zero. Note however that since the soil column remained saturated during the whole experiment, the van Genuchten parameters alpha, n and l were not sensitive. The Bromide diffusion coefficient was fixed to $1.67\ 10^{-9}\ m^2\ s^{-1}$. K_{sat} was not adjusted but calculated from the experimental outflow data using Darcy's law. Θs was also not adjusted but calculated from the bulk density data using a pedotransfer function.

Sorption properties of selected herbicides

Two herbicides, diuron and glyphosate, were selected to assess the heterogeneity of sorption properties along the profile of the ditch cross-section. Diuron was extensively used on the Roujan catchment for weed control in vineyards. After it was banned from the list of allowed active molecules in France in 2008, it was replaced by the broad-spectrum herbicide glyphosate. Both herbicides were still measured in the water column of the ditch at the outlet of the catchment in 2016. Glyphosate and diuron exhibit very different physicochemical properties (Table 3), which may lead to contrasting sorptive patterns along the soil profiles.

The adsorption parameters were assessed according to the procedure described in Dollinger et al. (2016), which was adapted from the OECD Guideline 106. Briefly, the soils were air-dried to a target humidity of 10 % then sieved to a size of 2 mm. 10 mL of the ^{14}C-labelled pesticide solution, with concentrations ranging from 5 to 1000 µg/L, were equilibrated with 1 and 2 g of dry soil in glass centrifuge tubes for glyphosate and diuron adsorption experiments, respectively. The tubes were shaken for 24 h, and the radioactivity in the supernatant was measured after centrifugation. Pesticide concentrations in soils were assessed by mass balance between initial and equilibrium concentrations. Both linear (Eq. 3) and Freundlich models (Eq. 4) were fitted to the experimental data.

$$C_s = Kd\ C_w \quad (3)$$

$$C_s = Kf\ C_w^{\,n} \quad (4)$$

$$H = \frac{n_{des}}{n_{ads}} \quad (5)$$

where C_s is the amount of sorbed pesticides in the soil at equilibrium (µg kg^{-1}), C_w is the equilibrium concentration in the supernatant (µg/L), *Kd* is the linear sorption coefficient (L/kg), *Kf* ($\mu g^{(1-n)}\ L^n/kg$) and n are the Freundlich coefficients and H is the apparent hysteresis index with n the non-linearity parameter of the Freundlich model and subscripts *ads* and *des* standing for adsorption and desorption isotherms, respectively.

The detailed procedure for the determination of herbicide desorption parameters can be found in Dollinger et al. (2016). Briefly, after 24 h of equilibration with a 100 µg/L pesticide solution, the activity in the supernatant was measured and the residual supernatant was removed. An equivalent volume of fresh electrolyte was added, and the tubes were shaken again for 24 h. Five successive desorption steps of 24 h each were then performed. The amount of pesticides sorbed to soils at each step was calculated

by mass balance based on radioactivity counting, and experimental data were fitted to Freundlich isotherms (Eq. 5). The hysteresis between adsorption and the corresponding desorption isotherms was represented by the H parameter (Eq. 3), which was calculated as proposed by Barriuso et al. (1994). Sorption is considered to be hysteretic when H <0.7; the lower the value of H is, the more irreversible the sorption is.

Table 3 **Physico-chemical properties of the studied pesticides.**

Properties		Glyphosate	Diuron
Formula		$C_3H_8NO_5P$	$C_9H_{10}Cl_2N_2O$
Molecular mass	g mol^{-1}	169.1	233.1
Aqueous solubility at 20 °C	g l^{-1}	10.5 to 12.0	0.42
Log Kow at pH 7		− 4.1 to − 3.2	2.7
pKa_1 – pKa_2 – pKa_3		2.2–5.5–10.2	13.2

From ANSES, 2017, FOOTPRINT, 2015, ChemID, 2017 and chemicalize.org 2017.

Results

Morphology of the ditch bed and bank profiles

Based on field morphological descriptions, two different soil profiles were distinguished along the cross-section: (i) the bank profile, which is composed of 4 horizons, and (ii) the ditch bed profile, which is composed of 5 horizons (Table 2 and Figure 2).

The bank soil profile corresponds to the soil pit observed in the vicinity of the ditch by Andrieux et al. (1993). According to the World Reference Base, this soil is a tilled gleyic Cambisol (colluvic, clayic). The structure of the first horizon (Ap, which extends from the surface to a depth of 0.4 m) is affected by tillage and deep ploughing operations. The upper cambic horizons B and Br (described in Table 1) are developed above another deep cambic horizon IIBr (Figure 2A) that feature both a high clay content and high bulk density values. However, more hydromorphic features and denser root systems are observed closer to the ditch bank surface than they are in the bank soil profile, which is located further away. The ditch bed soil profile corresponds to a succession of 3 ditch-specific horizons (H1, H2, and H3) and the Br and IIBr horizons, which are shared with the bank profile. The H1, H2, and H3 horizons are significantly different from the other horizons. H1 and H2, which are enriched in sand and have platy structures, are different from the bank horizon B, which is siltier and is dominated by a subangular blocky structure. The third horizon, H3, is similar to the bank horizon B in terms of texture but features a stratified structure that differs from that of the bank horizons. These differences indicate that the H1, H2, and H3 horizons were formed by the deposition of field-eroded particles during successive flood events subsequent to the creation of the ditch. The contours of the 3 horizons specific to the ditch bed (H1, H2 and H3; Figure 2A) thus likely delimit the section of the original ditch. The shape of the horizons is probably due to the regular management of the ditch, including dredging operations. At the location where the profiles were observed, the original ditch only slightly incises the Br horizon that prevailed prior to the creation of the ditch.

The B and Br horizons have very similar physicochemical properties (Table 2), although horizon B has a slightly greater organic carbon content and a lower bulk density. However, the porosities of horizons B and Br are larger in the vicinity of the ditch surface due to the higher density of the ditch vegetation root system. The upper two ditch bed soil horizons (H1 and H2) contain 1.5 to 2 times more organic carbon than horizon B, which is consistent with the presence of vegetation and higher water contents during the year. Moreover, the bulk densities of the specific ditch bed horizons are significantly lower than those of the other horizons, which is in accordance with their textures, organic matter contents, and dense root channels network. Therefore, the overall porosity of the ditch bed soil profile is higher than that of the bank profile.

In summary, the ditch bed profile and the bank profile have contrasting textural, chemical and structural

properties. Moreover, the vertical gradient of the analysed soil properties across the ditch bed horizons is sharper than that across the bank horizons. Both lateral and vertical gradients of soil properties, such as organic matter content or bulk density, are present within the limited spatial area of one square metre between the ditch and the bank. It is therefore expected that flow and sorption properties differ between the ditch and bank soils.

Heterogeneity and anisotropy of water pathways and associated soil pore structure

The results of the displacement experiments and dye staining of the active macroporosity (ω_{dye}) allowed us to compare the hydraulic conductivity and preferential flow patterns of the different horizons and sampling axes in the two soil profiles (Figure 3, Table 4) and to relate these flow patterns to the macroporosity patterns (Figures 4 and 5). The inverse modelling procedure provides a complementary estimation of the flow mechanisms and soil hydrodynamic properties (Table 4). The main interest of the modelling results is the opportunity to estimate the contribution of the fast flow to the global outflow.

The horizontal and vertical saturated hydraulic conductivity values (K_{sat}) at the column scale calculated from the percolation flux data range from very large ($1.7 \cdot 10^{-4}$ m s^{-1} for H2-V) to rather small ($6.9 \cdot 10^{-6}$ m s^{-1} for Br-H) values (Table 4). Regardless of the horizon, no systematic differences were observed in the measured K_{sat} values between the two sampling axes. With the exception of the second horizon in the ditch bed (H2), the anisotropy of the hydraulic conductivity was small in all samples. Therefore, a mean saturated hydraulic conductivity value was calculated for each horizon, and these values are reported in Table 4. The mean saturated hydraulic conductivity of the B horizon is slightly smaller than those of the H1 and the H2 horizons, despite important differences in their textures, organic matter contents and structures, as observed in Section *Morphology of the ditch bed and bank profiles*. Horizon H2 is the most conductive horizon due to the large value of its observed vertical K_{sat}, which may be caused by specific local macropore features, such as the snail shells observed in this horizon. The Br horizon is 4 to 15 times less conductive than the other horizons. Accordingly, as generally observed in structured soils, both ditch bed and bank soil profiles exhibit decreasing soil hydraulic conductivity with depth (e.g., Sammartino et al., 2015; Udawatta and Anderson, 2008), but the upper horizons of the ditch bed profile have higher permeability values than those of the bank profile.

The dye tracing experiments reveal information about the active macroporosity patterns (Figure 4) and, thus, about the heterogeneity of the soil structures between the horizons. In all columns, the dye percolated across the column demonstrating the presence of connected macroporosity along the height of the column. However, the magnitude of this connected macroporosity varied greatly between the horizons. Roots were found to be the main source of flow paths in most horizons, as most stained areas surrounded living or decayed root channels. However, not all living or decayed root channels were stained. Roots were present throughout the entirety of both profiles, but denser networks were located near the ditch surface. Consistently, on average, the active porosity was largest in the cores sampled in the upper horizons of the ditch bed profile (Figures 2 & 4, Table 4). The B horizon exhibits a large anisotropy in ω_{dye}, yielding a very large value of approximately 20 % in the horizontal direction. This anisotropy may be partly explained by the fact that the sampling location of the horizontal column is almost in the ditch sidewalls and is slightly further away for the vertical column (Figure 2). The H1 and H2 horizons both exhibit a large active porosity, as H2 has the largest ω_{dye} values of all of the horizons. The numerous snail shells, combined with the granular structure present in H2, are likely responsible for its greater active porosity than H1. The active porosity of the Br horizon is significantly smaller than those of the other horizons. Finally, in accordance with the observed variations in saturated hydraulic conductivity, the ditch bed profile exhibits, on average, a larger active porosity than the bank profile. Indeed, although the linear correlation is not statistically significant, K_{sat} generally increases when ω_{dye} increases (Figure 5).

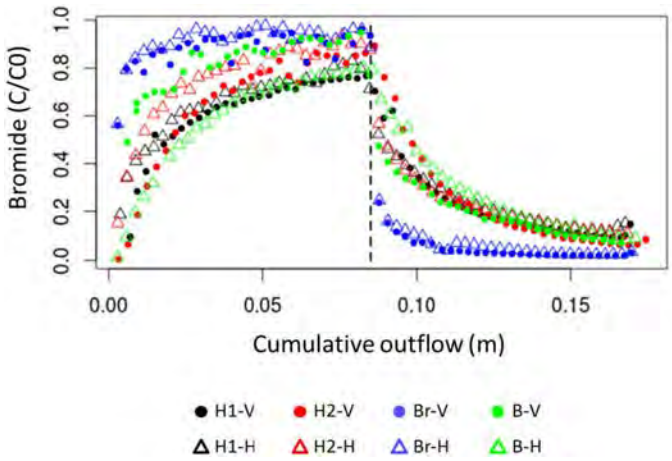

Figure 3. **Bromide breakthrough curves. The black dashed lines represent the shift between contaminated and clear water injection.**

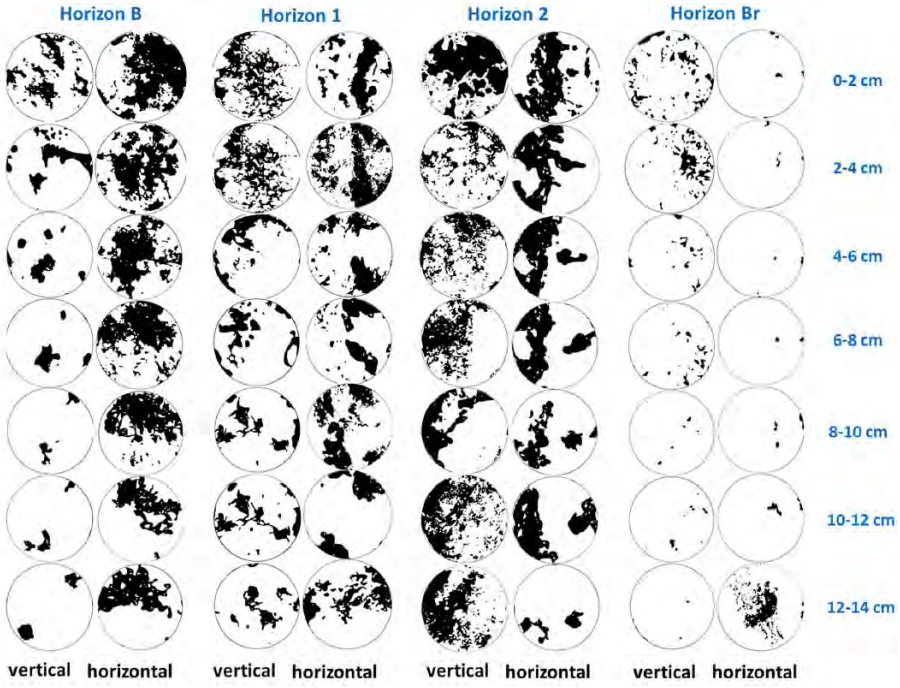

Figure 4. **Imaging of preferential flow patterns within the soil columns. The black areas represent the stained areas at different depths along the soil cores.**

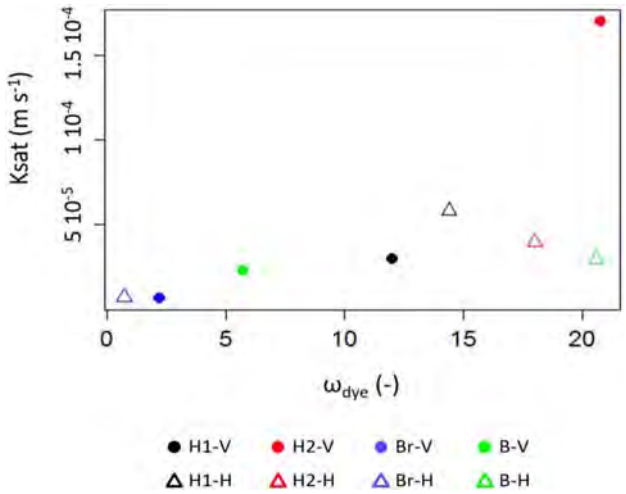

Figure 5. Evolution of the hydraulic conductivity with the active macroporosity fraction in the set of soil columns.

Table 4 Hydrodynamic properties of the ditch-bed and banks soil horizons.

Columns	[a] K_{sat}	[a] *Mean* K_{sat}*	[a] ω_{dye}	[b] θr_s	[b] θs_s	[b] Ks_s	[b] θs_f	[b] Ks_f	[b] ω	[b] $Disp_s$	[b] $Disp_f$	[b] θs_{Tot}	[a] θs	[b] Relative contribution of preferential flow
	m s^{-1}	m s^{-1}	%	m^3 m^{-3}	m^3 m^{-3}	m s^{-1}	m^3·m^{-3}	m s^{-1}	%	m	m	m^3 m^{-3}	m^3 m^{-3}	%
B-V	$2.34 \cdot 10^{-5}$	$2.68\ 10^{-5}$	5.7 ± 3.5	0.093	0.55	$3.01 \cdot 10^{-5}$	0.150	$3.07 \cdot 10^{-4}$	10.0	0.13	0.5	0.51	0.48	53.1
B-H	$3.02 \cdot 10^{-5}$		20.6 ± 3.5	0.093	0.45	$8.95 \cdot 10^{-6}$	0.492	$7.76 \cdot 10^{-5}$	21.0	0.27	24.25	0.46	0.48	69.7
H1-V	$2.99 \cdot 10^{-5}$	$4.41\ 10^{-5}$	12.0 ± 3.6	0.075	0.41	$1.35 \cdot 10^{-5}$	0.367	$1.13 \cdot 10^{-4}$	17.0	0.1	0.07	0.40	0.52	63.2
H1-H	$5.82 \cdot 10^{-5}$		14.4 ± 2.8	0.075	0.45	$2.26 \cdot 10^{-5}$	0.450	$3.79 \cdot 10^{-4}$	10.0	0.23	30	0.45	0.52	65.1
H2-V	$1.70 \cdot 10^{-4}$	$1.05\ 10^{-4}$	20.8 ± 5.2	0.077	0.55	$4.91 \cdot 10^{-5}$	0.440	$5.98 \cdot 10^{-4}$	22.0	0.1	0.1	0.52	0.52	77.5
H2-H**	$3.99 \cdot 10^{-5}$		18.0 ± 3.5	0.077	0.49	$1.18 \cdot 10^{-5}$	0.430	$3.0 \cdot 10^{-4}$	10.0	0.03	25.84	0.48	0.52	73.3
Br-V	$6.90 \cdot 10^{-6}$	$7.38\ 10^{-6}$	2.2 ± 2.0	0.092	0.40	$1.08 \cdot 10^{-6}$	0.300	$9.80 \cdot 10^{-5}$	6.0	0.1	0.47	0.39	0.44	85.3
Br-H	$7.86 \cdot 10^{-6}$		0.7 ± 1.1	0.092	0.40	$1.08 \cdot 10^{-6}$	0.300	$9.80 \cdot 10^{-5}$	7.0	0.1	0.47	0.39	0.44	87.2

[a] Values obtained from the experimental data.
[b] Values obtained from the inverse modelling of the bromide breakthrough curves.
* Mean K_{sat} is the mean saturated hydraulic conductivity for a given horizon.
** The values of the hydrodynamic parameters obtained from inverse modelling result from adjustments of a dual permeability model except for the column H2-H for which a dual porosity + mobile-immobile model was used. θr_F always equals 0. For H2-H the saturated water content of immobile compartment: $\theta s_{IM} = 0.35$, the Ks_s and Ks_f are the K_{sat} values in the slow and fast porous compartments and the K_{sat} of the immobile compartment is null.

Figure 3 depicts the succession of bromide concentrations measured at the column outlets during displacement experiments. The results are expressed as the ratio of outlet to inlet concentrations. These concentration evolutions could all be satisfactorily simulated using a dual-permeability model except the H2-H for which a dual-porosity model with a mobile-immobile conceptualization of the matrix compartment was needed. For each set of parameters allowing a good reconstitution of the water flow and the bromide leaching pattern (Table 4), the estimated ω were statistically equivalent to the one obtained with dye tracing (linear correlation: slope = 0.97, intercept = 0, $R^2 = 0.92$, p-value = $5 \cdot 10^{-5}$). This highlights the reliability of the simulated parameters, despite the equifinality issue inherent to the large number of fitted parameters.

For all displacement experiments, quantifiable bromide concentrations were measured in the first 50 ml of leachates, which were collected between 15 s and 7 min after injection began. This suggests that preferential flow occurred in all of the columns (e.g., Paradelo et al., 2016), which is consistent with the observation of connected macroporosity in the columns. Additionally, two major shapes of breakthrough curves can be distinguished.

In the columns of horizons B and H, the curve features a gentle increase and decrease in concentration during the injection and rinsing phases, respectively, as well as a maximum concentration that is less than the injected concentration. If it is assumed that macropore flow occurred almost instantaneously at a concentration close to the injected concentration, it follows that, throughout the displacement experiment in these columns, matrix flow was a significant contributor to outflow, as bromide concentration remained below the injected concentration. Although the volume of the injected bromide

solution was chosen to be larger than the overall pore volume of the columns, this volume was likely not sufficient to ensure a renewal of matrix pore water. This hypothesis is confirmed by the modelling results indicating that even if preferential flow contributed up to 77 % to the global outflow for this group of columns, the hydraulic conductivity of the fracture never exceeded 25 time that of the matrix (Table 4).

The other breakthrough curve shape is observed in the columns of the Br horizon and exhibits a sharp increase and early plateau in bromide concentrations during the injection phase, in which the plateau concentration is close to the injected concentration value. Additionally, a sharp decrease in concentration is observed during the rinsing phase. This pattern is not consistent with the small observed macroporosity of the Br horizon but can be explained by the very poor permeability of the soil matrix. In this case, most of the flow bypasses the soil matrix and flows through a few connected macropores. This hypothesis is confirmed by the modelling results indicating that preferential flow contributed to >85 % to the global outflow for this group of columns and that the hydraulic conductivity of the fracture was >90 time higher than that of the matrix (Table 4).

In accordance with recent studies relating soil macroporosity and hydraulic conductivity in structured soils, K_{sat} generally rises along with an ω increase (Figure 5). As ω is related to the root channels density, which decreases with the distance from the ditch surface, the saturated hydraulic conductivity is overall greater in the upper horizons of the ditch bed than in the banks. The contribution of preferential flow to the global outflow, is however greater in the deep bed and bank horizon. This can be explained by the contrasted hydraulic conductivity of the macroporal compartment relative to that of the matrix compartment (Ks_f/Ks_s) and by ω ($R^2 = 0.95$, p-value = $6 \cdot 10^{-4}$).

In sum, it is mainly in their upper horizons that the bank and ditch bed profiles differ in their patterns of water and solute transport. The top horizons of the ditch bed exhibit larger transport properties due to their larger active macroporosities, which are related to their denser rooting patterns. Thus, in contrast with the soil profile from which it originates, the ditch bed profile exhibits larger infiltration and percolation capacities. However, the deeper percolation of water and solutes is limited in both profiles by their common bottom Br horizon, which exhibits low permeability. The differences in the flow patterns may induce significant contrasts in the transfer and retention of herbicides. Indeed, water pathways determine the material surface area that is in contact with the soil solution and its effective contact time during downward seepage. This conditions the herbicide sorption equilibria.

Pesticide sorption heterogeneities among the ditch bed and bank soil profiles

The heterogeneities in herbicide sorption properties among the horizons are presented in Table 5. The H1 and H2 horizons exhibit the greatest diuron adsorption capacities and lowest desorption capacities, whereas adsorption on B and Br is low and very easily reversible. Therefore, the sorption capacities of the ditch bed profile are larger than those of the bank profile. For glyphosate, the adsorption coefficient of the B horizon is higher than that of the H1 horizon but is lower than that of the H2 horizon, and the desorption hysteresis of the B horizon is smaller and larger than those of the H1 and H2 horizons, respectively. The Br horizon exhibits a lower adsorption coefficient than the B horizon, but they both exhibit a similar desorption hysteresis. Based on the properties of these horizons, it remains unclear whether the ditch bed profile or the bank profile has the greater retention capacity.

Table 5 Sorption coefficients of the herbicides on ditch soils.

Molecule	Horizon	Kf_{ads}	n_{ads}	Kd_{ads}	Kf_{des}	n_{des}	H
		$\mu g^{(1-n)} l^n kg^{-1}$	–	$l\,kg^{-1}$	$\mu g^{(1-n)} l^n kg^{-1}$	–	–
Diuron	B	4.49	0.84	1.86	110.58	0.12	0.98
	H1	14.79	0.83	5.17	114.66	0.32	0.39
	H2	10.57	0.82	3.52	118.74	0.25	0.31
	Br	4.12	0.81	1.49	114.31	0.09	0.97
Glyphosate	B	157.66	0.94	109.90	666.99	0.28	0.29
	H1	77.60	0.93	51.69	675.64	0.14	0.15
	H2	165.24	0.96	129.86	533.29	0.36	0.37
	Br	124.36	0.91	75.38	505.00	0.29	0.32

In summary, the heterogeneities in the sorption coefficients of the two studied pesticide within a given profile are more substantial under the ditch bed than in the banks. Generally, due to the enrichment in organic matter of the ditch bed horizons, the sorption capacities of hydrophobic molecules in the ditch bed profile should be greater than those in the bank profile. Concerning ionisable compounds with low hydrophobicity, a higher sorption capacity of ditch bed profiles is not straightforward. The desorption hysteresis are generally significant in the ditch bed and are weaker or null in the bank soils. This should lower the release of pesticides previously adsorbed in the ditch bed soils as compared to the bank soils.

Conclusion

This study provides the first description of the range of soil properties influencing the magnitude of the water and pesticide exchanges occurring between surface water and groundwater along a ditch cross section profile. These ditch bed soil properties were also for the first time compared with those of the surrounding field soils. The in-situ and laboratory characterization of the physico-chemical properties evidenced distinct soil profiles between both the ditch bed and banks profiles. The ditch bank profile was equivalent to the surrounding field profile. In particular, the ditch bed upper horizons contain up to 2 times more organic carbon than the bank soils. These upper ditch bed horizons being also located closer to the ditch surface than the bank soils, they contain a denser network of plant roots which increases their active macroporosity and in turn their hydraulic conductivity. The deeper horizons share however, great similarities in both profiles, in particular their poor macroporosity, hydraulic conductivity and organic carbon content.

In conclusion, the physicochemical and sorptive properties of specific ditch bed horizons contrast with those of the ditch banks and neighbouring field soils. These differences may thus have different effects on the risk of groundwater contamination by pesticides. On one hand, ditch beds exhibit higher organic matter contents than field soils, possibly limiting the percolation of hydrophobic pesticides due to increased retention in the soil matrix. On the other hand, the upper horizons of ditch beds present larger active macroporosity and transport property values, which favour percolation. The final balance between the two effects, in terms of overall groundwater contamination risk, depends on the local hydrological conditions.

3. Assessment and conclusion

Assessment and conclusion by applicant:

The study reports the properties of a soil from a ditch in an agricultural area in the south of France. Mainly, the hydraulic parameters of the different soil layers of the ditch and the surrounding banks are considered and modelled and tracer experiments with bromide are presented. Sorption experiments with glyphosate were conducted and Freundlich sorption coefficients for the different soil horizons are reported. However, insufficient data to check validity of the experiment are reported (mass balances, chemical properties of test substance, solution agent, analytical information (method,

LOD, LOQ), temperature, considered concentrations, stability of the test item). No actually measured concentrations in the field are reported.

The study is therefore classified as reliable with restrictions (Category 2).

1. Information on the study

Data point:	KCA 7.1.3.1.1
Report author	Dollinger, J. et al.
Report year	2015
Report title	Glyphosate sorption to soils and sediments predicted by pedotransfer functions
Document No	Environ Chem Lett (2015) 13:293-307
Guidelines followed in study	None
Deviations from current test guideline	None
GLP/Officially recognised testing facilities	No, not conducted under GLP/Officially recognised testing facilities (literature publication)
Acceptability/Reliability:	Reliable with restrictions (no new experimental data is presented)

2. Full summary of the study according to OECD format

Glyphosate is the most applied herbicide for weed control in agriculture worldwide. Excessive application of glyphosate induces water pollution. The transfer of glyphosate to freshwater and groundwater is largely controlled by glyphosate sorption to soils and sediments. Sorption coefficients are therefore the most sensitive parameters in models used for risk assessment. However, the variations in glyphosate sorption among soils and sediments are poorly understood. Here we review glyphosate sorption parameters and their variation with selected soils and sediment. We use this knowledge to build pedotransfer functions that allow predicting sorption parameters, Kd, Kf and n, for a wide range of soils and sediments. We gathered glyphosate sorption parameters, 101 Kf, n and equivalent Kd, and associated soil properties. These data were then used to perform stepwise multiple regression analyses to build the pedotransfer functions. The linear (Kd) and Freundlich (Kf, n) pedotransfer functions were bench marked against experimental data. We found the following major points: (1). Under current environmental conditions, sorption is best predicted by the Kd pedotransfer function. (2) The pedotransfer function is Kd = 7.20*CEC – 1.31 *Clay + 24.82 (Kd in L/kg, CEC in cmol/kg and clay in %). (3) Cation exchange capacity (CEC) and clay content are the main drivers of Kd variability across soils and sediments. Freundlich parameters are additionally influenced by pH and organic carbon. This suggests that the formation of complexes between glyphosate phosphonate groups and soil–exchanged polyvalent cations dominates sorption across the range of analyzed soils.

Materials and Methods

Physical and chemical properties of glyphosate

Glyphosate [N–(Phosphomethyl)glycine] is a weak acid with strong hydrophilicity and very high water solubility (Table 1). Speciation of this zwitterionic molecule varies with the pH of the surrounding environment (Figure 1). The main species within the soil pH range are GH_2^- and GH^{2-}, corresponding to net negative charges of one and two, respectively (Figure 1).

Table 1 Physicochemical properties of glyphosate

Properties		References
Formula	$C_3H_8NO_5P$	ANSES (2015), FOOTPRINT (2015)
Molecular mass (g mol^{-1})	169.1	ANSES (2015), FOOTPRINT (2015)
Aqueous solubility at 20 °C (g L^{-1})	10.5 to 12.0	ANSES (2015), FOOTPRINT (2015)
Log Kow at pH 7	−4.1 to −3.2	ANSES (2015), FOOTPRINT (2015)
pKa_1–pKa_2–pKa_3	2.2–5.5–10.2	ANSES (2015), FOOTPRINT (2015)
Vapor pressure at 25 °C (mPa)	1.31×10^{-2}	ANSES (2015), FOOTPRINT (2015)
Henry's law constant at 25 °C (Pa m^3 mol^{-1})	2.10×10^{-7}	ANSES (2015), FOOTPRINT (2015)

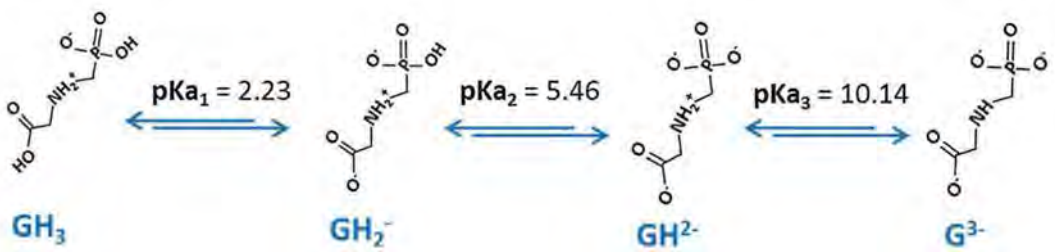

Figure 1 Speciation of glyphosate through the entire soil pH range from Albers et al. (2009), Borggaard (2011) and Maqueda et al. (1998)

Data mining

We extensively reviewed the literature to assemble a database of observed glyphosate sorption coefficients to both soils and sediments and the associated substrate properties (Table 2). We found 23 studies reporting sorption parameters for one or more soils or sediments. The soils or sediments for which glyphosate sorption measurements were carried out originated from four continents (Europe, Asia and North and South America) and exhibited highly varied texture and properties. The experimental conditions varied greatly. For example, the initial concentrations in the liquid phase ranged from 0.01 to more than 1000 mg/L. Only coefficients of sorption to unmodified soils or sediments were included in the database. Measured coefficients of sorption to organic soils were included in the database, but only those measured for sorption to mineral soils, i.e., with an organic matter content lower than 20 % (IUSS 2014) were used for the statistical analyses. Several studies have reported that sorption coefficients depend strongly on the background electrolyte. Therefore, only sorption coefficients obtained with classical background electrolyte, either Milli–Q water or $CaCl_2$, were included in the database. Among the 101 sorption parameters registered in the database (Table 2), 69 were measured with $CaCl_2$, as the background electrolyte. Statistical analyses were only performed for sorption parameters measured with $CaCl_2$ (designated as "sample A").

Sorption isotherms

For sample A, approximately two–thirds of the sorption models were nonlinear Freundlich (Table 3). To establish a pedotransfer function for Kd, we approximated equivalent Kd values by linearizing the Freundlich models over the actual range of the initial aqueous concentrations of the batch experiment used for model fitting (Table 3). The relative difference between Kf and its equivalent, Kd (Kd_{eq}), was approximately 30 % on average.

Statistical analyses

Pedotransfer functions aim to predict the sorption parameters Kd, Kf and n from selected substrate properties. Some of the properties, especially CEC, iron– and aluminum oxides or phosphorus content, were not available for all soils or sediments (Table 2). This lack of data induced a subsampling of sample A for the establishment of pedotransfer functions for the Kd and Kf parameters. This sample is designated as "sample B". The sample used for the establishment of the pedotransfer function for the n parameter excluded sorption studies that investigated only one concentration and, thereby, did not consider the possibility that n differs from 1. This sample is designated as “sample C”.

The statistical analyses were performed using the R statistical computing software. Correlation analyses were performed using the default "1 m" function of the R software. The three pedotransfer functions for the estimation of linear and nonlinear sorption models were established by forward and backward stepwise multiple regression analyses of the substrate properties and the Kd_{eq}, Kf and n parameters. The stepwise multiple regression analyses were performed using the default "step" function of the R software.

The validity of the Kd pedotransfer function is strongly supported by the fact that sorption processes do not depend on the pesticide concentration. However, in sample A, the n values ranged from 0.48 to 1.05, with a mean value of 0.83, indicating saturation of the sorption sites at high glyphosate concentrations. A complementary multiple regression between n, the substrate properties and the experimental conditions (C_{max} and *R)* was performed. The resulting equation (see Eq. 4) indicates the linearity range under various conditions.

Finally, we evaluated the accuracy of the predicted equilibrium partitioning of glyphosate between the soil and water by using the sorption parameters provided by the Kd or Kf/n pedotransfer functions. The evaluation was performed for 11 initial concentrations (0.01 , 0.04, 0. 10, 0.40, 1,4, 10, 40, 100, 400 and 1000 mg/L) in the liquid phase by comparing the predicted soil–to–water glyphosate concentration ratios, as obtained by the pedotransfer–estimated sorption parameters, to those obtained by the batch–fitted sorption parameters. The aqueous and soil concentrations were calculated for all sample B soils and sediments using the numerical solver as described previously.

Table 2 Glyphosate sorption parameters and associated soil or sediment properties' database

Substrate type and origin	Texture	pH	CEC	Organic carbon	Clay	Phosphorus	Fe_{ox} and Al_{ox}	Kf	*n*	Aqueous concentration min–max	Solid/ liquid ratio	Aqueous phase	References
	Sand-silt-clay (%)		cmol kg^{-1}	%	%	mg kg^{-1}	g kg^{-1}	L kg^{-1} n^{-1}		mg L^{-1}	g mL^{-1}		
Soil (Italy)	63.4:22.6:14.0	8.11[a]	na	0.70	14.00	na	na	43.01	0.79	0.20–120.00	1/5	$CaCl_2$	Accinelli et al. (2005)
Soil (USA)	93.5:2.7:3.8	7.20 [a]	na	0.94	3.80	na	na	62.16	0.88	0.20–120.00	1/5	$CaCl_2$	Accinelli et al. (2005)
Soil (France)	Sandy loam	5.10 [a]	na	0.82	10.50	1240.00	298.73	34.50	0.97	0.73–60.13	1/5	$CaCl_2$	Al-Rajab et al. (2008)
Soil (France)	Silt clay loam	6.30 [a]	na	1.45	30.60	3240.00	48.57	33.60	1.00	0.73–60.13	1/5	$CaCl_2$	Al-Rajab et al. (2008)
Soil (France)	Clay loam	7.90 [a]	na	1.91	34.90	2740.00	35.67	16.60	1.00	0.73–60.13	1/5	$CaCl_2$	Al-Rajab et al. (2008)
Soil (Finland)	Sandy loam	6.10[b]	na	0.47	17.00	1.60	na	166.00	0.97	2.00–10.00	1/5	H_2O	Autio et al. (2004)
Soil (Finland)	Clay	5.80[b]	na	2.88	46.00	3.00	na	55.00	0.92	2.00–10.00	1/5	H_2O	Autio et al. (2004)
Soil (Finland)	Clay	5.60[b]	na	0.54	58.00	1.10	na	249.00	0.91	2.00–10.00	1/5	H_2O	Autio et al. (2004)
Soil (Finland)	Sandy loam	5.80[b]	na	2.57	13.00	27.40	na	44.00	0.90	2.00–10.00	1/5	H_2O	Autio et al. (2004)
Soil (Finland)	Sandy loam	5.70[b]	na	0.72	4.00	17.10	na	55.00	1.00	2.00–10.00	1/5	H_2O	Autio et al. (2004)
Soil (Finland)	Clay	6.00[b]	na	7.06	41.00	4.10	9.66	97.00	1.03	2.00–10.00	1/5	H_2O	Autio et al. (2004)
Soil (Finland)	Clay	6.00[b]	na	2.96	47.00	1.50	11.22	41.00	1.02	2.00–10.00	1/5	H_2O	Autio et al. (2004)
Soil (Finland)	Sandy loam	6.40[b]	na	5.93	4.00	3.30	9.26	97.00	0.85	2.00–10.00	1/5	H_2O	Autio et al. (2004)
Soil (Finland)	Sandy loam	5.90[b]	na	1.77	4.00	0.90	6.70	51.00	0.86	2.00–10.00	1/5	H_2O	Autio et al. (2004)
Soil (Finland)	Clay	8.10[b]	na	2.67	41.00	38.70	na	58.00	0.93	2.00–10.00	1/5	H_2O	Autio et al. (2004)
Soil (Finland)	Clay	7.90[b]	na	2.50	30.00	22.40	na	113.00	0.87	2.00–10.00	1/5	H_2O	Autio et al. (2004)
Soil (Finland)	Sandy loam	7.10[b]	na	2.35	21.00	8.80	na	93.00	0.90	2.00–10.00	1/5	H_2O	Autio et al. (2004)
Soil (Finland)	Sandy loam	6.80[b]	na	0.75	8.00	2.80	na	90.00	0.86	2.00–10.00	1/5	H_2O	Autio et al. (2004)
Soil (Finland)	Clay	6.00[b]	na	7.05	41.00	5.80	na	179.00	1.26	2.00–10.00	1/5	H_2O	Autio et al. (2004)
Soil (Finland)	Sandy loam	6.30[b]	na	5.93	4.00	6.40	na	121.00	0.98	2.00–10.00	1/5	H_2O	Autio et al. (2004)
Soil (Finland)	Silty loam	5.40[b]	na	7.90	5.00	10.00	4.48	159.00	0.93	2.00–10.00	1/5	H_2O	Autio et al. (2004)
Soil (Finland)	Silty loam	5.60[b]	na	4.50	4.00	3.60	4.29	102.00	1.05	2.00–10.00	1/5	H_2O	Autio et al. (2004)
Soil (Finland)	Silty loam	5.40[b]	na	1.30	8.00	3.50	4.57	37.00	0.76	2.00–10.00	1/5	H_2O	Autio et al. (2004)
Soil (Finland)	Muddy clay	6.90[b]	na	12.60	57.00	52.00	na	84.00	0.91	2.00–10.00	1/5	H_2O	Autio et al. (2004)
Soil (Finland)	Organic soil	5.20[b]	na	26.00	79.00	5.10	17.09	303.00	1.11	2.00–10.00	1/5	H_2O	Autio et al. (2004)
Sediment (France)	35.9:39.1:25.0	8.44[a]	12.50	1.58	25.00	19.00	2.78	51.69	1.00	0.005–1.00	1/10	$CaCl_2$	Bailly et al. (2015)
Sediment (France)	40.3:33.1:26.6	8.54[a]	12.10	1.56	26.60	6.00	2.62	129.86	1.00	0.005–1.00	1/10	$CaCl_2$	Bailly et al. (2015)
Sediment (France)	4.7:58.5:36.8	8.63[a]	14.40	0.73	36.80	5.00	3.27	75.38	1.00	0.005–1.00	1/10	$CaCl_2$	Bailly et al. (2015)
Sediment (France)	7.7:57.2:35.1	8.71[a]	14.20	0.96	35.10	5.00	3.48	109.90	1.00	0.005–1.00	1/10	$CaCl_2$	Bailly et al. (2015)
Sediment (France)	9.7:54.6:35.7	7.30[a]	23.20	0.54	35.70	11.00		302.63	1.00	0.005–1.00	1/10	$CaCl_2$	Bailly et al. (2015)
Sediment (France)	25.5:42.0:32.5	7.93[a]	26.10	3.88	32.50	73.00	na	262.41	1.00	0.005–1.00	1/10	$CaCl_2$	Bailly et al. (2015)
Sediment (France)	77.9:13.9:8.2	6.03[a]	6.34	0.47	8.20	142.00	na	89.07	1.00	0.005–1.00	1/10	$CaCl_2$	Bailly et al. (2015)
Sediment (France)	7.8:62.6:29.6	6.19[a]	17.60	3.67	29.60	144.00	na	318.82	1.00	0.005–1.00	1/10	$CaCl_2$	Bailly et al. (2015)
Soil (Sweden)	7.3:46.2:46.5	7.20[b]	28.40	4.00	46.50	na	na	118.00	0.95	0.01–0.10	1/10	$CaCl_2$	Bergström et al. (2011)
Soil (Sweden)	3.3:40.6:56.1	7.40[a]	33.60	0.00	56.10	na	na	165.00	1.03	0.01–0.10	1/10	$CaCl_2$	Bergström et al. (2011)

Table 2 continued

Substrate type and origin	Texture	pH	CEC	Organic carbon	Clay	Phosphorus	Fe_{ox} and Al_{ox}	Kf	n	Aqueous concentration min–max	Solid/liquid ratio	Aqueous phase	References
	Sand-silt-clay (%)		cmol kg^{-1}	%	%	mg kg^{-1}	g kg^{-1}	L kg^{-1} n^{-1}		mg L^{-1}	g mL^{-1}		
Soil (Sweden)	87.8:4.5:7.7	7.40[a]	4.70	2.00	7.70	na	na	40.00	0.92	0.01–0.10	1/10	$CaCl_2$	Bergström et al. (2011)
Soil (Sweden)	95.4:4.6:0.0	6.40[a]	1.80	1.00	0.00	na	na	28.70	0.82	0.01–0.10	1/10	$CaCl_2$	Bergström et al. (2011)
Soil (Spain)	82.0:11.0:7.0	7.90[a]	5.20[c]	1.00	7.00	na	36.70	93.00	0.78	0.10–5.00	2/5	H_2O	Candela et al. (2007)
Soil (Spain)	59.0:13.0:10.0	7.30[a]	4.60[c]	0.00	10.00	na	126.50	154.00	0.74	0.10–5.00	2/5	H_2O	Candela et al. (2007)
Soil (Malaysia)	Sandy loam	6.70	7.10[c]	1.30	10.00	na	na	83.80	0.85	0.10–5.00	1/5	$CaCl_2$	Cheah et al. (1997)
Soil (Malaysia)	Muck	4.70	54.10[c]	30.50	32.50	na	na	417.00	0.78	0.10–5.00	1/5	$CaCl_2$	Cheah et al. (1997)
Soil (France)	10.0:44.0:46.0	7.60[a]		3.90	46.00	na	4.40	33.90	1.00	0.10–5.00	1/5	H_2O	Dousset et al. (2007)
Soil (France)	53.0:25.0:22.0	6.60[a]		1.50	22.00	na	5.10	51.80	1.00	0.10–5.00	1/5	H_2O	Dousset et al. (2007)
Soil (Denmark)	Sandy	7.67	12.60	1.70	15.00	na	na	30.90	0.78	0.03–67.00	1/20	H_2O	de Jonge and Wollesen de Jonge (1999)
Soil (Denmark)	Sandy	6.13	12.60	1.70	15.50	na	na	78.50	0.75	0.03–67.00	1/20	$CaCl_2$	de Jonge and Wollesen de Jonge (1999)
Soil (Denmark)	Sandy	6.30	12.60	1.70	15.50	na	na	78.40	0.75	0.03–67.00	1/20	$CaCl_2$	de Jonge and Wollesen de Jonge (1999)
Soil (Denmark)	Sandy	6.53	12.60	1.70	15.50	na	na	48.40	0.77	0.03–67.00	1/20	$CaCl_2$	de Jonge and Wollesen de Jonge (1999)
Soil (Chili)	Clay loam	4.79[a]		6.60	18.00	na	na	12.13	1.00	1000.00–2500.00	1/10	H_2O	Kogan et al. (2003)
Soil (Finland)	Clay	6.02[a]		7.10	41.00	4.20	9.66	98.69	1.02	2.00–10.00	1/5	H_2O	Laitinen et al. (2008)
Sediment (Germany)	Sandy	7.7[c]		0.34	0.00	0.00	0.61	1.89	0.48	0.10–100.00	1/2	$CaCl_2$	Litz et al. (2011)
Soil (France)	Rendzina over limestone	8.4[a]	6.40	1.86	8.80	3590.00	2.51	17.60	0.76	0.20–10.00	1/5	H_2O	Mamy and Barriuso (2005, 2007)
Soil (France)	Rendzina over limestone	8.2[a]	7.10	1.86	9.30	2720.00	2.58	34.80	0.80	0.20–10.00	1/5	$CaCl_2$	Mamy and Barriuso (2005, 2007)
Soil (France)	Clay loam	8.36[a]	17.80	2.00	37.60	2490.00	15.20	32.90	0.86	0.20–10.00	1/5	H_2O	Mamy and Barriuso (2005, 2007)
Soil (France)	Clay loam	8.2[a]	20.60	1.69	37.70	2760.00	14.96	41.90	0.80	0.20–10.00	1/5	$CaCl_2$	Mamy and Barriuso (2005, 2007)
Soil (France)	Clay loam	6.3[a]	16.40	1.01	27.40	1460.00	8.58	60.50	0.88	0.20–10.00	1/5	H_2O	Mamy and Barriuso (2005, 2007)
Soil (France)	Clay loam	7.6[a]	15.90	0.96	23.50	1310.00	7.00	276.00	0.77	0.20–10.00	1/5	$CaCl_2$	Mamy and Barriuso (2005, 2007)
Soil (Greece)	13.4:64.1:22.6	8.0[a]	28.30[c]	0.00	22.60	na	3.40	13.79	0.77	50.00–300.00	1/25	$CaCl_2$	Piccolo et al. (1994)
Soil (UK)	46.3:36.8:17.0	5.8[a]	18.30[c]	3.73	17.00	na	63.10	40.64	0.77	50.00–300.00	1/25	$CaCl_2$	Piccolo et al. (1994)
Soil (Germany)	81.5:12.6:6.0	4.6[a]	30.70[c]	9.23	6.00	na	14.80	51.14	0.58	50.00–300.00	1/25	$CaCl_2$	Piccolo et al. (1994)
Soil (France)	1.7:82.4:16.0	8.3[a]	11.40[c]	0.45	16.00	na	22.80	152.85	0.44	50.00–300.00	1/25	$CaCl_2$	Piccolo et al. (1994)
Soil (Brazil)	46.0:7.0:47.0	5.2[a]	14.18	3.20	47.00	89.00	222.80	162.90	0.98	0.42–6.72	1/5	$CaCl_2$	Prata et al. (2003)
Soil (Brazil)	38.0:60.0:56.0	5.0[a]	12.32	2.50	56.00	59.00	277.10	215.70	0.99	0.42–6.72	1/5	$CaCl_2$	Prata et al. (2003)

Substrate type and origin	Texture	pH	CEC	Organic carbon	Clay	Phosphorus	Fe_{ox} and Al_{ox}	Kf	n	Aqueous concentration min–max	Solid/liquid ratio	Aqueous phase	References
	Sand-silt-clay (%)		cmol kg^{-1}	%	%	mg kg^{-1}	g kg^{-1}	L kg^{-1} n^{-1}		mg L^{-1}	g mL^{-1}		
Soil (Denmark)	Sandy	5.3[a]	na	na	1.64	na	2.21	403.50	1.00	0.30	1/5	$CaCl_2$	Strange-Hansen et al. (2004)
Soil (China)	–	7.20[a]	23.60	4.57	34.30	na	209.50	31.19	0.82	21.00–169.00	1/25	H_2O	Wang et al. (2006)
wetland Sediment (Canada)	Sandy	6.70[a]	13.30	3.20	9.10	na	na	172.90	1.00	1.00	1/10	$CaCl_2$	Xu et al. (2009)
Wetland sediment (Canada)	Sandy	6.40[a]	16.80	3.80	11.30	na	na	152.60	1.00	1.00	1/10	$CaCl_2$	Xu et al. (2009)
Wetland sediment (Canada)	Sandy	6.40[a]	24.80	6.80	4.90	na	na	251.90	1.00	1.00	1/10	$CaCl_2$	Xu et al. (2009)
Wetland sediment (Canada)	Sandy	7.20[a]	33.10	8.70	5.60	na	na	193.10	1.00	1.00	1/10	$CaCl_2$	Xu et al. (2009)
Wetland sediment (Canada)	Sandy	7.10[a]	31.90	9.60	6.70	na	na	124.90	1.00	1.00	1/10	$CaCl_2$	Xu et al. (2009)
Soil (Denmark)	Sandy	3.70[b]	na	1.32	4.20	50.55	3.21	107.40	0.62	0.04–65.00	1/18	$CaCl_2$	de Jonge et al. (2001)
Soil (Denmark)	Sandy	3.60[b]	na	1.06	4.20	63.49	2.47	80.60	0.62	0.04–65.00	1/18	$CaCl_2$	de Jonge et al. (2001)
Soil (Denmark)	Sandy	3.60[b]	na	1.28	4.20	87.39	2.98	83.50	0.66	0.04–65.00	1/18	$CaCl_2$	de Jonge et al. (2001)
Soil (Denmark)	Sandy	3.80[b]	na	1.06	4.20	72.15	2.53	79.40	0.68	0.04–65.00	1/18	$CaCl_2$	de Jonge et al. (2001)
Soil (Denmark)	Sandy	4.20[b]	na	1.20	4.20	18.32	2.73	121.20	0.60	0.04–65.00	1/18	$CaCl_2$	de Jonge et al. (2001)
Soil (Denmark)	Sandy	4.30[b]	na	1.33	4.20	27.70	3.36	141.20	0.63	0.04–65.00	1/18	$CaCl_2$	de Jonge et al. (2001)
Soil (Denmark)	Sandy	4.20[b]	na	1.30	4.20	44.58	3.43	118.10	0.67	0.04–65.00	1/18	$CaCl_2$	de Jonge et al. (2001)
Soil (Denmark)	Sandy	4.30[b]	na	1.40	4.20	44.50	3.24	111.50	0.62	0.04–65.00	1/18	$CaCl_2$	de Jonge et al. (2001)
Soil (Denmark)	Sandy	4.50[b]	na	1.26	4.20	12.07	3.23	126.80	0.56	0.04–65.00	1/18	$CaCl_2$	de Jonge et al. (2001)
Soil (Denmark)	Sandy	4.70[b]	na	1.26	4.20	18.56	2.95	120.00	0.58	0.04–65.00	1/18	$CaCl_2$	de Jonge et al. (2001)
Soil (Denmark)	Sandy	4.60[b]	na	1.21	4.20	36.31	2.76	92.00	0.59	0.04–65.00	1/18	$CaCl_2$	de Jonge et al. (2001)
Soil (Denmark)	Sandy	4.90[b]	na	1.36	4.20	32.08	3.27	116.20	0.61	0.04–65.00	1/18	$CaCl_2$	de Jonge et al. (2001)
Soil (Denmark)	Sandy	5.20[b]	na	1.33	4.20	9.08	3.46	154.00	0.62	0.04—65.00	1/18	$CaCl_2$	de Jonge et al. (2001)
Soil (Denmark)	Sandy	5.50[b]	na	1.14	4.20	13.07	3.44	138.80	0.65	0.04–65.00	1/18	$CaCl_2$	de Jonge et al. (2001)
Soil (Denmark)	Sandy	5.40[b]	na	1.29	4.20	24.28	3.65	136.60	0.63	0.04–65.00	1/18	$CaCl_2$	de Jonge et al. (2001)
Soil (Denmark)	Sandy	5.50[b]	na	1.20	4.20	25.57	3.32	119.80	0.63	0.04–65.00	1/18	$CaCl_2$	de Jonge et al. (2001)
Soil (Denmark)	Sandy loam	6.20[b]	na	1.28	10.80	6.19	6.45	214.70	0.56	0.04–65.00	1/18	$CaCl_2$	de Jonge et al. (2001)
Soil (Denmark)	Sandy loam	6.20[b]	na	1.26	10.80	13.26	5.26	165.10	0.60	0.04–65.00	1/18	$CaCl_2$	de Jonge et al. (2001)
Soil (Denmark)	Sandy loam	6.30[b]	na	1.25	10.80	24.52	5.35	137.60	0.67	0.04–65.00	1/18	$CaCl_2$	de Jonge et al. (2001)
Soil (Denmark)	Sandy loam	6.40[b]	na	1.23	10.80	58.74	5.71	106.40	0.71	0.04–65.00	1/18	$CaCl_2$	de Jonge et al. (2001)
Soil (Denmark)	Sandy loam	6.30[b]	na	1.21	10.80	8.75	5.28	171.70	0.58	0.04–65.00	1/18	$CaCl_2$	de Jonge et al. (2001)
Soil (Denmark)	Sandy loam	6.30[b]	na	1.40	10.80	15.56	5.04	144.00	0.59	0.04–65.00	1/18	$CaCl_2$	de Jonge et al. (2001)
Soil (Denmark)	Sandy loam	6.30[b]	na	1.44	10.80	24.79	4.94	151.30	0.65	0.04–65.00	1/18	$CaCl_2$	de Jonge et al. (2001)

Table 2 continued

Substrate type and origin	Texture Sand-silt-clay (%)	pH	CEC cmol kg^{-1}	Organic carbon %	Clay %	Phosphorus mg kg^{-1}	Fe_{ox} and Al_{ox} g kg^{-1}	Kf L kg^{-1} n^{-1}	n	Aqueous concentration min–max mg L^{-1}	Solid/liquid ratio g mL^{-1}	Aqueous phase	References
Soil (Brazil)	81.7:2.0:16.3	4.00[a]	2.00	0.83	16.30	28.77	212.00	31.32	1.00	3405.00	2/5	$CaCl_2$	da Cruz et al. (2007)
Soil (Brazil)	81.7:2.0:16.3	5.00[a]	2.00	0.83	16.30	28.77	212.00	17.89	1.00	3405.00	2/5	$CaCl_2$	da Cruz et al. (2007)
Soil (Brazil)	81.7:2.0:16.3	6.00[a]	2.00	0.83	16.30	28.77	212.00	19.59	1.00	3405.00	2/5	$CaCl_2$	da Cruz et al. (2007)
Soil (Brazil)	81.7:2.0:16.3	7.00[a]	2.00	0.83	16.30	28.77	212.00	15.52	1.00	3405.00	2/5	$CaCl_2$	da Cruz et al. (2007)
Soil (Brazil)	27.7:42.0:30.3	4.00[a]	4.00	0.38	30.30	3.12	289.40	0.87	1.00	3405.00	2/5	$CaCl_2$	da Cruz et al. (2007)
Soil (Brazil)	27.7:42.0:30.3	5.00[a]	4.00	0.38	30.30	3.12	289.40	0.83	1.00	3405.00	2/5	$CaCl_2$	da Cruz et al. (2007)
Soil (Brazil)	27.7:42.0:30.3	6.00[a]	4.00	0.38	30.30	3.12	289.40	1.37	1.00	3405.00	2/5	$CaCl_2$	da Cruz et al. (2007)
Soil (Brazil)	27.7:42.0:30.3	7.00[a]	4.00	0.38	30.30	3.12	289.40	0.90	1.00	3405.00	2/5	$CaCl_2$	da Cruz et al. (2007)
Soil (Brazil)	19.7:26.0:54.3	4.00[a]	11.00	2.56	54.30	16.93	236.70	4.45	1.00	3405.00	2/5	$CaCl_2$	da Cruz et al. (2007)
Soil (Brazil)	19.7:26.0:54.3	5.00[a]	11.00	2.56	54.30	16.93	236.70	3.44	1.00	3405.00	2/5	$CaCl_2$	da Cruz et al. (2007)
Soil (Brazil)	19.7:26.0:54.3	6.00[a]	11.00	2.56	54.30	16.93	236.70	2.51	1.00	3405.00	2/5	$CaCl_2$	da Cruz et al. (2007)
Soil (Brazil)	19.7:26.0:54.3	7.00[a]	11.00	2.56	54.30	16.93	236.70	2.01	1.00	3405.00	2/5	$CaCl_2$	da Cruz et al. (2007)

Note that sorption parameters included in the database were measured on unmodified soil or sediment and with background electrolyte being either water (H_2O) or calcium chloride ($CaCl_2$). Some parameters were not included in the database because of unit incoherencies (e.g., Jacobsen et al. 2008)

na not available

[a] pH_{H2O}

[b] pH_{CaCl2}

[c] CEC meq/100 g

Table 3 Statistical characteristics of the database subsamples

	Sample A					Sample B					Sample C				
	Nobs.	Mean	Median	Min	Max	Nobs.	Mean	Median	Min	Max	Nobs.	Mean	Median	Min	Max
Kf (L kg^{-1} n^{-1})	69	108.16	111.50	0.83	403.50	36	96.32	63.00	0.83	297.02	51	118.89	118.10	1.89	297.02
n	69	0.83	0.88	0.48	1.05	36	0.94	1.00	0.75	1.05	51	0.77	0.75	0.48	1.05
Kd_{eq} (L kg^{-1})	69	73.96	38.89	0.06	403.50	36	87.02	39.05	0.83	318.82	51	72.61	44.78	0.06	318.82
pH	69	6.10	6.30	3.60	8.71	36	6.68	6.85	4.00	8.71	51	6.20	6.30	3.60	8.71
OC (%)	69	1.79	1.29	0.00	9.60	36	2.62	1.69	0.00	9.60	51	1.50	1.29	0.00	6.44
CEC (cmol kg^{-1})	36	13.25	12.55	1.80	33.60	36	13.25	12.55	1.80	33.60	19	15.21	12.60	1.80	33.60
Clay (%)	69	18.32	10.80	0.00	56.10	36	25.36	24.25	0.00	56.10	51	16.11	10.80	0.00	56.10
P_{OLSEN} (mg kg^{-1})	52	297.88	25.18	0.00	3240.00	26	321.32	16.93	3.12	2760.00	40	382.36	29.89	0.00	3240.00
Fe_{ox}–Al_{ox} (g kg−1)	49	80.87	5.04	0.61	298.73	19	157.32	212.00	2.58	289.40	36	28.00	3.44	0.61	298.73

Sample A all data with $CaCl_2$ as the background electrolyte. *Sample B* data used for the calibration of Kd and Kf pedotransfer functions. *Sample C* data used for the calibration of the **n** pedotransfer function

OC organic carbon, *CEC* cation exchange capacity, Fe_{ox}–Al_{ox} iron- and aluminum oxides, *Nobs.* number of observations

Results and Discussion

Database and sample characteristics

The soils and sediments used in the glyphosate sorption measurements displayed great variability in their origins and properties. This variability was preserved in the subsampling of the database for pedotransfer function calibration, as seen in Table 3. Indeed, the three subsamples of the database displayed similar distributions of properties and parameters values. The 0.01–1000 mg/L concentration range (Table 4) was also preserved by the subsampling of the database. This range covers all possible environmental glyphosate concentrations from concentrations found during spraying to those found in runoff and groundwater. It is interesting to note that the data presented in Table 5 exhibited highly significant correlations between some basic soil properties: The CEC was correlated with organic carbon or iron– and aluminum oxides, and the clay content was correlated with iron– and aluminum oxides. In contrast, there was no correlation between clay and CEC, suggesting a large influence of the within–sample variation in clay mineralogy (Table 5).

Table 4 Initial aqueous concentration used for the linear approximation if Freundlich isotherms

	Initial aqueous concentrations (mg L^{-1})	Frequency of use in experimental design (%)
Class 1	0.01–0.02–0.04–0.06–0.08	56
Class 2	0.10–0.20–0.40–0.60–0.80	59
Class 3	1.00–2.00–4.00–6.00–8.00	55
Class 4	10.00–20.00–40.00–60.00–80.00	32
Class 5	100.00–200.00–400.00–600.00–800.00–1000.00	12

Table 5 The Pearson correlation coefficients matrix among soil properties

Parameters	CEC (cmol kg^{-1})	OC (%)	Clay (%)	Phosphorus (mg kg^{-1})	Fe_{ox} and Al_{ox} (g kg^{-1})
pH	0.407*	NS	0.250*	0.339*	NS
	(36)	(69)	(69)	(52)	(49)
CEC	–	0.666***	NS	NS	−0.691**
		(36)	(36)	(26)	(19)
OC	–	–	NS	NS	NS
			(69)	(52)	(49)
Clay	–	–	–	NS	0.631***
				(52)	(49)
Phosphorus	–	–	–	–	NS
					(49)

The number in brackets corresponds to the number of observations for the given correlation. "***", "**" and "*" represent correlation significance levels of 0.001, 0.01 and 0.05, respectively

NS correlation is not significant, *OC* organic carbon, *CEC* cation exchange capacity, Fe_{ox}–Al_{ox} iron- and aluminum oxides

Table 6 The Pearson correlation coefficients matrix between sorption parameters and soil properties or experimental conditions

Parameters	pH	CEC (cmol kg^{-1})	OC (%)	Clay (%)	Phosphorus (mg kg^{-1})	Fe_{ox} and Al_{ox} (g kg^{-1})	C_{max} (mg L^{-1})	log(R)
Kd_{eq}	NS	0.659***	0.380**	NS	NS	NS	−0.364**	NS
	(69)	(36)	(69)	(69)	(52)	(49)	(69)	(69)
Kf	NS	0.659***	0.255*	NS	NS	−0.527***	−0.551***	−0.432***
	(69)	(36)	(69)	(69)	(52)	(49)	(69)	(69)
n	0.531***	NS	0.351*	0.760***	0.361*	0.560***	−0.666***	0.489***
	(51)	(19)	(51)	(51)	(40)	(36)	(51)	(51)

The number in brackets corresponds to the number of observations for the given correlation. "***", "**", and "*", represent correlation significance levels of 0.001, 0.01 and 0.05, respectively

NS correlation is not significant, *OC* organic carbon, *CEC* cation exchange capacity, Fe_{ox}–Al_{ox} iron- and aluminum oxides, C_{max} maximal initial concentration (mg L^{-1}), *log(R)* log-transformed solid–liquid ratio (g mL^{-1})

Table 7 Pedotransfer function for the estimation of linear (Kd) and Freundlich (Kf–n) sorption isotherms

Pedotransfer function	Sample	Soil parameters	Equation	R^2	RMSEP
Kd	B	CEC, Clay	Kd = 24.821 + 7.199 * CEC − 1.307 * Clay	0.48***	7.59 (8.7 %)[a]
Kf	B	CEC, Clay, OC	Kf = 50.904 + 9.246 * CEC − 1.985*Clay − 11.811 * OC	0.52***	16.33 (16.9 %)[b]
n	C	Clay, pH	*n* = 0.505 + 0.007 * Clay + 0.024 * pH	0.62***	0.006 (0.8 %)[c]

OC organic carbon (%), *CEC* cation exchange capacity (cmol kg^{-1}), clay (%)

*** Correlations are significant at the level 0.001

[a] RMSEP expressed as a percentage of the mean Kd value (87.02 L kg^{-1})

[b] RMSEP expressed as a percentage of the mean Kf value (96.32 L kg^{-1} n^{-1})

[c] RMSEP expressed as a percentage of the mean n value (0.77)

Glyphosate sorption: mechanisms and prediction

The Pearson correlation coefficients (Table 6) showed that the Kd, q and Kf values are primarily correlated with CEC and, secondarily, with organic carbon content and Fe_{ox}–Al_{ox} content. They also show that n exhibits significant correlation with all of the selected soil properties, with the exception of CEC. The multiple regression analysis (Table 7) provided pedotransfer functions that accurately fit the observed Kd_{eq}, Kf and n values. The functions account for 48–62 % of the variation in the sorption parameters. Visual inspection of the disparity between the measured and predicted Kd_{eq}, Kf and n sorption parameters did not reveal systematic departures from the regression, except for one outlier corresponding to high Kd_{eq} and Kf values measured on a sediment containing a particularly high organic carbon content (Figure 2). The multiple regression analyses high–lighted the points that CEC is the main predictor of Kd_{eq} and Kf variation and that clay is a useful predictor. Furthermore, we found that organic carbon was a predictor for Kf only. The analyses also revealed that clay and pH are significant predictors of *n*. These results suggest that the formation of complexes between the glyphosate phosphonate groups and the soil exchanged polyvalent cations is the dominating sorption mechanism across the entire range of analyzed soils. This is indicated by the primary role of CEC in controlling Kd_{eq} and Kf variability. Given the high correlation between CEC and Fe_{ox}–Al_{ox} in our sample, it is likely that the influence of the latter property was masked by that of the former.

Additionally, we found that clay content explained only approximately 5 % of the Kd_{eq} and Kf variability (Tables 6, 7). Significant correlations were found between organic carbon and Kd_{eq} or Kf (Table 6), although organic carbon only slightly increased the R^2 value obtained in the multiple regression analyses of Kf. Organic carbon appeared to be strongly correlated with CEC, indicating the significant contribution of organic matter to CEC; this correlation may explain the correlation of organic carbon with the sorption parameters. There is a general consensus that a rise in pH negatively affects the sorption of glyphosate. However, the multiple regression analyses did not detect any influence of pH on Kd_{eq}, and Kf variability.

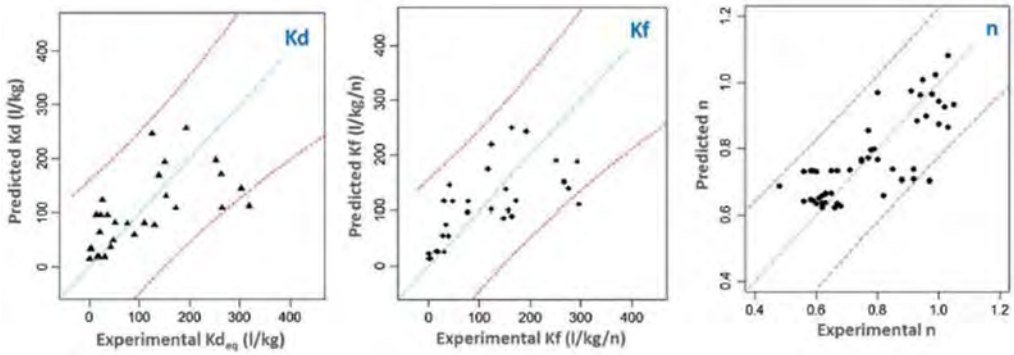

Figure 2 Multiple regression analysis of the sorption coefficients (Kd, Kf, *n)* and soil properties. The sorption coefficients predicted from the pedotransfer functions presented in Table 7 were plotted against the sorption coefficienls (Kf, *n*) fitted from the experimental data and for Kd_{eq}, against the linearized sorption coefficients.

Here, pH and clay explained most of the n parameter variability (Tables 6 and 7). The positive correlation of n with pH may be related to the increased negative charges for both glyphosate (Figure 1) and the soil, favoring the formation of complexes with soil–exchanged polyvalent cations. Despite the increasing electrostatic repulsion, a rise in pH appears to reduce the potential saturation of sorption sites for high initial concentrations by favoring cation bridging between glyphosate and the soil. The variability of the sorption parameters that is not predicted by the multiple regressions may be largely attributed to the varying experimental conditions among the studies measuring glyphosate sorption to soils and sediments (Table 2). If different parameters are considered to be possible predictors in the multiple regressions, they enable a fit to a regression function (Eq. 4) with a better performance (R^2 = 0.69) than that of the regression using only basic soil properties as predictors for *n*.

$$n = 0.920 - 0.028 \times \log(C_{max}\ (mg/L)) + 0.064 \times \log (R(g\ m/L)) + 0.005 \times clay\ (\%) \qquad (4)$$

A small R implies a limited amount of sorption sites.

Correlations between Kf, Kd_{eq} and the solid–to–liquid ratio or the maximal initial concentration (Table 6) are further evidence of the influence of the experimental conditions on the sorption. However, unlike the case of the *n* parameter, inclusion of the experimental conditions (C_{max}, *R*) in the multiple regression analyses did not increase the predictive performance of the regression for Kd_{eq} and Kf. It must be noted that the pedotransfer functions could be improved with additional experimental sorption studies designed to closely mimic the environmental conditions and with pH and CEC analyzed with the standardized methods [pH_{H2O}, Metson CEC (cmol/kg)].

Use of pedotransfer functions for risk assessment

The linear sorption coefficient Kd can be predicted by a pedotransfer function requiring the knowledge of only two properties, the clay content and CEC. The prediction performance is good with an RMSEP of less than 10 % of the mean glyphosate Kd_{eq} (Table 7). However, Figure 3a shows that the errors in the predicted soil–to–water concentration ratios vary largely according to the initial concentration of water. The errors are moderate for initial liquid–phase concentrations below 10 mg/L, indicating that the Kd pedotransfer function predicts sorption relatively accurately for concentrations below this

threshold. The 10 mg/L may correspond to the threshold above which the concentration independence of the sorption process can no longer be assumed. This assumption can be checked by examining the variation in n given by Eq. 4. Figure 4 presents the departure from linearity assumed to occur when *n* is below 0.9 across a range of clay content values and initial glyphosate concentrations.

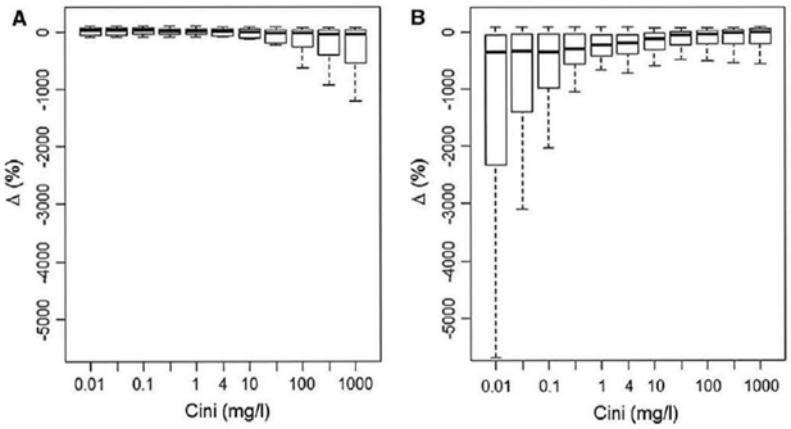

Figure 3 Distributions of the prediction errors for linear sorption isotherms and nonlinear sorption isotherms. Δ represents the difference (%) at a given initial concentration between the predicted and the measured ratio of concentrations between soil and water. a Ratios predicted by the Kd pedotransfer function (linear isotherm estimation) and b ratios predicted by the Kf and *n* pedotransfer function (nonlinear isotherm estimation)

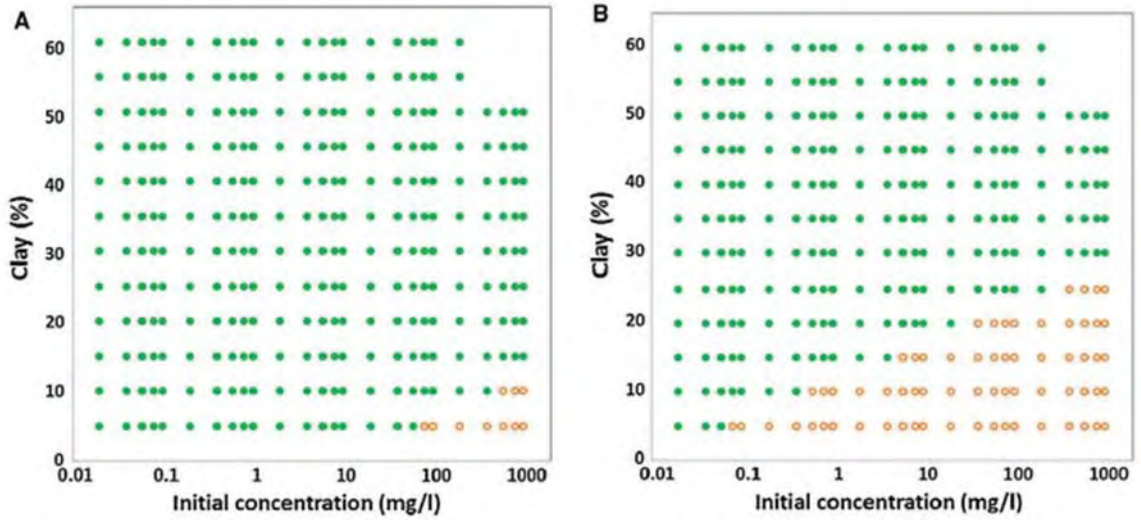

Figure 4 Linearity range of sorption isotherms in relation to the clay content and initial glyphosate concentrations in the liquid phase. Plain green dots represent 0.9 <n <1.05, and empty orange dots represent n values lower than 0.9 (bottom right), A n values were calculated from Eq. 4 with a solid–to–liquid ratio of 1:1 (g/ml). B n values were calculated from Eq. 4 with a solid–to–liquid ratio of 1:20 (g/ml). Note that for a solid–to–liquid ratio of 1:1, the saturation of sorption sites occurs at initial concentration higher than 100 mg/L for clay content varying between 0 and 10 %, whereas for the 1:20 ratio, the saturation for the same clay content starts at initial concentrations of approximately 0.1 mg/L.

The Freundlich isotherms can be satisfactorily predicted by two pedotransfer functions requiring the knowledge of four properties, namely the organic carbon and clay contents, CEC and pH (Table 7). As seen in Figure 4, the prediction errors of the soil–to–water concentration ratio exceed 1000 % for concentrations between 0.01 and 0.40 mg/L and 500 % for concentrations up to 10 mg/L (Figure 3b). Thus, the sorption estimated by the combination of *n* and Kf pedotransfer functions is significantly underestimated for initial concentrations below 10 mg/L. This may be due to the multiplication of

properties used to estimate the sorption parameters and the accumulation of inherent bias of the two pedotransfer functions. However, it must also be noted that for concentrations higher than 10 mg/L, the predictions using the estimated Freundlich model parameters show slightly smaller errors than those using the estimated linear isotherms. The application of the Kf pedotransfer function is therefore only advisable for estimating sorption for very high liquid–phase concentrations, a condition that is relatively rarely found in the current environmental conditions.

Conclusion

Sorption to soils and sediments controls the fate of glyphosate in the environment and thus the potential risk of freshwater and groundwater contamination. Glyphosate sorption appeared to be controlled mainly by cation exchange capacity, clay and organic carbon content and pH. This suggests that the mechanism driving glyphosate sorption over the range of soil and sediment investigated is the complex formation between the phosphonate group of glyphosate and the soil–exchanged polyvalent cations. Robust pedotransfer function for the estimation of glyphosate Kd was built from multiple regression analysis of the literature data. This Kd pedotransfer function enables prediction of glyphosate sorption for a wide range of soils and sediments with a limited number of properties and with reasonable accuracy for most environmental conditions.

3. Assessment and conclusion

Assessment and conclusion by applicant:
The article estimates pedotransfer functions for the adsorption of glyphosate to soil based on based on review of existing literature data. No new experimental data is presented.
The article is therefore classified as reliable with restrictions (Category 2).

Te

1. Information on the study

Data point:	KCA 7.1.2.1.1
Report author	Ghafoor, A. et al.
Report year	2011
Report title	Measurements and modeling of pesticide persistence in soil at the catchment scale
Document No	The Science of the total environment (2011) Vol. 409, No. 10, pp. 1900–8.
Guidelines followed in study	OECD 106 Guidance
Deviations from current test guideline	Not sufficient information provided to check validity
GLP/Officially recognised testing facilities	No, not conducted under GLP/Officially recognised testing facilities
Acceptability/Reliability:	Reliable with restrictions (Not all information provided to check validity of the results, no results reported for adsorption experiment)

2. Full summary of the study according to OECD format

Degradation of pesticides in soils is both spatially variable and also one of the most sensitive factors determining losses to surface water and groundwater. To date, no general guidance is available on suitable approaches for dealing with spatial variation in pesticide degradation in catchment or regional scale modeling applications. The purpose of the study was therefore to study the influence of various soil physical, chemical and microbiological characteristics on pesticide persistence in the contrasting cultivated soils found in a small (13 km^2) agricultural catchment in Sweden and to develop and test a simple model approach that could support catchment scale modeling. Persistence of bentazone, glyphosate and isoproturon was investigated in laboratory incubation experiments. Degradation rate constants were highly variable with coefficients of variation ranging between 42 and 64 % for the three herbicides. Multiple linear regression analysis and Mallows Cp statistic were employed to select the best set of independent parameters accounting for the variation in degradation. Soil pH and the proportion of active microorganisms (r) together explained 69 % of the variation in the bentazone degradation rate constant; the Freundlich sorption co–efficient (K_f) and soil laccase activity together explained 88 % of the variation in degradation rate of glyphosate, while soil pH was a significant predictor ($p < 0.05$) for isoproturon persistence. However, correlations between many potential predictor variables made clear interpretations of the statistical analysis difficult. Multiplicative models based on two predictors chosen ‘a priori’, one accounting for microbial activity (e.g. microbial respiration, laccase activity or the surrogate variable soil organic carbon, SOC) and one accounting for the effects of sorption on bioavailability, showed promise to support predictions of degradation for large–scale modeling applications, explaining up to 50 % of the variation in herbicide persistence.

Materials and methods

Study site and soils

The study was carried out in the E21 monitoring catchment in Östergötland, southern Sweden. The total catchment area of 13 km^2 consists of 95 % agricultural land, with main crops of winter and spring sown cereals, rape, potatoes and peas. The soils, which are derived from glacial and post–glacial fluvial sediments and glacial till (moraine), have a wide range of texture, from loamy sand to clay. Soil samples were collected from 60 locations in the catchment (1 location every 20 ha) on a grid pattern. Five soil samples from each location were taken in the surface 20 cm, bulked, homogenized by passing through a 2 mm sieve, put into plastic bags and stored at 4°C until use (within 48 days). Sixteen of these sampled locations were selected for further study to cover the range of measured textures, organic matter contents and pH values.

Soil pH was measured on fresh samples after shaking the samples in de–ionised water (1:2.5) at room temperature (Swedish Standard Institute, 1994). Particle size distributions were evaluated using the standard pipette method (Day, 1965). The contents of clay, sand, and silt are usually correlated with one another (Iqbal et al., 2005). Thus the geometric mean particle diameter, d_g, was derived from the fundamental particle size classes as (Shirazi and Boersma, 1984):

[1]

$$d_g = exp(\sum_i m_i ln(X_i))$$

where *m* is the mass fraction of particle size class i and X is the mean diameter of that class. For the Swedish system, x–values are 0.001, 0.03 and 1.03 mm for clay, silt, and sand, respectively. Total organic C and N were measured using a Leco CN 2000 (LECO Corp., St. Joseph, MI, USA). Water contents at a pressure potential of –100 cm (pF 2) were measured on a sand table (Jamison, 1958). Ammonium–lactate extractable phosphorus and potassium were measured according to the method described by Egner et al. (1960).

The physical and chemical characteristics of the 16 soils are given in Table 1. There was a relatively wide range of SOC contents, ranging from 0.9 to 10.2 %. Soil pH ranged from 6.0 to 7.6. Soil texture is very variable for such a small catchment: clay, sand and silt contents ranged from 4–45 %, 12–87 %, and 8–54 % respectively, and 8 of the 11 USDA texture classes are represented. Ammonium–lactate extractable phosphorus and potassium ranged from 56–148 mg/kg and 54–209 mg/kg, respectively.

Table 1. Physico–chemical properties of soils.

Soils	pH	Texture			Textural class	SOC	$CaCO_3$	Total N	Water content at pF_2 (−100 cm)	Geometric mean particle diameter (d_g)	Available P	Available K
		Sand	Silt	Clay								
		%	%	%	International	%	%	%	g/g	mm	mg kg^{-1}	mg kg^{-1}
1	7.6	49	32	18	Loam	1.6	9.2	0.16	0.253	0.095	58	68
2	6.2	87	8	4	Sand	1.2	0.1	0.08	0.115	0.588	63	69
3	7.0	43	27	30	Clay Loam	2.3	0.1	0.22	0.363	0.049	99	116
4	7.1	58	25	17	Sandy Loam	2.1	0.4	0.21	0.3	0.131	89	84
5	6.9	68	17	15	Sandy Loam	2.1	0.2	0.21	0.285	0.199	111	114
6	6.5	70	21	9	Sandy Loam	1.1	0.1	0.09	0.175	0.263	90	120
7	6.5	85	9	6	Loamy Sand	1.6	0.1	0.15	0.169	0.494	159	70
8	7.6	55	28	17	Sandy Loam	2.6	0.2	0.25	0.265	0.118	56	68
9	6.4	12	45	44	Silty Clay	6.7	0.3	0.54	0.643	0.010	57	205
10	6.9	17	54	29	Silty Clay Loam	10.2	0.5	0.87	0.540	0.020	73	170
11	6.9	22	33	45	Clay	2.5	0.9	0.25	0.383	0.014	134	162
12	7.3	56	24	20	Sandy Loam	5.4	0.4	0.53	0.477	0.110	142	209
13	6.0	63	27	10	Sandy Loam	0.9	0.1	0.08	0.240	0.198	132	126
14	6.1	83	11	6	Loamy Sand	1.3	0.1	0.13	0.227	0.460	148	54
15	7.5	35	39	25	Clay Loam	3	0.1	0.28	0.410	0.046	101	97
16	7.1	31	40	29	Clay Loam	1.9	0.2	0.19	0.347	0.033	89	164

Chemicals

Unlabelled isoproturon (N,N–dimethyl–N′–[4–(1–methylethyl) phenyl]urea; 99 % purity), bentazone (3–(1–methylethyl)–1 H–2,1,3–benzothiadiazin–4(3 H)–one 2,2–dioxide; 97 % purity) and glyphosate (N–(phosphonomethyl)glycine, 98 % purity) were purchased from Dr. Ehrenstorfer GmbH, Augsburg, Germany. Ring (^{14}C) isoproturon (4.044 MBq/mg; purity >95 %) and [P–methylene–^{14}C]glyphosate (5.155 MBq/mg, purity >99 %) were purchased from Izotop, Institute of Isotopes, Budapest, Hungary. ^{14}C–labelled bentazone (3–(1–methylethyl–1 H–2,1,3–benzothiadiazin–4(3 H)–one 2,2–dioxide–[phenyl–U–^{14}C]; 5.211 MBq/mg; 100 % purity) was a gift from BASF, Limburgerhof, Germany. Table 2 gives the structural formulae and some physical and chemical properties of the three compounds. The 3–methyl–2–benzothiazolinone hydrazone (MBTH), 3–(dimethylamino) benzoic acid (DMAB) and 2,2′–azinobis(3–ethyl–benzthiazoline–6–sulfonic acid) (ABTS) were supplied by Sigma–Aldrich Sweden AB.

Table 2. Selected pesticides and their properties (data from the e–Pesticide Manual (3.0), British Crop Protection Council, 2003).

Herbicides	Structural formulae	pKa	mol wt	Solubility in water (mg L^{-1})
Bentazone	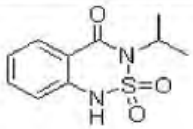	3.3	240.3	570
Glyphosate	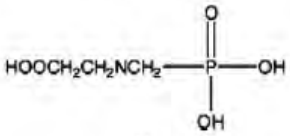	2.3, 5.7,10.2	169.1	10,500
Isoproturon	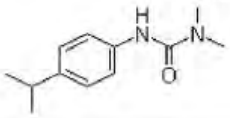	n.a	206.3	65

Degradation

Incubation experiments for each soil/pesticide combination were carried out on two replicate samples. A sub–sample of each soil (7 g) was spiked with glyphosate dissolved in water (0.7 mg herbicide/mL water) or isoproturon or bentazone dissolved in methanol (0.7 mg herbicide/mL methanol). The soil was dried, after which an additional amount of fresh soil (63 g) was thoroughly mixed into the spiked soil to give an initial concentration of 10 μg/g dry weight (d.w.) of soil (procedure adopted from Brinch et al. (2002)). Water contents were adjusted to and maintained at pF 2 throughout the experiment by the addition of de–ionized water as necessary. The samples were incubated in aerated glass tubes in the dark at 20°C for 64 days. Duplicate samples (5 g) were taken after 0, 2, 4, 8, 16, 32 and 64 days of incubation for measurement of the residual concentrations of glyphosate, isoproturon, and bentazone.

Analyses of bentazone and isoproturon in soil samples were carried out by HPLC as described by Larsbo et al. (2009), while for glyphosate, the GC–MS method developed by Börjesson and Torstensson (2000) was employed. The data from the incubation study were fitted to first–order degradation kinetics using non–linear regression:

[2]

$$c = c_0 e^{-kt}$$

where c is the mass of compound in the soil (μg/g) at a given time t (days), c_0 is the original mass of compound added to the soil (μg/g), and k (day^{-1}) is the first–order degradation rate coefficient. Degradation half–lives (DT_{50}, days) were calculated as ln(2)/k.

Adsorption

The adsorption experiments were carried out according to the OECD 106 guideline (Organization for Economic Cooperation and Development, 2000) on two replicates. Soil (four grams d.w. for glyphosate, two grams d.w. for isoproturon and bentazone) was shaken to pre–equilibrate with 0.01 M $CaCl_2$ (39 mL for glyphosate, 1.5 mL for bentazone and isoproturon) for 24 h at 20°C in test tubes (50 mL plastic tubes (Sarstedt) for glyphosate and 10 mL glass tubes for bentazone and isoproturon). Thereafter, the soil slurry was spiked with a 1 mL mixture of labeled (ca 7000–11000 dpm) and unlabeled pesticides in 0.01 M $CaCl_2$ to give 5 initial concentrations in the range of 0.1–10 μg/g soil. The tubes were shaken for 24 h and then centrifuged for 20 min at 4000 rpm. After mixing with 10 mL of Insta–Gel Plus (glyphosate) or 6 mL of Ultima Gold emulsifying cocktail (bentazone and isoproturon) (PerkinElmer, Waltham, MA, USA), the radioactivity was measured in the supernatant (10 mL for glyphosate, 1 mL for bentazone and isoproturon) using a LS 6000TA liquid scintillation counter (Beckman Instruments, Fullerton, CA, USA). Tubes without soil and ^{14}C–labelled substances were included for subtraction of background radiation and tubes without soil were used to give the initial amount of ^{14}C activity. No significant adsorption of the tested substances occurred on the tubes.

The sorption measurements for each pesticide in the 16 soils were fitted to the Freundlich equation using

non–linear regression:
[3]

$$S = K_f c_e^n$$

where S is the adsorbed amount (μg/g), c_e is the equilibrium concentration (μg/mL), K_f is the Freundlich constant ($\mu g^{1-n}\, mL^n/g$), and n (–) is an exponent that expresses the degree of isotherm nonlinearity.

Manganese peroxidase and laccase enzyme activities
Manganese peroxidase (MnP, EC 1.11.1.13) activity
Ten g of soil was mixed with 20 mL of a 1:1 mixture of 500 mM lactic acid/sodium succinate buffer (pH 4.5) in a Waring blender and homogenized for 3×30 seconds at high speed. The aliquots were centrifuged in 50 mL centrifuge tubes at 4000 rpm for 15 min at 4°C. The supernatant was filtered through 0.45 μm filter paper. Manganese peroxidase (MnP) activity was measured according to the method described by Castillo et al. (1994). Briefly, the assay is based on the oxidative coupling of MBTH and DMAB in the presence of H_2O_2, Mn^{+2} and MnP. This reaction gives a deep purple–blue color with a broad absorption band with a peak at 590 nm. The reaction mixture contained 300 μL 6.6 mM DMAB, 100 μL 1.4 mM MBTH, 30 μL 30 mM$MnSO_4$, 10 μL 10 mM H_2O_2 and 1.56 mL of sample extract in a total volume of 2 mL. A reagent blank without any sample extract was also run. Time zero was registered at the moment of addition of H_2O_2 and the increase in absorbance was then followed at 590 nm for 5 min by using a Shimadzu UV 1800–A spectrophotometer fitted with a time scan function. The initial rates were calculated by using linear regression. MnP activity (mU/min/g soil) in soil was calculated as:
[4]

$$\text{Unit of enzyme } g^{-1}\text{soil} = \frac{\text{Abs}/\textit{min} \times 0.002}{E_m \times \text{mL of sample} \times \text{Dry weight of soil} \times \text{mL of buffer added}}$$

where E_m is the molar extinction coefficient (0.053 μM^{-1}/cm). One unit is defined as the amount of enzyme needed to form 1 μmol of product in 1 min.

Laccase (EC 1.10.3.2) activity
Laccase activity was measured by monitoring the oxidation of ABTS (Wolfenden and Willson, 1982) in a citrate/phosphate (100 mM citrate, 200 mM phosphate) buffer (pH 4.5) at 420 nm. Briefly, five g of soil was extracted with 20 mL 100 mM citrate/phosphate buffer (pH 4.5) for 1 h and then centrifuged for 15 min at 4000 rpm. The supernatant was filtered through a 0.45 μm filter. The reaction mixture contained 900 μL soil extract and 100 μL 30 m MABTS solution. The absorbance was measured at 420 nm at 25°C for 1 min with Shimadzu UV 1800–A spectrophotometer. Absorbance per minute (Abs/min) was calculated from the linear range of the curve and laccase activity was calculated as:
Unit of enzyme g^{-1}soil
[5]

$$= \frac{\text{Abs}/\ \textit{min} \times \text{mL of buffer added} \times 1000 \times \text{Volume}_{\text{reaction mixture}(\mu L)}}{E_m \times \text{Volume}_{\text{enzyme solution}(\mu L)} \times \text{Dry weight of soil}}$$

where Em is 0.036 μM^{-1}/cm.

Respiration
Respiration was measured as described previously (Stenström et al., 2001) with some modifications. Two replicates of soil (10 g d.w.) were weighed into 250 mL respirometric jars. The jars were installed inside a respirometer, and the accumulation of CO_2 trapped in KOH solution (0.2 M; 10 mL) was determined automatically twice every hour for each jar by measuring the electrical conductivity. The soil samples were incubated until a constant basal respiration rate (BR) was established (after about 3 days) at a constant temperature of 22°C and with a moisture content adjusted to pF 2. A substrate was prepared, consisting of glucose (7.5 g), $(NH_4)_2SO_4$ (1.13 g), KH_2PO_4 (0.35 g) and talcum powder (10 g), and 0.19 g of this mixture was thoroughly mixed into each jar. Empty jars were incubated as controls. The BR was calculated by linear regression of accumulated CO_2 produced versus time. The

instantaneous rate of CO_2 formation after addition of the substrate (substrate–induced respiration, SIR) was calculated using non–linear regression. The SIR was divided into the CO_2 production rate of active, exponentiallly growing (r) and dormant, non–growing (*K*) microorganisms as described by Stenström et al. (2001).

^{14}C–DHP mineralization

Synthetic ^{14}C–ring–labeled dehydrogenated polymerizate (^{14}C–DHP) of coniferyl alcohol (gift from Paul Ander, Department of Forest Products, SLU) with a molecular weight of 4–10 kDa and a specific activity of 0.16 MBq/mg was used to quantify lignin degrading activity in situ. The ^{14}C–DHP was added as a DMF–water suspension to 10 g dw of soil in 20 mL plastic jars. The final radioactivity was approximately 13,000 dpm per sample. The water contents were adjusted to pF 2. The plastic jars were each installed into air–tight glass jars together with scintillation vials containing NaOH (0.2 M; 4 mL) to trap carbon dioxide. The glass jars were incubated in the dark at 20°C and the base traps were changed regularly. The amount of ^{14}C in the base traps was measured on an LS 6000TA liquid scintillation counter (Beckman Instruments, Fullerton, CA, USA) after mixing with 4 mL of Insta–gel Plus and incubated in the dark overnight. The ^{14}C liberated was corrected for the background radiation in controls without soil. Kinetic parameters describing ^{14}C–DHP mineralization were determined by non–linear regression according to first–order kinetics:

[6]

$$P = P_{max}\left(1-e^{-kt}\right)$$

where P is the accumulated ^{14}C–CO_2 released (% of the added ^{14}C) at time t, P_{max} is the maximum ^{14}C mineralized (% of applied) and k is the mineralization rate constant (day^{-1}).

Statistical analysis

General regression models (GRM) for best–subset–regression were fitted to the data, where replicate 1 was cross–validated with replicate 2 under the assumption of homogeneous variance. Hence, the two replicates were pooled for variance estimation, and all possible combinations of regressors examined with respect to explanatory power of the response variable (k). When the best–subset–regression models were built, our objective was to identify the subset of explanatory variables that combine optimal orthogonality with maximum explanatory power, in order to explain the variance of the response variable across soil samples. Orthogonality is synonymous with independence across regressor variables, and many methods have been suggested for estimating the ideal subset. Mallow's Cp statistic (Mallows, 1973) is an effective way to punish a linear combination of potential regressors with respect to multi–collinearity and accumulated error (Ryan, 1997). Mallow's Cp is identical to Akaike's information criteria when the generic variance σ^2 is known ‘a priori’. Since we estimate σ^2 from our data, Mallow's Cp is a better choice. Statistical analyses were performed with STATISTICA™ (StatSoft, 1995).

Results and discussion

Degradation

The results from the degradation experiments are presented in Table 3. Bentazone, glyphosate and isoproturon degradation in soils generally followed first–order kinetics (all R^2>0.91 and statistically significant at $p<0.001$). The degradation rate constants listed in Table 3 show considerable differences between soils with coefficients of variation ranging from 42 to 64 % for the three compounds. Degradation rate constants for bentazone were in the range 0.005–0.034/day which corresponds to half–lives of 20 to 139 days. Our data are consistent with those (8–133 days) reported by others (Rodriguez–Cruz et al., 2006; Thorstensen and Lode, 2001). Degradation rate constants for isoproturon were in the range 0.011–0.104/day which corresponds to half–lives of 7–63 days. Again, this degree of variation is similar to that reported in the literature for isoproturon, with values ranging from 1.4 to 40 days (Larsbo et al., 2009; Rodriguez–Cruz et al., 2006; Walker et al., 2001). The degradation rates of glyphosate (0.006–0.05/day, which correspond to half–lives of 14–116 days) are also consistent with other studies where the DT_{50} values in a variety of different soil types have been reported in the range of 1.7 to 197.3 days (Giesy et al., 2000; Sorensen et al., 2006).

Table 3. Degradation rate constant of bentazone, isoproturon, and glyphosate in different soils.

Soils	Bentazone		Isoproturon		Glyphosate	
	k (day^{-1})	R^2	k (day^{-1})	R^2	k (day^{-1})	R^2
1	0.024 ± 0.002[a]	0.963	0.045 ± 0.002	0.981	0.044 ± 0.006	0.93
2	0.013 ± 0.001	0.984	0.031 ± 0.000	0.977	0.018 ± 0.001	0.95
3	0.019 ± 0.001	0.980	0.024 ± 0.001	0.986	0.032 ± 0.002	0.86
4	0.021 ± 0.001	0.986	0.044 ± 0.003	0.940	0.046 ± 0.002	0.88
5	0.015 ± 0.001	0.959	0.016 ± 0.001	0.980	0.031 ± 0.001	0.87
6	0.015 ± 0.002	0.972	0.041 ± 0.001	0.968	0.033 ± 0.003	0.97
7	0.010 ± 0.000	0.983	0.032 ± 0.005	0.990	0.024 ± 0.000	0.95
8	0.018 ± 0.002	0.976	0.062 ± 0.006	0.968	0.050 ± 0.001	0.89
9	0.032 ± 0.001	0.984	0.027 ± 0.000	0.941	0.017 ± 0.004	0.98
10	0.034 ± 0.001	0.986	0.015 ± 0.001	0.960	0.006 ± 0.001	0.95
11	0.014 ± 0.000	0.936	0.027 ± 0.003	0.983	0.013 ± 0.001	0.96
12	0.015 ± 0.002	0.961	0.034 ± 0.001	0.967	0.029 ± 0.001	0.96
13	0.006 ± 0.000	0.987	0.023 ± 0.003	0.964	0.022 ± 0.000	0.95
14	0.005 ± 0.000	0.910	0.011 ± 0.001	0.933	0.027 ± 0.000	0.97
15	0.017 ± 0.002	0.985	0.104 ± 0.002	0.937	0.028 ± 0.001	0.96
16	0.023 ± 0.002	0.968	0.077 ± 0.007	0.939	0.032 ± 0.004	0.98
Mean	0.018		0.039		0.028	
CV %	46		64		42	

[a] indicates the ± standard deviation of two replicates.

Correlations between variables

Soil physical, chemical and microbial parameters

Correlations between basic soil properties, microbiological parameters, sorption strength and the degradation rate of pesticides are reported in Table 4. As is quite typical, the sandy soils in our catchment (large dg values) generally had lower pH and SOC contents than the finer–textured loamy and clayey soils (Table 4). Activities of ligninolytic enzymes (MnP and laccase) were highly variable in our soils. Sinsabaugh et al. (2008) found a coefficient of variation for phenol oxidase (e.g., laccase) and peroxidase (e.g., MnP) activities among ecosystems of nearly 300 %. This variability can be attributed to differences in both the enzymology of various enzyme–producing white–rot species and differences in growth and enzyme production responses of the fungi to different soil and environmental factors (Sinsabaugh, 2010). Correlation analysis suggested that significantly higher enzyme activities in our soils were associated with higher soil organic carbon and soil pH (Table 4). MnP was positively correlated with SOC ($r = 0.78$; $p < 0.0001$). For peat soils, Sinsabaugh et al. (2008) also found that peroxidase activity increased with SOC. The activity of laccase was positively correlated with soil pH ($r = 0.55$; $p < 0.001$). This has also been found in other studies (Sinsabaugh, 2010; Sinsabaugh et al., 2008). Laccases deprotonate at high soil pH, which reduces their redox potential and increases their solubility, both of which may enhance their reaction potential (Sinsabaugh, 2010). Because laccases are widely produced for varied purposes, it is arguable that the diversity of the soil enzyme pool and potentially its range of action may also increase with soil pH (Sinsabaugh et al., 2008). Soil pH is also known to be an important predictor of microbial diversity (Sinsabaugh, 2010). Thus, SIR was positively correlated with soil pH, as well as SOC and available potassium, whereas it was negatively correlated with d_g and available P. The proportion of active microorganisms (r) was positively correlated with SOC, available K, and MnP whereas it was negatively correlated with d_g.

Table 4.Linear correlation coefficients.

Laccase	SIR	r	DHP k	Bentazone k	Isoproturon k	Glyphosate k
0.324						
−0.084	0.646***					
−0.504**	−0.019	0.13				
0.204	0.761***	0.787***	0.077			
0.546**	0.429*	−0.054	−0.274	0.130		
0.588**	−0.026	−0.536**	−0.012	−0.10	0.413	
−0.423	0.525**	0.555**	0.347	0.274	−0.14	−0.538**
−0.225	0.629***	0.761***	0.284	0.694	−0.23	0.413
−0.404	−0.078	0.498**	−0.162	0.112	0.11	−0.924***

	pH	c_g	SOC	P	K (Potassium)	MnP
d_g	0.621**					
SOC	0.186	−0.479*				
P	−0.32	0.299	−0.254			
K (potassium)	0.057	−0.605**	0.645***	0.018		
MnP	−0.132	−0.172	0.777***	0.043	0.700**	
Laccase	0.546**	−0.305	−0.274	−0.432*	−0.26	−0.588**
SIR	0.458*	−0.699***	0.494*	−0.489*	0.516**	0.323
r (active)	−0.015	−0.455*	0.834***	−0.448*	0.579**	0.548**
DHP k	0.099	−0.032	0.509**	0.229	0.253	0.649***
Bentazone k	0.449*	−0.655**	0.736***	−0.705***	0.477*	0.361
Isoproturon k	0.592**	−0.295	−0.169	−0.268	−0.115	−0.308
Glyphosate k	0.516**	−0.053	−0.503**	−0.223	−0.492*	−0.503**
Bentazone K_f	−0.286	−0.178	0.551**	0.035	0.610**	0.803***
Isoproturon K_f	0.025	−0.496*	0.814***	−0.221	0.697***	0.719***
Glyphosate K_f	−0.523**	0.059	0.428*	0.054	0.444*	0.363

*, **, and *** indicate significance at $p<0.1$, 0.05 and 0.01, respectively.

Pesticide degradation

Glyphosate degradation was significantly positively correlated to soil pH and laccase activity and negatively correlated with SOC and K_f. The strong relationship between glyphosate degradation and the Freundlich sorption coefficient is illustrated in Figure 1. A negative correlation between glyphosate adsorption and degradation in soil has also been reported by others (Zablotowicz et al., 2009).

Figure 1. Relationship between the degradation rate constant k (day^{-1}) for glyphosate and the Freundlich sorption coefficient (K_f, $\mu g^{1-n} mL^n g^{-1}$).

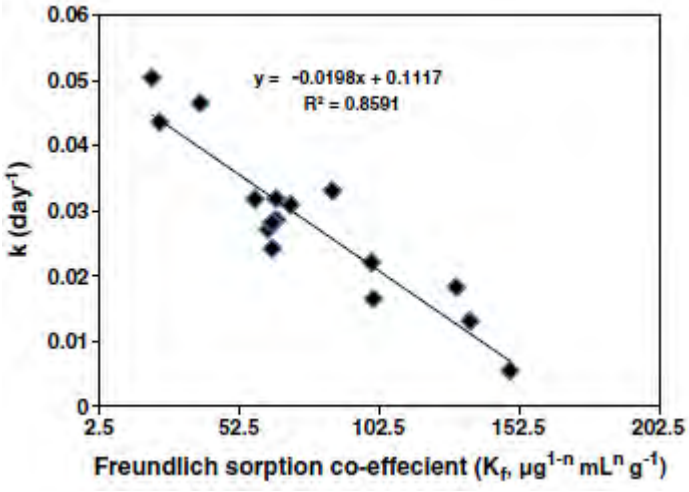

In this catchment, the finer-textured loamy and clay soils of higher pH showed faster degradation than sandy soils of low pH (Figure 2A and Table 3). Soil bacterial diversity and richness decline as pH decreases (Sinsabaugh et al., 2008) and other studies have also found pesticide persistence to increase as soil pH decreases (Walker et al., 2001). However, caution should be exercised in interpreting our data, since pH and SOC are strongly (positively) correlated if the three locations with highly organic (peaty) topsoils are excluded.

Figure 2B shows that the influence of SOC on pesticide degradation was rather complicated. An increase in soil organic matter increases biological activity and pesticide degradation rates in soil by providing conditions favorable to microbial growth (Thorstensen and Lode, 2001). On the other hand, pesticide sorption in soil, which is often positively related to SOC (Kah et al., 2007), may reduce the bioavailability of pesticides (Boivin et al., 2005; Kah et al., 2007; Sorensen et al., 2006; Thorstensen and Lode, 2001). Many studies have therefore demonstrated strong negative relationships between pesticide sorption and degradation in soils (Bolan and Baskaran, 1996; Dyson et al., 2002; Lehmann et al., 1992). In our study we observed a strong negative relationship between glyphosate degradation and its Freundlich sorption coefficient (Figure 1). The competing effects of organic matter content on microbial activity and sorption (bio–availability) mean that both positive and negative relationships

between sorption and degradation have been reported, as well as non–monotonic relation–ships which display an optimum (Bolan and Baskaran, 1996), as in Figure 2B for isoproturon.

Figure 2. Relationships between soil pH (A) and organic carbon content (B) and the degradation rate constants of all three pesticides.

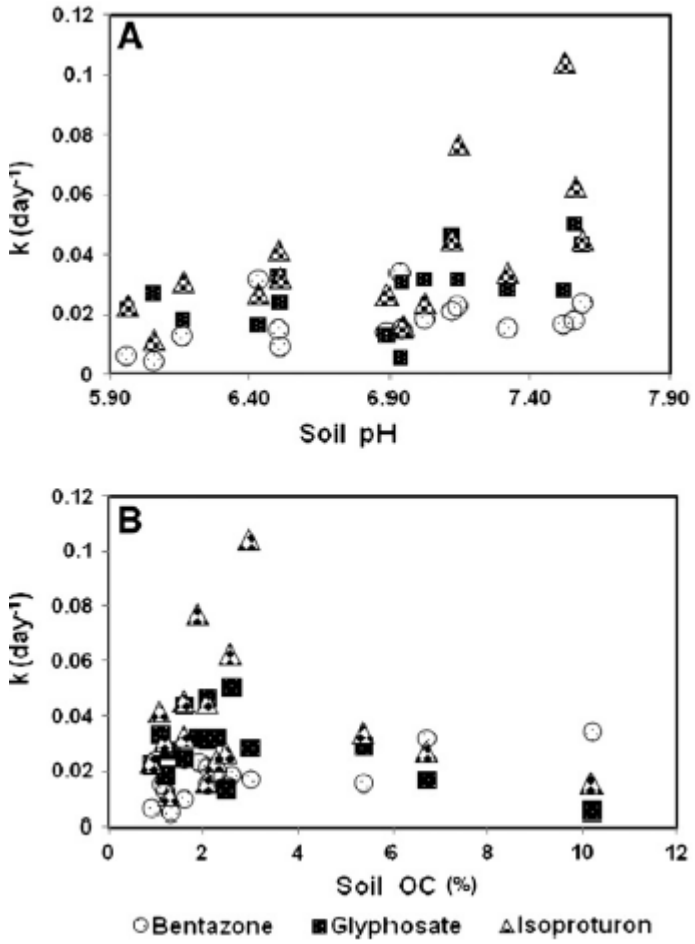

Regression analysis

Table 5 shows the results of best-subset regression analysis. The use of Mallows Cp led to the selection of five out of 12 potential regressor variables: soil pH, SOC, r, laccase, and K_f. Soil pH and r together explained 69 % of the total variation in the bentazone degradation rate constant. There was, however, a problem with this model, arising from the skewed distribution of r, which resulted in heteroscedasticity. After applying Box–Cox transformation to the original r variable (rBC), we obtained a regression equation for which the residual distributions were approximately normal homoscedastic:

[7]

$$k = 0.006(\text{pH}) + 0.004(\text{rBC}) - 0.012$$

$$R^2 = 0.57, \text{Adj } R^2 = 0.51, F(2,14) = 8.75, p < 0.01$$

As an alternative model, pH and SOC explained 56 % of the variation in bentazone degradation, with an acceptable behaviour of the residuals (Table 5). This is because SOC and *r* are strongly correlated (Table 4). For glyphosate, 88 % of the variation in degradation rate coefficient could be explained by the Freundlich co–efficient K_f and soil laccase activity. Soil pH was the most significant predictor (pb 0.05) for isoproturon degradation and the inclusion of two more terms (SOC and r) significantly increased R^2 from 0.29 to 0.42 (Table 5).

Table 5. Best subset regression models relating first–order degradation rate constants for bentazone, glyphosate and isoproturon to soil parameters (β is the unscaled regression coefficient).

Pesticide	Intercept	Soil pH	SOC	r	Laccase	K_f	Overall performance
Bentazone	−0.030	β = 0.006 p < 0.05 F (1, 15) = 8.25	–	β = 0.007 p < 0.001 F (1, 15) = 25.2	–	–	Adj R^2 = 0.69 F (2, 14) = 17.8 p < 0.001
	−0.024	β = 0.005 p = 0.07 F (1, 15) = 3.85	β = 0.002 p < 0.01 F (1, 15) = 13.9	–	–	–	Adj R^2 = 0.56 F (2, 14) = 10.6 p < 0.01
Glyphosate	0.04	–	–	–	β = 0.000011 p < 0.05 F (1, 15) = 7.5	β = −0.0002 p < 0.0001 F (1, 15) = 60.7	Adj R^2 = 0.88 F (2, 14) = 56.5 p < 0.000
Isoproturon	−0.14	β = 0.030 p < 0.05 F (1, 15) = 7.08	–	–	–	–	Adj R^2 = 0.29 F (1, 15) = 7.08 p < 0.05
	−0.17	β = 0.032 p < 0.01 F (1, 15) = 11.6	β = −0.008 p < 0.05 F (1, 15) = 4.9	β = 0.02 p = 0.13 F (1, 15) = 2.7	–	–	Adj R^2 = 0.42 F (3, 13) = 4.57 p < 0.05

As discussed above, these predictor variables are more or less strongly correlated, both with each other and with other potential predictors (Table 4). Furthermore, multiple linear regression models comprising linear additive terms (e.g. for SOC and K_f) cannot reproduce observed non–monotonic relationships between degradation rate coefficients and either sorption constants or soil organic carbon content (see Figure 2B). It may therefore be more fruitful to develop models based on a mechanistic understanding of the processes controlling degradation. For microbial degradation, Allen and Walker (1987) suggested that degradation rates should be controlled by some measure of microbial activity multiplied by a factor related to the bio–availability of the compound. We can write:

[8]

$$k = k_{ref} \cdot (B)^m \cdot (A)^n$$

where *k* is the degradation rate constant, k_{ref} is a pesticide–specific reference rate coefficient which, in addition to the influence of variables not included in the model, should be related to the inherent degradability of the compound as determined by its molecular structure, *m* and *n* are constants, *A* is some measure of microbial activity and B is some measure of bioavailability. We tested six different forms of Eq. 8, combining three potential descriptors of microbial activity (laccase activity, SIR, and SOC) with two for bioavailability, K_f or the calculated fraction of pesticide in soil solution, Fs, given by:

[9]

$$F_s = \frac{m_g}{m_g + K_f c_e^{n-1}}$$

where m_g is the gravimetric water content at pF 2 and c_e is the equilibrium concentration of the pesticide in solution at the start of the incubation experiment, which was iteratively calculated from the applied amount, the gravimetric moisture content and the parameters of the Freundlich equation. Although pH could also have been considered, we chose SOC as a surrogate variable for microbial activity, since it was strongly correlated to the microbial parameters MnP, SIR and r.

The data for all three pesticides were fitted to the logarithmic form of Eq. (8). The parameter values were estimated by introducing three 'class' variables into the data set (B, G, and I for bentazone, glyphosate and isoproturon, respectively, which take values of either 1 or zero) and k_{ref} values were obtained as regression coefficients for G, I and B. Table 6 shows that several of the models fitted the data well, especially models 1, 3 and 5, which had R^2 values ranging from 39 to 50 % and regression co–efficients that were all significant ($p<0.1$). As an example, Figure 3 shows a comparison of measured k with predictions using model 1 (i.e. Eq. (8) based on K_f and SIR). In contrast, model 6 (using Fs with SOC as a surrogate measure of microbial activity) gave the poorest results, with no significant effect of SOC and clear bias in the residuals (not shown). However, after excluding glyphosate from the model, the overall regression became highly significant ($p<0.0001$) and the distribution of residuals was unbiased. It is interesting that bioavailability, as reflected in the parameter F_s, emerges here as a

significant factor controlling degradation rates of bentazone and isoproturon, something which was not readily apparent from the classical correlation and regression analysis. Furthermore, although K_f is a very good predictor of glyphosate degradation (Figure 1), F_s is not. The reason for this is not clear.

Figure 3. Comparison of measured degradation rate constants with those predicted using model 1 (see Table 6).

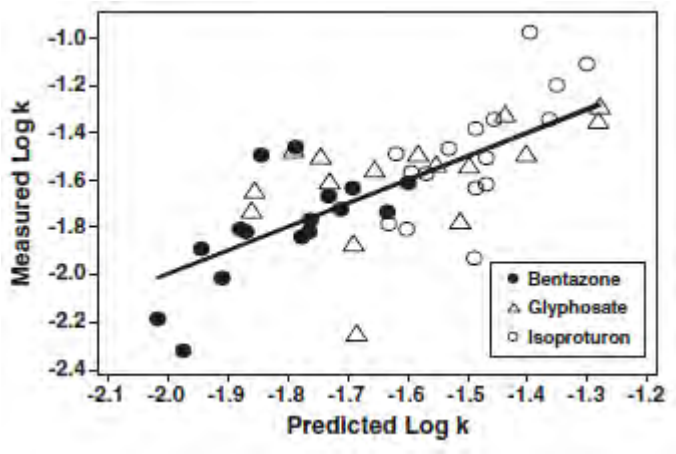

No single model of pesticide degradation can be generally valid (Kah et al., 2007) as the mode of degradation varies considerably between compounds (e.g. chemical hydrolysis, co–metabolic or metabolic microbial degradation). However, although further testing is required, these results suggest that at least for some particular classes of pesticides, a multiplicative model based on soil organic carbon content and the sorption co–efficient (e.g. models 3 and 6, Table 6) may be an effective and practical way to account for the effects of microbial activity and bio-availability on pesticide degradation in the context of modeling applications at catchment or regional scales.

Table 6. Parameter values and their significance for different models developed to predict degradation rate for all three pesticides together.

With K_f in the models					With F_s in models				
Model	Parameters	Values	P value	Centered R^2	Model	Parameters	Values	P value	Centered R^2
1	Log ($k_{ref\,(B)}$)	−2.274	<.0001	0.50	4	Log ($k_{ref\,(B)}$)	−1.797	<.0001	0.42
	Log ($k_{ref\,(G)}$)	−0.893	0.0006			Log ($k_{ref\,(G)}$)	−0.659	0.1515	
	Log ($k_{ref\,(I)}$)	−1.472	<.0001			Log ($k_{ref\,(I)}$)	−1.182	<.0001	
	Log K_f	−0.500	0.0005			Log F_s	0.433	0.0179	
	Log SIR	0.366	0.0006			Log SIR	0.176	0.1134	
2	Log ($k_{ref\,(B)}$)	−2.825	<.0001	0.45	5	Log ($k_{ref\,(B)}$)	−2.586	<.0001	0.49
	Log ($k_{ref\,(G)}$)	−2.106	<.0001			Log ($k_{ref\,(G)}$)	−1.510	0.0076	
	Log ($k_{ref\,(I)}$)	−2.296	<.0001			Log ($k_{ref\,(I)}$)	−1.991	<.0001	
	Log K_f	−0.218	0.1408			Log F_s	0.404	0.0149	
	Log Laccase	0.353	0.0057			Log Laccase	0.344	0.0038	
3	Log ($k_{ref\,(B)}$)	−2.166	<.0001	0.39	6	Log ($k_{ref\,(B)}$)	−1.659	<.0001	0.38
	Log ($k_{ref\,(G)}$)	−0.715	0.0179			Log ($k_{ref\,(G)}$)	−0.295	0.4889	
	Log ($k_{ref\,(I)}$)	−1.336	<.0001			Log ($k_{ref\,(I)}$)	−0.972	<.0001	
	Log K_f	−0.530	0.0029			Log F_s	0.538	0.0030	
	Log SOC	0.242	0.0773			Log SOC	−0.029	0.8036	

3. Assessment and conclusion

<u>Assessment and conclusion by applicant</u>:

The study describes degradation and sorption experiments with glyphosate among other substances on several Swedish agricultural soils. The analytical methods used in both experiments are not explained in detail, no LoD or LoQ are provided. For the sorption experiment, no results are provided. No mass balances and measurement per sample date are provided for both experiments.

The study is therefore classified as reliable with restrictions (Category 2).

1. Information on the study

Data point:	KCA 7.1.4.1.1
Report author	Gjettermann, B. et al.
Report year	2011
Report title	Kinetics of Glyphosate Desorption from Mobilized Soil Particles
Document No	Soil Science Society of America journal (2011), Vol 75, No 2, pp. 434–443
Guidelines followed in study	None
Deviations from current test guideline	No
GLP/Officially recognised testing facilities	No, not conducted under GLP/Officially recognised testing facilities
Acceptability/Reliability:	Reliable with restrictions (Study not sufficiently described to check validity of results)

2. Full summary of the study according to OECD format

Desorption kinetics of chemical compounds can be important both for their mobility in soil and for the significance of particle–facilitated transport. We studied desorption of glyphosate [N–(phosphonomethyl) glycine] on mobilized particles from two soil columns (50–cm height, 30–cm diameter), i.e., particles leached by free drainage from the bottom and particles mobilized by splash erosion and collected next to the top of the column. Leaching and splash erosion were driven by three, 30–mm irrigation events following surface application of ^{14}C–labeled glyphosate. Fresh leachate samples were investigated within 30 min of sampling, and desorption from splash–eroded particles in suspension (100 mg solid/L) was followed for 48 h (starting 2.0 min after immersion). Glyphosate concentrations were determined by measuring the ^{14}C activity using liquid scintillation counting. Similar fractional amounts of glyphosate (on average, 10–20 % in 20 min) desorbed from leached and from splash–eroded particles (>20 nm) shortly after leaching or immersion, respectively, indicating that the processes of desorption from the different sources of particles were similar. In leachate, about 45 to 79 % remained particle bound after 20 min, while calculated values at equilibrium were 20 % or less. Equilibrium was established after about 5 to 10 h in suspensions with splash–eroded particles, except for one sample. These direct observations, supported by estimated values of the Damköhler number, lead to the conclusion that desorption kinetics are important for evaluating the significance of dissolved and particle–facilitated transport of glyphosate. To quantify particle–facilitated glyphosate transport, the water and solid phases in the leachate should consequently be separated within a few minutes after leaching.

Materials and methods

Experimental Setup

The investigated sandy loam soil and parts of the experimental setup have previously been described in detail by Gjettermann et al. (2009), who focused on the influence of soil structure on particle–facilitated pesticide leaching. Two undisturbed cylindrical soil columns (B1 and B2) were carefully excavated from a recently tilled (plowed and drilled) experimental plot, encapsulated with polyurethane foam, and trimmed at the bottom end (50–cm cylinder length, 30–cm diameter). As reference, two columns (A1 and A2) were excavated from an untilled plot. The coding of the columns used in the glyphosate experiments by Gjettermann et al. (2009) has been kept to facilitate comparison. Particular care was observed not to disturb the surfaces of the columns or to block large macropores while trimming the bottom ends. The investigated sandy loam soil (an Agrudalf) is located at the University of Copenhagen research farm Roerrendegaard at Taastrup, Denmark, and has previously been described by Petersen et al. (2001). The contents of coarse sand (200–2000 μm), fine sand (20–200 μm), silt (2–20 μm), clay (<2 μm), and organic C in the upper 30 cm were 29, 40, 18.5, 12.5, and 1.2 %, respectively. A schematic presentation of the experimental setup is given in Figure 1. All irrigation water applied to the columns (influent) had a composition similar to rainwater (Miljøstyrelsen, 1996) containing 0.017 mmol/L

$CaCO_3$, 0.018 mmol/L KNO_3, 0.021 mmol/L $MgSO_4$, 0.126 mmol/L NaCl, and 0.94 mmol/L NH_4Cl. The pH was 6.32 and the electrical conductivity was 0.047 mS cm^{-1}. Water was applied to the column with a pump (FMI Pump QG 150, Fluid Metering Inc., Syosset, NY) through a motor–driven, slowly rotating sprinkling device with 90 syringe needles (Trumo, 25G), to ensure a uniform application rate of 15.0 mm/h (1.06 L/h). The sprinkling device was placed 54 cm above the surface of the column. The drop size was determined at the used intensity by sampling and weighing about 20 drops (10 repetitions). The mass of a drop was 6.4 ± 0.5 mg, corresponding to a (spherical) drop diameter of 2.3 ± 0.9 mm.

Figure 1. Schematic illustration of the experimental setup for the leaching experiments and for the collection of splash–eroded soil particles.

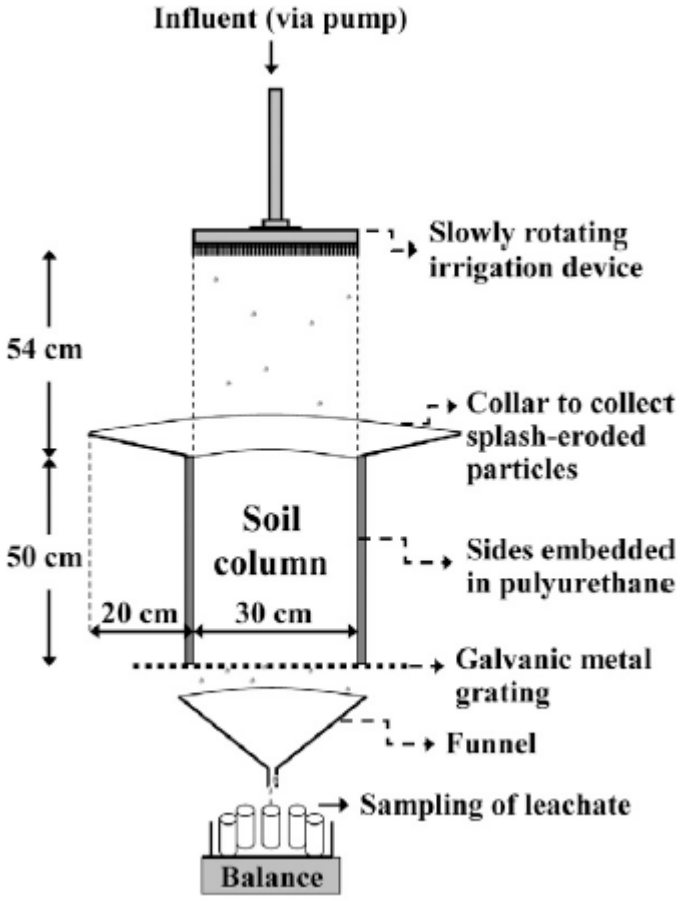

The columns were rewetted at the start of the experiment by irrigation, which was stopped 35 min after the first appearance of leachate. One day later, ^{14}C–labeled glyphosate mixed with the commercial glyphosate product Roundup Bio (Monsanto Europe, Antwerp, Belgium) was applied uniformly to the surface. The glyphosate stock solution had a specific concentration activity of 0.80 MBq/mg and contained 4.4 % ^{14}C–labeled glyphosate, 93.5 % unlabeled glyphosate, and 2.1 % aminomethylphosphonic acid (AMPA). The applied dose of glyphosate (12.5 mg/column) was comparable to current agricultural practice. A total of 13 mL of solution (stock solution and rinse water) was applied during the glyphosate application.

Three irrigations were applied to the soil columns 5, 8, and 12 d after rewetting, respectively. Each event lasted 2.0 h and had a constant intensity of 15.0 mm/h. Water drained freely from the column during and after each irrigation event. The mass of drainage water (leachate) was measured continuously. The leachate was sampled continuously, yielding a total of 21 samples, each containing 30 to 50 mL of leachate. The top ends of the columns were covered with plastic whenever possible to minimize evaporation.

A new plastic collar was mounted around the tops of the columns before each irrigation event to collect water splashes and soil particles (splash–eroded particles) that were eroded by drops and thrown over the sides (height up to 1 cm above the soil surface) with the droplets. All of these water droplets were collected on the collar. The water droplets generally evaporated within a few hours. The particles left were scraped off the collar 24 h after the irrigation event, allowed to air dry, and sieved through a 100-μm sieve. The mass of air–dry particles <100 μm was determined. This material was used for the desorption experiments.

Measurements

The ^{14}C activity of unfiltered and filtered leachate samples was measured with a Wallac 1414 (Perkin Elmer Corp., Waltham, MA) liquid scintillation counter (LSC) using 10 mL of scintillation cocktail (InstaGel, PerkinElmer) to a 9–mL sample. Using ^{14}C–labeled pesticides has the consequence that also metabolites, for example the major metabolite of ^{14}C–glyphosate (^{14}C–AMPA) were measured by LSC. The detection limit of the ^{14}C LSC analysis was 16.4 disintegrations min^{-1} (0.038 μg ^{14}C–glyphosate/L) and the method had trueness for quantification on ^{14}C standard buttons (PerkinElmer) of 100.2 ± 0.8 %. The effect of quenching was automatically adjusted by the LSC, and increasing quench induced by increasing particle concentration was accurately measured. Gjettermann et al. (2009) found good agreement between these determinations and direct chemical measurements of glyphosate plus AMPA, and they showed that AMPA constituted only a minor part (up to 17.5 %) in leachate samples from the investigated columns.

Particle concentration in the leachate was determined indirectly from the measured turbidity. Turbidity was measured with a turbidity meter (Tintometer GmbH, Dortmund, Germany). Samples were shaken and immediately transferred to glass vials. Turbidity was then measured after exactly 60 s. With the chosen procedure, isolated soil particles were <30 to 50 μm (equivalent spherical diameter), assuming a particle density of 1600 to 2650 kg/m^3. The mass of particles was estimated in 70 randomly selected leachate samples of known volume to establish a relationship between turbidity and concentration of particles. The samples were centrifuged (30 min at 4100 × *g*) and washed twice with deionized water. Finally, the particles were dried at 105°C before determining the mass. The correlation between turbidity *T* (in nephelometric turbidity units [NTU]) and the concentration of soil particles in the leachate was used to calculate the concentration of particles: concentration of particles (mg/L) = 110 ln(*T*) − 241 (R^2 = 0.74, 70 samples). For turbidity <20 NTU, equivalent to particle concentrations of less than approximately 88 mg/L, the relationship was poor and this limit was therefore used as the detection limit.

Desorption was investigated in five leachate samples from each of the tilled soil columns (Samples 2, 8, and 14 from the first irrigation event and Sample 21 from the other two events; see Table 1). The samples were selected to illustrate the development in glyphosate levels during the three irrigation events. Only one leachate sample (Sample 2, first irrigation) from each of the untilled columns was investigated, the amount of sediment being too small (considerably below the detection limit) and the uncertainty of the determination on individual samples too high during the later phases of the drainage events (Gjettermann et al., 2009). Approximately 40 mL of leachate sample was collected and a stopwatch was activated. A 10–mL sample was immediately filtered (0.02–μm inorganic, anopore filter, Frisenette, Knebel, Denmark) into a clean glass and the time (about 1.5 min) was recorded. Nine milliliters of the filtrate was later extracted for ^{14}C–activity measurement. After 5 min, another 10 mL of leachate was extracted and filtered for activity measurement. This was repeated after another 5 to 10 min and, if the amount of the original sample allowed it, after approximately 30 min. The so–called reaction time associated with each filtration, t_r, was assigned as the time span from the midpoint [$(t_{beg} + t_{end})/2$] of the sampling interval to when filtration had just been performed.

The concentrations of soil particles in the leachate used for the desorption experiments were not measured but estimated as the average of measured concentrations in the directly preceding and succeeding samples (first irrigation) or as the concentration measured in the directly preceding sample (second and third irrigations). The sample size did not allow combined determination of both particle concentration and desorption, and larger samples would have compromised the need for fast separation of colloids from the water phase. The uncertainty associated with this procedure was estimated from concentration difference between consecutive samples measured by Gjettermann et al. (2009), the

absolute average concentration difference being assigned as *D*.

Detectable splash erosion occurred from both of the tilled columns (B) in all events, but not from the untilled columns (A). Sieved and air–dried, splash–eroded particles generated during each irrigation event from the tilled columns were immersed (at time zero) in stirred artificial rainwater (irrigation water) yielding a suspended particle concentration of $C_{particle}$ = 100 mg/L. Samples of 10 mL were extracted and filtered, and the ^{14}C activity of the filtered samples was determined five or six times, typically 2.0, 10.0, 60, 120, 1440, and 2880 min after immersion (equivalent to t_r) as described above for the leachate.

Table 1 summarizes all analytical results available on the leachates.

Table 1. Overview of analyses conducted on leachate samples from each of the three irrigation events.

Sample no.	First irrigation	Second and third irrigation
1	pesticide (colloidal and soluble fractions), ph, conductivity and turbidity	
2	sorption and desorption kinetics of pesticide	total concentration of pesticide, colloidal and soluble organic c, ph, conductivity and turbidity.
3–7	pesticide (colloidal and soluble fractions), ph, conductivity and turbidity	
8	sorption and desorption kinetics of pesticide	total concentration of pesticide, colloidal and soluble organic c, ph, conductivity and turbidity.
9–13	pesticide (colloidal and soluble fractions), ph, conductivity and turbidity	
14	sorption and desorption kinetics of pesticide	total concentration of pesticide, colloidal and soluble organic c, ph, conductivity and turbidity.
15–20	pesticide (colloidal and soluble fractions), ph, conductivity and turbidity	
21		sorption and desorption kinetics of pesticide

Data Analyses

The specific activity of the applied glyphosate stock solution was checked by LSC analysis at each application time. The measured specific activity was used to convert the measured ^{14}C activity into glyphosate concentration units. The concentration of particle–bound glyphosate (C_p) in the leachate was defined as the difference between the measured concentration in the suspension (total concentration, Cs) and the measured concentration in the filtrate (dissolved glyphosate, Cd). The particle–bound fraction of leached glyphosate was calculated as C_p/C_s. Rates of change of the particle–bound fraction were estimated by least squares linear regression, i.e., from fitting experimental data to the simple approach presented by

[1]

$$\frac{100C_p}{C_s} = -\alpha t_r + \beta$$

where the rate α (% min^{-1}) and β (%) are constants (positive α values indicate desorption) and t_r is the time of reaction (min).

Equation [1] was also fitted to the first data points from experiments with splash–eroded particles in an attempt to obtain similar time scales of desorption from the different sampling types of particles (leached and splash eroded). In this analysis, C_s was obtained as the sum of particle–bound and dissolved concentrations at equilibrium ($C_{p,eq}$ and $C_{d,eq}$, respectively), and C_p was calculated as the difference between C_s and C_d.

At long experimental periods ($0 < t_r \leq 48$ h), however, the desorption from splash–eroded particles was not linear and the points were therefore also described according to

[2]

$$\frac{dC_d}{dt} = -k\left(C_d - C_{d,eq}\right)$$

where C_d (µg/L) is the dissolved concentration (<20 nm), t is the time (h), $C_{d,eq}$ (µg/L) is the "equilibrium" dissolved concentration, and k is a rate constant (h^{-1}). This approach has been termed a linear driving force approximation (LeVan et al., 1997) or a first–order mass transfer model (Lick et al., 1997). Assuming that C_d at time t = 0 h when the particles were suspended [$C_d(0)$] = 0, Eq. [2] can be integrated into

[3]
$$C_d = C_{d,eq}\left[1 - \exp\left(-kt_r\right)\right]$$

where t_r is the time of reaction. The Solver function in Excel (Wraith and Or, 1998) was used to adjust the model parameters $C_{d,eq}$ and k by minimizing the difference between predicted and measured C_d values (maximizing R^2). Because the chemical or physical processes involved in the desorption are expected to be similar in the two data sets, the choice of a linear vs. an exponential model is based solely on the number of data points available and the time scale used to observe the different particles.

For the splash–eroded particles, the total content of glyphosate in the sample was not measured (the results had to be discarded due to an error in the laboratory). It therefore had to be estimated. Gjettermann et al. (2009) reported a K_d value of 503 L/kg for the bulk topsoil (and 496 L/kg for AMPA). It has previously been shown that particles larger than about 0.1 mm are not present in drainage from the investigated field site (Holm et al., 2003), indicating that coarse sand and parts of the fi ne sand fraction either are not mobile or are immobilized on the way through the soil column. For this soil, it may generally be expected that the Fe and Al oxides that sorb glyphosate is mainly present in the fraction <20 µm. Hence, K_d for the investigated leached particles will be larger than that for the bulk soil. Based on the texture of the topsoil, 40 % of the constituents were >0.100 mm. Hence, an estimate of K_d was obtained as 503 L/kg / 0.60 = 8.4 × 102 L/kg. This is a conservative estimate because it assumes no sorting of particles below the 0.1–mm limit within the soil columns. Estimates of the concentration of particle–bound glyphosate at equilibrium, $C_{p,eq}$ (µg/L) were obtained from the fitted $C_{d,eq}$, the soil/water ratio (particle concentration $C_{particle}$, kg/L), and K_d as $C_{p,eq} = C_{particle}K_dC_{d,eq}$. Hence, in the absence of direct measurements, the total glyphosate concentration was calculated as

[4]
$$\begin{aligned} C_s &= C_{d,eq} + C_{p,eq} \\ &= C_{d,eq}\left(1 + C_{particle}K_d\right) \end{aligned}$$

The Damköhler number, D_a, is a measure of the relative importance of kinetics to equilibrium processes in transport (Bold et al., 2003). The D_a is defined as the ratio between the transport and the reaction time scales, and can be calculated as

[5]
$$D_a = \frac{k}{\left(U/L\right)}$$

where L (cm) is the transport distance (e.g., length of column, cm) and U (cm/h) is the water velocity in the soil.

Results and Discussion

Desorption in Leachate from Tilled Soil

Measured dissolved glyphosate concentrations in the leachate from the tilled soil generally increased with time (Figure 2), and the particle–bound fraction decreased (Figure 3). Thus, one immediate finding of the experiment is that considerable amounts of glyphosate desorbed from leached soil particles

(>20 nm) during the investigated period (about 20 min). Desorption was particularly large for the first irrigation on Column B1 (Figure 2), probably reflecting leaching of highly pesticide–enriched particles. Thus, the initially (about 1.5 min after sampling) measured concentration of glyphosate on particles was 19 to 24 mg/kg for this irrigation event, while it was between 7.7 and 3.5 mg/kg for the other irrigations on Column B1 and all irrigations on Column B2. The data do not indicate that concentrations of dissolved glyphosate reached stable levels.

The concentration of leached particles, $C_{particle}$ (Table 2), could be a critical factor for the α values describing glyphosate desorption. Higher concentrations of particles should result in lower desorption rates due to a higher final equilibrium value (c.f. Eq. [4]). The particle concentrations showed little variation from sample to sample within events (Table 2, D ≤24 mg/L), although it often varied significantly from the beginning to the end of an irrigation event (Gjettermann et al., 2009). Thus, the uncertainty associated with the estimated $C_{particle}$ values in Table 2 is probably on the order of 24 mg/L or less. The concentrations ranged between 123 and 292 mg/L and were higher for Column B1 than for Column B2. The expected dissolved mass fraction at equilibrium, $C_{d,eq}/C_s$ can be estimated by rearranging Eq. [4] and inserting the measured particle concentrations from Table 2. According to this calculation, the mass of sorbed glyphosate at equilibrium in the leached samples will account for 20 % or less of the mass in solution. Hence, with the investigated range of particle concentrations and the high initial fractions of particle–bound glyphosate (Figure 3), the samples are far from equilibrium and particle concentrations should not be important for the relative amount of desorbed pesticide or the desorption rates.

Figure 2. Concentration of dissolved glyphosate (C_d) in leachates from two soil columns, B1 (left) and B2 (right), at different reaction times (t_r, 0–30 min): (a) and (b) data for the first irrigation event (Samples 2, 8, and 14); (c) and (d) data for the second and third irrigation events (Sample 21).

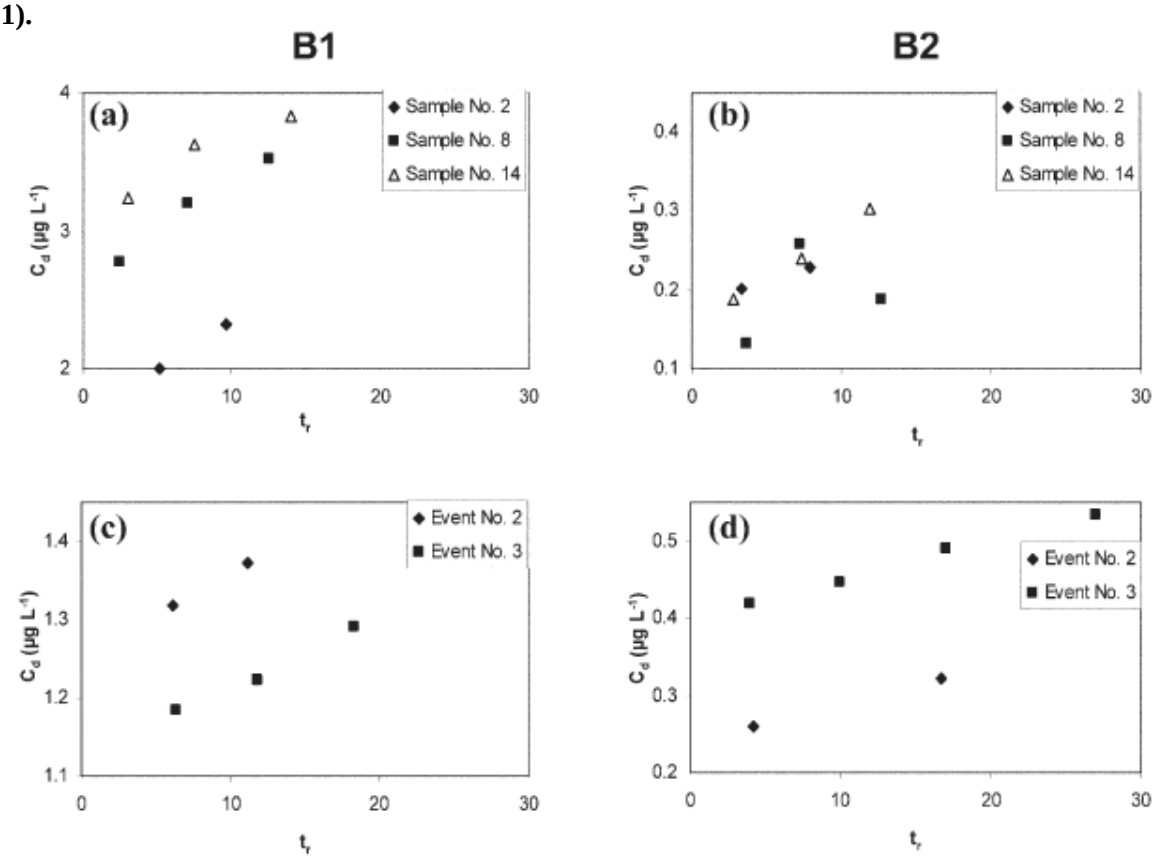

Table 2. Relative desorption rate (α), intercept parameter (β), concentration of soil particles ($C_{particle}$) in the investigated leachate, and average absolute particle concentration difference between consecutive samples (D) derived from experiments on leachates; α, β, and coefficient of determination (R^2) obtained by fitting data from different soil columns (B1, B2, A1, and A2), irrigation events (1–3), and samples (2, 8, 14, and 21) to Eq. [1].

Column	Irrigation no.	Sample no.	α	β	R^2†	$C_{particle}$	D
			% min^{-1}	%		— mg L^{-1} —	
B1	1	2	0.94	78		292	
	1	8	0.80	72	0.98	276	9 (6)‡
	1	14	0.56	67	0.92	268	
	2	21	0.41	53		212	13 (19)
	3	21	0.33	58	0.99	263	6 (5)
B2	1	2	0.48	85		199	
	1	8	0.39	87	0.11	134	24 (20)
	1	14	0.98	89	1.00	151	
	2	21	0.69	67		123	14 (13)
	3	21	0.51	60	0.99	166	11 (13)
A1	1	2	0.37	21		264	23(21)
A2	1	2	−1.03	8	1.00	190	21(26)

† Not applicable when the number of samples was <3.
‡ Standard deviation in brackets ($14 < n < 21$).

In general, Eq. [1] fitted well to the measured fractions of particle–bound glyphosate (Figure 3). The coefficients of determination were high ($R^2 \geq 0.92$), except for Sample 8 from the first irrigation on Column B2 (Table 2). By using this equation with the parameter values from Table 2, it was estimated that 7 to 20 % (on average, 12 %) of the leached glyphosate was desorbed from soil particles (>20 nm) within the first 20 min after sampling, corresponding approximately to the time scale of the observations. The reaction time (t_r) associated with the first filtration varied somewhat between events due to differing lengths of the sampling intervals. The 20–min relative desorption may be overestimated if the last measureements were close to the equilibrium concentrations (which was probably not the case according to the above calculations), and it may be underestimated if desorption took place much faster before the first filtrations (1.5 min after sampling).

The reaction time, defined as the time from the midpoint of the sampling interval, can be considered as an estimate of the time span after leaching. Hence, an estimate of the particle–bound fraction of glyphosate at a given time after leaching can be obtained from Eq. [1] by using parameters from Table 2. The data indicate that 45 to 79 % of the leached glyphosate was still particle bound 20 min after leaching (Figure 3). Thus, the rates of desorption measured shortly after sampling could not fully account for the amounts of glyphosate being desorbed 20 min after leaching.

The particle–bound fraction measure in leachate from the tilled soil 1.5 min after sampling varied between 51 and 89 % (Figure 3). This is in accordance with results reported by Gjettermann et al. (2009). It is probable that such figures depend considerably on the conditions that eventually lead to bypass flow and leaching. The applied methods were chosen to minimize desorption in the leachate before sampling and phase separation.

Figure 3. Particle (>20–nm) bound fraction of glyphosate in leachates from two soil columns, B1 (left) and B2 (right), at different reaction times (t_r, 0–30 min): (a) and (b) data for the first irrigation event (Samples 2, 8, and 14); (c) and (d) data for the second and third irrigation events (Sample 21).

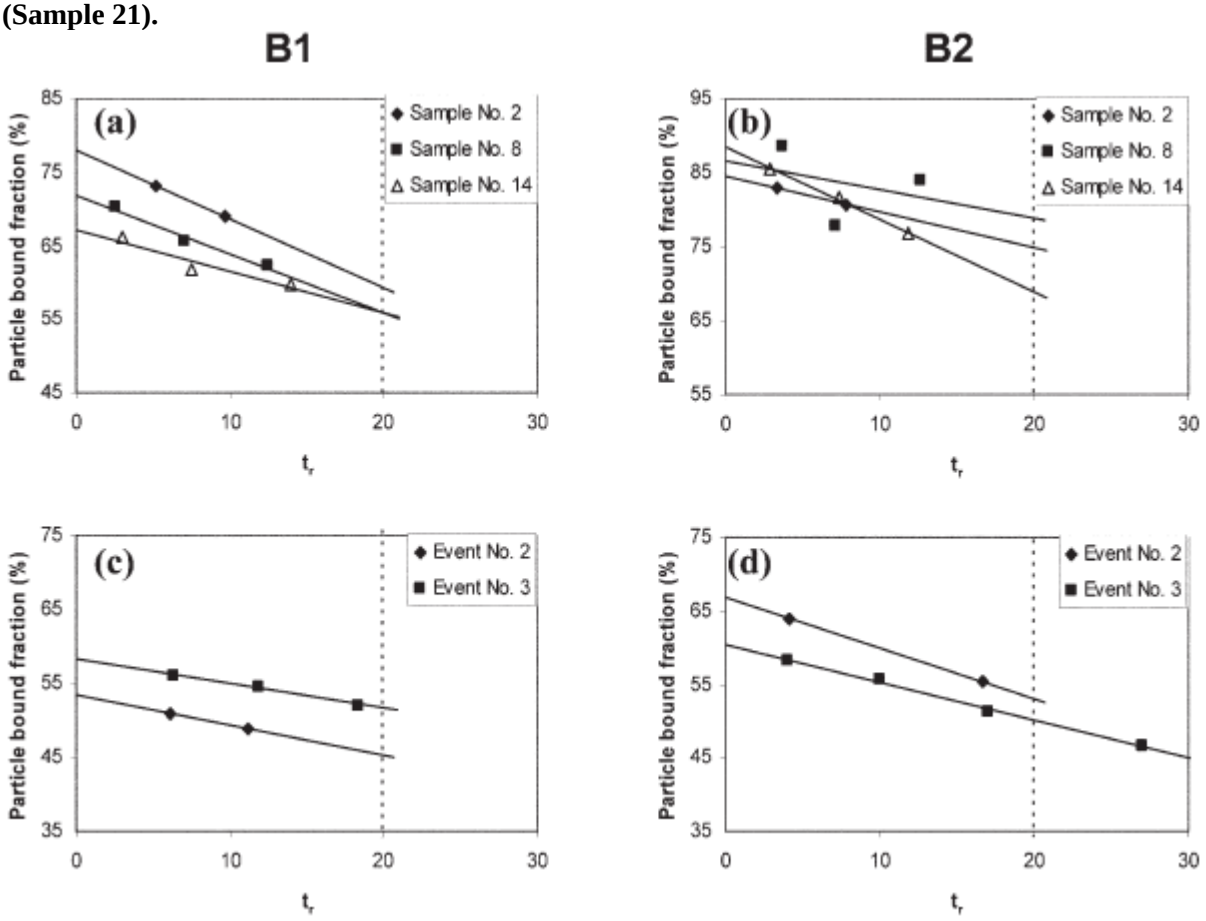

The particle–bound fractions of glyphosate measured in the leachate from the two untilled soil columns (A1 and A2) 1.5 min after sampling were 19 and 14 %, respectively. This conforms to previously reported results that the fraction of particle–bound glyphosate in recently produced leachate can be much smalller with a minimally disturbed soil structure than with a tilled structure (Gjettermann et al., 2009). The particle–bound fraction decreased with time after sampling in the A1 sample, indicating desorption, whereas it increased in the A2 sample, indicating sorption (Table 2). By inserting the estimated K_d (= 8.4×10^2 L/kg) in Eq. [4], the fractions of particle–bound glyphosate at equilibrium were estimated to be 18 and 14 % for the A1 and A2 samples, respectively. Hence, leached glyphosate from the untilled soil columns appears to have been close to equilibrium, which is probably why both sorption and desorption may have occurred, as indicated by the measurements.

The individual desorption rates are relatively uncertain, being based on only two to four measured particle–bound fractions (Figure 3). More observations could have been obtained, but only if the sample sizes had been increased correspondingly. This would have increased the time of reaction and hence desorption taking place before the measurements. The trends observed are similar for all samples, however, corroborating the conclusion that the particle–bound glyphosate in the solution leaching from the tilled columns was not in equilibrium with the surrounding water phase.

Desorption from Splash–Eroded Particles

Noticeable splash erosion occurred during all irrigation events involving the tilled columns. The amounts of (air–dry) splash–eroded particles varied between 31 and 70 mg per event independent of irrigation number and column. All fine–earth particle sizes were present, in accordance with earlier findings that eroded material is typically unsorted (Heilig et al., 2001; Hairsine and Rose, 1991; Al–Durrah and Bradford, 1982). Larger particles were removed by using the 100–µm sieve in consequence

of the earlier reported finding that particles smaller than about 0.1 mm are not present in drainage water from the investigated field site (Holm et al., 2003). The fine particles released considerable amounts of glyphosate after being suspended. Hence, dissolved glyphosate concentrations increased with time, with gradually decreasing rates (Figure 4a and 4b). The rates were still relatively high after 1 h. After a few hours, concentrations were high compared with concentrations measured in most leachates (Figure 2), except from the first irrigation on Column B1. An equilibrium concentration of dissolved glyphosate appeared to be reached after about 5 to 10 h, except for the first irrigation event on Column B2; equilibrium was not attained within 48 h in this case. Glyphosate desorption decreased successively with irrigation event number.

Equation [3] fitted well to the measured dissolved concentration as a function of time (0–48 h) (Figure 4a and 4b; Table 3). Coefficients of determination, R^2, varied between 0.87 and 0.98. The rate constant of desorption, k, was found to be in the range 0.57 to 1.19 h^{-1}, largest for the first irrigation event on Column B1. The equilibrium concentration, $C_{d,eq}$, was in the range 1.56 to 4.1 µg/L, decreasing successively with each additional irrigation event.

Table 3. Parameters and key data derived from experiments on splash-eroded particles. Rate constants (k), dissolved concentrations at equilibrium ($C_{d,eq}$), and coefficient of determination (R^2) obtained by fitting Eq. [3] to all data (reaction time t_r 0–48 h) from the two columns (B1 and B2) and three irrigation events. Relative desorption rate (α), intercept parameter (β), and R^2 obtained by fitting Eq. [1] to data for relatively short time scales: results based on the first three data points (t_r = 2, 10, and 60 min) and desorption rate based on the first two data points (t_r = 2 and 10 min).

Column	Irrigation no.	From Eq. [3], 0–48 h			From Eq. [1]			
					2–60 min			2–10 min
		k	$C_{d,eq}$	R^2	α	β	R^2	α
		h^{-1}	µg L^{-1}		% min^{-1}	%		% min^{-1}
B1	1	1.19	4.0	0.98	0.56	71	0.94	1.62
	2	0.75	2.19	0.91	0.54	79	0.98	1.09
	3	0.59	1.83	0.94	0.48	82	0.98	1.06
B2	1	0.57	4.1	0.92	0.41	81	0.99	0.79
	2	0.58	2.59	0.95	0.55	87	1.00	0.40
	3	0.99	1.56	0.87	0.50	73	0.98	1.10

The equilibrium concentrations, $C_{d,eq}$, the previously estimated K_d = 8.4 × 102 L/kg, and the constant particle concentration $C_{particle}$ = 100 × 10^{-6} kg/L were used when calculating total concentrations (Eq. [4]), particle–bound fractions, and relative desorption rates (Eq. [1]). Accordingly, the fitted dissolved concentrations at equilibrium (Table 3) represent about 92 % of the total concentrations. The linear relationship Eq. [1] fitted well to the three data points representing the particle-bound fraction vs. time (2 to 60 min) after dissolving the splash–eroded particles, R^2 being in the range 0.94 to 1.00 (Figure 4c and 4d; Table 3). The relative desorption rates (α) were estimated to be in the range 0.41 to 0.56 % min^{-1} (average 0.51 % min^{-1}), with no systematic dependence on irrigation event or column (Table 3). Hence, at these rates, 8 to 11 % (average 10 %) would be desorbed during a 20–min time period. The rates tended to be slightly smaller than desorption rates measured in the leachate at a similar or somewhat shorter time scale (α for Columns B1 and B2 in Table 2, average value 0.61 % min^{-1}). For the period 2 to 10 min, the measured relative desorption rates were in the range 0.40 to 1.62 % min^{-1} (Table 3; average value 1.01 % min^{-1}), i.e., generally somewhat larger than for the period 2 to 60 min. This was expected also from the good fit of all the data to Eq. [3]. The rates obtained for the 2– to 10–min period were of the same order of magnitude, although generally larger than desorption rates measured in the leachate at a similar or somewhat longer time scale (α for Columns B1 and B2 in Table 2). Calculated from rates obtained for the 2– to 10–min period, 8 to 32 % (average 20 %) would desorb in 20 min right after the first fractionation. Overall, similar desorption rates were found for leached and splash–eroded particles when determined at similar time scales. This indicates that similar desorption processes were involved for the two types of particles.

The initial glyphosate concentrations (mg/kg) were somewhat higher on splash–eroded particles than on leached particles. For the first measurements on leached particles made 1.5 min after sampling, the range of concentrations was 4 to 24 mg/kg; for measurements on splash–eroded particles made 2.0 min after immersion, the range of estimated concentrations was 13 to 36 mg/kg. The concentrations decreased systematically with succeeding irrigation event for both types of particles. The splash–eroded particles may have been enriched with glyphosate when the water droplets evaporated on the collar after irrigation; however, concentrations on splash–eroded particles from the first irrigations (about 44 mg/kg according to Table 3 and Eq. [4]) were within a realistic range for the uppermost soil layer shortly after spraying. Thus, by assuming that the applied glyphosate was distributed in the uppermost 2– to 5–mm soil layer having a bulk density of 1.6 g/cm^3, an expected average glyphosate concentration of 55 to 22 mg/kg can be calculated for the layer.

The splash–eroded particles were air dry, and the particle–bound fraction of the glyphosate must therefore have been close to 100 % right before the particles were immersed in water (at $t_r = 0$). At t_r = 2.00 min, however, the particle–bound fraction had already decreased to between 74 and 85 % (Figure 4c and 4d). It is difficult to model this very rapid decrease as a function of time when seen at the shorter time scales. It indicates that a fraction (up to 26 %) of the glyphosate could have been very weakly bound. Physical effects of the immersion may also have affected the rapid glyphosate release.

From the linear models shown in Figure 4c and 4d, it can be calculated that about 60 to 76 % of the glyphosate was still particle bound 20 min after immersion of the particles in water. The values are of a similar magnitude as the estimated particle–bound fractions in the leachate 20 min after leaching (45–79 %, cf. above). In the study on leachate, it is probable that desorption had taken place in wet fractions of the soil columns before leaching and from leached particles in the leachate before the first fractionation. This may to some extent have reduced the initially measured fraction of particle–bound glyphosate and the measured desorption rates.

Figure 4. Desorption of glyphosate in suspensions containing splash–eroded soil particles from two soil columns, B1 (left) and B2 (right): (a) and (b) concentration of dissolved glyphosate (C_d) monitored at long time scales of reaction ($0 < t_r \leq 48$ h), the curves represent least squares fits of Eq. [3] to data points; (c) and (d) particle–bound fraction monitored at short time scales (2–60 min), the lines represent least squares fits of Eq. [1] to data points.

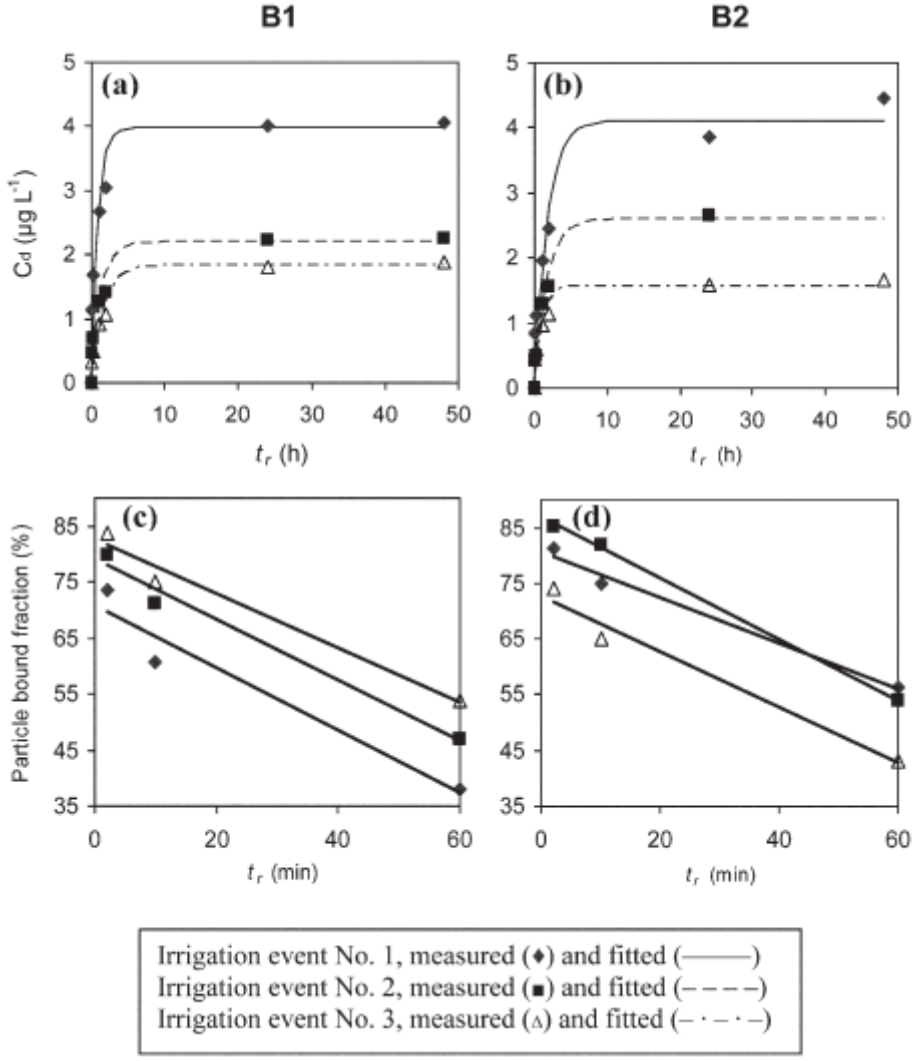

Can Desorption Kinetics be Ignored in Glyphosate Transport?

Bold et al. (2003) investigated the significance of kinetics in contaminant transport using an intraparticle diffusion model to account for the kinetic contaminant–particle interaction. They showed by sensitivity analysis that kinetic limitations of contaminant–particle interactions have to be taken into account for $0.01 < D_a < 100$. They also concluded that for $D_a < 0.01$, desorption of contaminants from particles is so slow that it can be neglected.

A range of possible outcomes of D_a for the present column experiments was estimated based on desorption rate coefficients obtained in the 0– to 48–h experiments on splash–eroded particles (k values in Table 3). The fluid velocity inside the column depends on whether it is moving through macropores or the matrix. Two extreme boundaries could be: (i) transport exclusively through a water–filled continuous macropore from the surface to the bottom of the column, and (ii) transport exclusively thought the soil matrix. For extreme (i), a continuous macropore with a diameter of 0.6 cm (area = 0.28 cm^2), and steady–state condition, the irrigating rate (1060 cm^3/h) would give rise to an average fluid velocity of approximately 3700 cm/h. For extreme (ii), a homogeneous soil matrix (column area = 707 cm^2), steady-state condition, and a water content equal to field capacity (about 30 %), the irrigation would give rise to an average fluid velocity of approximately 5 cm/h. For extreme (i), the D_a would be

in the range of 0.01 to 0.02 (cf. Eq. [4]), depending on the value of *k*. For extreme (ii), the D_a would be in the range of 6 to 12. These intervals, even the one for homogeneous matrix flow, are within the critical range estimated by Bold et al. (2003), indicating that kinetic limitations of glyphosate–particle interactions have to be taken into account in describing the transport. In reality, bypass flow and glyphosate transport below the 25–cm depth took place almost exclusively in earthworm channels in the size range 2 to 8 mm (Gjettermann et al., 2009), indicating conditions much closer to extreme (i) than (ii). Although we realize that the measured rates are not necessarily representative of the conditions throughout the soil columns, the results of this analysis indicate that particle mobilization and particle–facilitated transport could play a critical role in pesticide leaching under such conditions.

The interaction between contaminants and mobile particles has, in many studies, been described as an instantaneous equilibrium process (e.g., Prechtel et al., 2002; Villholth et al., 2000). To our knowledge, no study has described the importance of desorption kinetic behavior of contaminants in structured soil with special attention to facilitated transport. Turner et al. (2006), however, revealed that Cs desorption from illite particles was slower than Sr desorption and demonstrated that this difference in desorption kinetics resulted in greater colloid–facilitated transport of Cs in columns packed with a quartz porous medium. They estimated D_a to be in the range of 0.00035 to 0.086 for Cs and 0.97 to 2.0 for Sr. Van de Weerd and Leijnse (1997) also found that desorption of Am from humic particles was a slow process that could only be described by taking into account a kinetic interaction between Am and humic particles. These findings combined with the current investigations show that it is important to consider desorption kinetics as an integral part of the transport process when considering particle–facilitated transport of glyphosate and other non-instantaneously desorbing contaminants.

Conclusion

Glyphosate desorbed with similar fractional rates from leached and from splash–eroded particles (>20 nm) when investigated at similar relatively short time scales. Thus, 7 to 20 % of the total amount of leached glyphosate (average 12 %) desorbed in 20 min shortly after leaching, while on average between 10 and 20 % desorbed from splash-eroded soil particles in suspension in 20 min shortly after immersion. The similarities support the view that the particles investigated and the processes of desorption were similar for the two types of material. Concentrations of glyphosate on leached particles were always somewhat lower than concentrations on splash–eroded particles.

Equilibrium concentrations were generally obtained within 5 to 10 h in suspensions containing splash–eroded particles. Hence, depending on the time of fractionation of the collected samples (in the interval 0–10 h), very different relative amounts of particle–bound glyphosate may be found; to quantify particle–facilitated glyphosate transport, the water and solid phases should be separated immediately after leaching. Furthermore, an analysis of the Damköhler number indicates that desorption kinetics is important for glyphosate transport and for the significance of particle–facilitated transport.

2. Assessment and conclusion

Assessment and conclusion by applicant:

The study describes a leaching experiment with glyphosate in soil columns. The desorption of glyphosate from soil particles and its effect on interpretation of leaching experiments was in the focus of the study. Not all necessary information was reported to check the validity of the results (no mass balances, study set-up not clearly described, insufficient information on soil properties and soil origin, test item not sufficiently described, Temperature not provided, molecular identity of desorbed radioactivity not determined).

The study is therefore classified as reliable with restrictions (Category 2).

1. Information on the study

Data point:	KCA 7.1.4.1.1
Report author	Gjettermann, B. et al.
Report year	2011
Report title	Evaluation of Sampling Strategies for Pesticides in a Macroporous Sandy Loam Soil
Document No	Soil & sediment contamination (2011), Vol 20, No 5–8, pp. 986–994
Guidelines followed in study	None
Deviations from current test guideline	No
GLP/Officially recognised testing facilities	No, not conducted under GLP/Officially recognised testing facilities
Acceptability/Reliability:	Reliable with restrictions (Not sufficient information available to check validity of the results, scope of the study is not on leaching of glyphosate itself but on evaluating the usage of a dye to improve sampling strategies)

2 Full summary of the study according to OECD format

It is not straightforward to sample and demonstrate the presence and transport of pesticides in heterogeneous soil. Following leaching experiments with four differently structured 50–cm–long soil columns (tilled and untilled soil), the objective of this study was to investigate the extent that visual tracing of the dye Brilliant Blue could support in soil sampling for two strongly sorbing pesticides (^{14}C–labeled glyphosate and pendimethalin). About 830 samples were collected. No pesticide was found below 10–25 cm depth by random sampling, even though 0.21–0.31 % of the applied amounts were leached, and 0.18 % of the soil volume was sampled. With similar sampling efforts, the pesticides could generally be traced throughout the columns by sampling from stained soil volumes, only. None of the two particular sampling strategies for pesticides produced accurate mass balances or balances that were obviously better than the other. No pesticide was detected outside stained soil volumes, except for glyphosate in one sample. Below 30 cm, stained soil comprized on average 5 % of the total soil volume, leaving 95 % as expectedly pesticide–free. The results suggest that much more efficient sampling for sorbing pesticides can be obtained by using the dye and focusing on stained soil volumes.

Materials and methods

Soil Columns

The macroporous Rorrendegaard sandy loam soil investigated in this experiment is developed on till from the Weichselian glaciation. The contents of coarse sand (200–2000 µm), fine sand (20–200 µm), silt (2–20 µm), and clay (<2 µm) in the upper 30 cm is 29 %, 40 %, 18.5 %, and 12.5 %, respectively, and the organic C content is 1.2 %. At 50 cm depth, the number of vertically oriented earthworm channels (diameter: 3–8 mm) is typically in the range 200–600 m^{-2}. The soil has previously been described in detail by Petersen et al. (2001) and Gjettermann et al. (2009).

Undisturbed soil columns (diameter: 30 cm; 0–60 cm soil depth) were sampled in late autumn from two experimental plots with different tillage treatments (A and B). For each of the previous nine years the same cereal crop (wheat or barley) had been grown in the plots. Plot A had not been tilled for one year, and it had not been subjected to deep (>4–6 cm), loosening tillage for eight years. Plot B had been under traditional tillage (including annual ploughing) for at least nine years. It had been ploughed and drilled for wheat one month before sampling, and a new wheat crop had just been established. Treatment A (untilled) gave rise to a relatively stable soil structure with vertically oriented earthworm channels from the partially covered surface (old wheat stubble, weeds, and moss) to the bottom of the columns. Treatment B (tilled) did result in a more variable structure with stubbles being heterogeneously incorporated in the plough layer (0–25 cm). Fewer vertically oriented earthworm channels penetrated all the way to the surface. Columns (two per treatment) were manually excavated and encapsulated with

polyurethane to stabilize and seal the walls. Care was observed not to disturb the surface structure. The columns were trimmed to 50 cm length from the bottom end, avoiding sealing macropores, and placed on a galvanized metal grating. The columns were sealed with plastic foil at the upper end and stored at 2–3°C whenever not used in the experiments.

Leaching Experiments

The leaching experiments have been described in detail by Gjettermann et al. (2009) and were in brief as follows: Columns were rewetted by irrigation one day before pesticide application. Each pesticide was applied uniformly to the surface of one column per treatment. The pesticides were applied in doses similar to the ones used in agriculture, i.e. 12.51 mg glyphosate/column and 14.24 mg pendimethalin/column. Glyphosate was taken from a stock solution made from the commercial product Roundup Bio, ^{14}C–glyphosate, and blank formulation (all from Monsanto). The stock solution had a specific concentration activity of 0.80 MBq/mg. It contained both glyphosate and its major metabolite, AMPA (aminomethylphosphonic acid, CH_6NO_3P) (2.034 g/L in total) distributed on ^{14}C–glyphosate (4.4 %), unlabeled glyphosate (93.5 %), and AMPA (2.1 %). Pendimethalin was taken from another stock solution made from the commercial product Stomp mixed with ^{14}C–pendimethalin (both from BASF). This stock solution had a specific concentration activity of 4.55 MBq/mg. It contained ^{14}C–pendimethalin (4.2 %) and unlabeled pendimethalin (95.8 %).

Leaching was driven by irrigation water having a composition similar to rain water (Gjettermann et al., 2009). The water was applied uniformly at a fixed intensity (15 mm/h) to the top of the columns through a rotating irrigation device. Each column received three 2.0 hours irrigation events 5, 8, and 12 days after rewetting, respectively. Thus 30 mm of irrigation water was applied in each event, corresponding approximately to 7.6 % of the total soil pore volume. A 15 mm/h rain event in 2 h may be considered as an extreme for Danish conditions expected to occur about once every 10 years, even though short–time rain intensities are frequently much higher (Madsen et al., 2009). Water was allowed to drain freely from the bottom of the columns. Pesticide contents in the leachate were determined by measuring the ^{14}C–activity with liquid scintillation counting. Brilliant Blue was applied to the four columns (one per combination of soil treatment and pesticide) after the pesticide–leaching experiments. The dye was applied in aqueous solution (4.0 g/L) as a standard irrigation (i.e. 15 mm/h in two hours) after rewetting.

Sampling

Samples were obtained from 9 or 10 separate column sections prepared 1–2 days after dye application. Initially, the columns were sectioned into 7 or 8 depth intervals (cylindrical slices). All columns were cut at 15, 20, 25, 30, and 40 cm depth using a steel thread or a narrow–bladed saw to minimize smearing. Two more cross-sections were made at depths below 15 cm in three columns, whereas only one cross–section was obtained in one column representing treatment B. All cross–sections were carefully cleaned for traces of soil materials and dye being smeared during the cutting procedure. They were then subjected to intensive diffuse light and photographed using a 3.0 Mpx camera.

Soil sampling within the slices was conducted according to three different strategies: (1) 5–10 soil samples were taken from different, intensively blue–colored soil volumes in the vicinity of dyed (flow active) macropores; (2) 10 core samples were taken randomly within non–colored areas (as determined at the top–end); and (3) 10 completely randomized core samples were collected. Thus, typically 25–30 soil samples were taken per slice. However, due to extensive staining making it difficult to avoid blue soil, sampling according to strategy 2 was not performed above 5–10 cm depth. Furthermore, special procedures were followed in the uppermost slice. Following strategy 3, 10 samples were taken randomly in the 0–0.5 cm and the 0.5–1.5 cm depth intervals (the uppermost 1.5 cm was not included when sampling below). With strategy 1, sampling started at 0.5 cm depth (treatment A) or 1.5 cm depth (treatment B) because it was not possible to identify flow active macropores in the uppermost layer. Sampling according to strategy 1 was accompliced by scraping 1–2 mm of stained soil from the inside of biopores or cracks using a spatula. Sampling following strategies 2 and 3 was supported by coordinates generated by a random number generating program. It was done using a drill (diameter: 4.0 mm) throughout the entire soil layer. Hence with 10 samples per layer, roughly 0.18 % of the total soil volume was sampled. A total of 185–240 soil samples were obtained per column. Similar samples, according to the sampling strategy, were pooled within each soil layer.

Analyses
The pooled soil samples were air–dried, grounded using a ball–mill (350 rpm for 1 min), and mixed carefully. ^{14}C–activity was measured by LSC after heating of 250 mg soil to 800°C in a constant flow of oxygen (Packard Sample Oxidizer Model 507) followed by ^{14}C–CO_2 absorption by Carbosorb E (Packard) and Permafluor E+ (Packard). Two replicates were analyzed from each pooled soil sample. The concentrations of pesticides in soil were calculated from the specific concentration activity of the ^{14}C–labeled pesticides and the relationship between labeled and unlabeled pesticide in the applied pesticide solutions. The detection limits for glyphosate and pendimethalin in soil were 0.01 and 0.005 mg/kg, respectively.

All the blue-stained representations of flow patterns appearing on photos of the cross–sections were manually transferred to transparent plastic sheets, and the new binominal representations (images showing either color or no color) were digitized using the procedures described by Petersen et al. (1997). The only distinction made in this process was whether or not blue dye was visible on the photos as evaluated by one person. The photos were handled in systematic order governed by a random serial number assigned to each. The digitized images were then scaled in two mutually perpendicular directions, and the fractional dye–stained area (DC, %) was determined using the image processing program ImageJ (Collins, 2007). The thickness of the uppermost completely dyed in soil layer (maximum depth with DC = 100 %) was measured. Fractional volume of dyed soil in a given soil layer was calculated as the average of DC observed at the top and bottom ends.

Mass balances for the pesticides were established based on sampling strategy 1 and 3, respectively. For strategy 1, measured pesticide concentration in soil was multiplied with fractional volume of dyed soil and by the mass of soil to get the pesticide content of a given soil layer. Concentrations obtained with strategy 3 were applied in the uppermost 0.5 cm (treatment A) or 1.5 cm (treatment B) layers in the lack of strategy 1 observations. For strategy 3, the pesticide content of a given soil layer was obtained by multiplying the measured concentration by the mass of soil. A dry bulk density of 1.60 g/cm^3 (average value for all columns) was applied throughout in these calculations.

Results and Discussion

Distribution of Pesticides
Significant pesticide concentrations (above the detection limits) could be traced all the way through the columns by sampling strategy 1, except for glyphosate in treatment B at 25–50 cm depth. The concentrations generally decreased with depth (Figure 1). Below 30 cm depth, the pendimethalin concentrations approached the detection limits.

No significant amounts of the pesticides were found using sampling strategy 2, except in one sample (glyphosate in treatment A at 20–25 cm depth, cf. Figure 1). Thus, as a rule, pesticides were not detected by sampling outside blue-stained areas, not even at 5–10 cm depth, where considerable amounts of pesticide were found with the other sampling strategies. This is particularly noteworthy because three irrigations were carried out after pesticide application prior to application of the dye solution. Stronger sorption of the pesticides than of the dye may be part of the explanation. For the investigated (top–) soil, Gjettermann et al. (2009) reported soil–water partition coefficients (K_d–values) of 503 L/kg for glyphosate and 242 L/kg for pendimethalin. Hence, both pesticides sorb strongly to the soil material. For Brilliant Blue, Flury and Flühler (1995) have reported much smaller K_d–values in the range 0.19–5.78 L/kg. Somewhat stronger sorption than measured by Flury and Flühler has been found for soils rich in clay minerals (German–Heins and Flury, 2000; Ketelsen and Meyer–Windel, 1999). It should be noticed that the sampling strategy being based on coring from upper surfaces of the slices does not completely exclude the inclusion of blue-stained soil material.

It was not possible in any case to trace the pesticides all the way through the columns by using strategy 3. With treatment A, glyphosate was not found below 10 cm depth and pendimethalin not below 20 cm. The pesticides tended to be found at slightly greater depths with treatment B. However, no significant concentrations were found below 25 cm depth. Hence with completely randomized sampling, pesticides

were not found in significant amounts in the soil below 10–25 cm depth even though significant amounts (0.21–0.31 % of applied) were leached (Table 1) and 0.18 % of the soil volume was sampled. It was noticed that the strategy generally led to the inclusion of some blue–colored soil in the pooled samples when applied above 15–20 cm. Pesticide concentrations decreased strongly with depth in the 0–5 cm depth interval (Figure 1). By far the highest concentrations were found in the uppermost 5 mm of soil being completely dyed–in for both tillage treatments. Glyphosate concentrations measured in this layer were 8.59 and 10.5 mg/kg for the A and B treatment, respectively, while the corresponding numbers for pendimethalin were 24.6 and 14.1 mg/kg. Significant pesticide concentrations measured according to strategy 1 were always higher than concentrations obtained at the corresponding depths by strategy 3 (Figure 1). The differences between the two repeated measurements of pesticide concentrations of the soil samples were negligible (not shown).

Figure 1. Glyphosate and pendimethalin concentration (C_G and C_P, respectively) as a function of soil column depth obtained by the sampling strategies 1 (dyed), 2 (non–dyed), and 3 (random). Data for the two tillage treatments (A and B, average of 2 repeated measurements). Notice the broken 2nd axes.

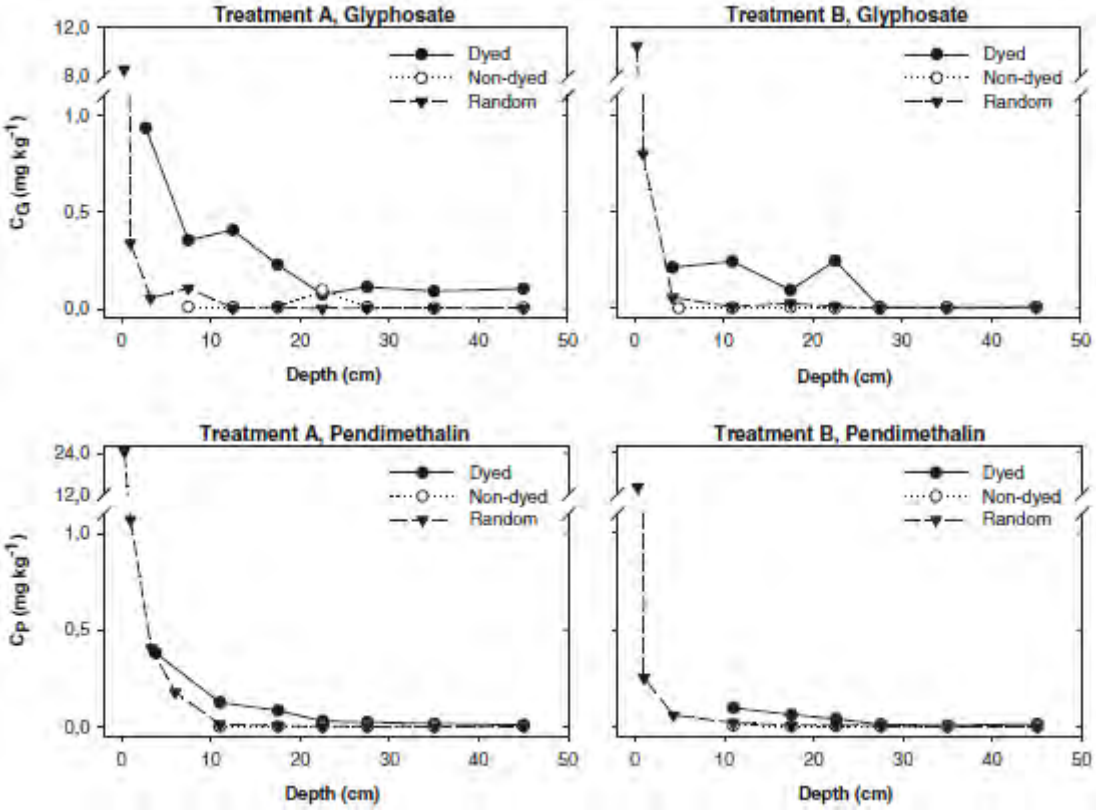

Table 1. Amounts of pesticides retrieved in columns estimated from two different column sampling strategies (1 and 3), and amounts lost with leachate (% of applied)

	Treatment A		Treatment B	
	Strategy 1	Strategy 3	Strategy 1	Strategy 3
Glyphosate found in column	63	50	67	61
Glyphosate leached	0.31	0.31	0.21	0.21
Pendimethalin found in column	110	123	65	63
Pendimethalin leached	0.23	0.23	0.21	0.21

Applied amounts per column, Glyphosate: 12.5 mg; Pendimethalin: 14.2 mg.

Dye Patterns

The thickness of the uppermost completely dyed–in soil layer was about 0.5 cm for treatment A and about 3 cm for treatment B. Thus, the fractional volume of dyed soil was 100 % above 0.5–cm depth in columns subjected to treatment A and above 3 cm in columns subjected to treatment B. The fractional area covered with dye (DC) rapidly decreased with depth right below these depths. In the topsoil, DC tended to be larger for treatment B than for treatment A, whereas the opposite trend was observed in the subsoil (Figure 2).

Figure 2. Fractional area covered with dye (DC) at different soil depths. Average values for each of the two tillage treatments (A and B, n = 2) with the range shown by the bars. Notice the broken 2nd axis.

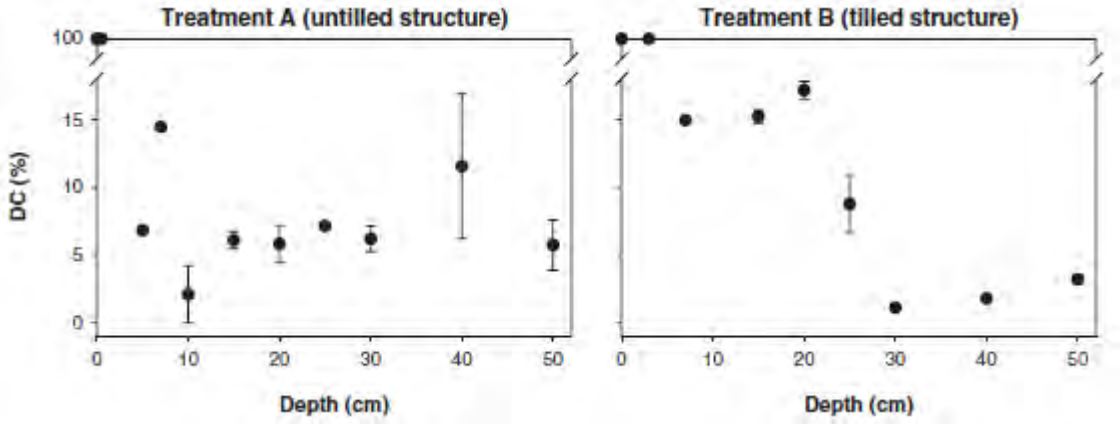

Below 30–cm depth, the stained flow pathways were mainly concentrated around vertically oriented earthworm channels comprising a relatively small fraction of the total soil volume. The dye had typically penetrated less than 1–2 cm into the soil matrix from these flow active macropores (4–10 per column). This is more than previously reported from studies conducted under field conditions (Petersen et al., 1997), probably due to the wet conditions prevailing in the columns with drainage at atmospheric pressure from 50–cm depth. For treatment A, a considerable fraction of the stained soil volume was found at the column walls in connection with large flow–active macropores that were cut during the excavation process. On average for all columns, the fractional volume of dyed soil below 30–cm depth comprized 5 %, leaving about 95 % as unstained and expectedly pesticide free.

Mass Balances

Under typical field conditions, half–lives (DT_{50} values) for glyphosate and pendimethalin are about 12 and 90 days, respectively (PPDB, 2010). However, under the low temperatures prevailing in the columns, both pesticides are expected to be slowly degradable. Furthermore, any non–volatile metabolites containing the ^{14}C would be included in the measurements. The columns were sealed with plastic foil, except when used in the experiments. Hence, losses due to degradation and evaporation are expected to be very small. Also, the fraction of applied pesticide (^{14}C) being leached was small (0.21–0.31 %) and unimportant for the mass balance (Table 1). Consequently, we expected a recovery close to 100 % based on the soil sampling alone. We found between 50 and 123 % with sampling strategy 3, and between 63 and 110 % with strategy 1, respectively (Table 1). Hence, none of the sampling strategies resulted in the expected (slightly less than) 100 % recovery in the columns although the balances tended to be better for strategy 1 than 3.

Both methods of constructing a mass balance obviously had large uncertainties. The largest concentrations (and amounts) of pesticide were found in the uppermost 0.5 cm of the profile, and the major uncertainty appears to be the sampling of this top layer. If, for instance, the actual depth of sampling was 6 mm rather than 5, the error to the mass balance would be 8–19 % for the investigated columns. However, any difference in mass recovery obtained with the two sampling strategies is not related to this uncertainty, since the same sampling of this uppermost thin soil layer was used in both cases. The method based on sampling strategy 1 does correctly include some pesticide from lower parts

of the columns. However, it may be biased if sampling for the pesticides did not fully represent the stained soil volumes. The mass recovery was of the same order of magnitude or considerably better than that obtained by Flury et al. (1995) working with a systematic very dense two–dimensional sampling scheme for herbicides in structured field soil.

Tracing Pesticides in Macroporous Soil

The magnitude of preferential flow contributing to the leaching of pesticide is difficult to quantify from studies on soil samples. Prichard et al. (2005) investigated the predominant source of pesticide residues detected in domestic wells located in an area with cracking clay soil. Although preferential flow through macropores within the field was a potential pathway, pesticide residues were retained in the top 15 cm of the soil. They deduced that the contribution of preferential transport to leaching was insignificant, despite the fact that lack of correlation of pesticide data between soil and water samples has previously been documented for soils with preferential flow (e.g. Sanchez et al., 2006; Laabs et al., 2000; Malone et al., 2000). Sanchez et al. (2006) found high concentrations of methidathion in the upper 25 cm of a soil profile but very low concentrations below this depth. They attributed high concentrations found sometimes in leachates from deeper layers to preferential flow processes. Laabs et al. (2000) similarly suggested that absence of pesticide residues in soil at depths below 25 cm combined with observed leaching indicated non–chromatographic transport of these substances in the soil profile. Malone et al. (2000) concluded that a sampling strategy including the mixing of horizontal slices with dimension 3.75 × 30 × 30 cm was not well suited to trace the movement of pesticides in the subsoil of structured soils. The present study support the interpretations made by Laabs et al. (2000), Malone et al. (2000), and Sanchez et al. (2006).

As expected, visible traces of Brilliant Blue were indicators for the occurrence of the pesticides in the soil. The measurements strongly suggest that both pesticides were transported exclusively within some fraction of the stained soil volume. With transport concentrated on a few macropores as in the subsoil of the present study, it should be possible to sample virtually all dye (and pesticide) at a given depth. Further developed, strategy 1 could therefore be used as the basis for better quantification of strongly sorbing pesticides in macroporous subsoil profiles. It is likely that the dye tracer should be applied under similar conditions (e.g. soil structure, soil moisture content, irrigation/precipitation amount and intensity) as the pesticides themselves.

Conclusions

Visible traces of Brilliant Blue transported under similar conditions as the two pesticides indicated the occurrence of both pesticides in the soil. The results suggest that efficient sampling for sorbing pesticides can be obtained by using the dye and focusing on stained soil volumes. None of the investigated sampling strategies led to mass balances that were accurate enough to detect small but significant amounts of pesticide leaching.

3. Assessment and conclusion

Assessment and conclusion by applicant:

The study describes a leaching experiment on soil columns with a dye and glyphosate and pendimethalin. Some important information about study conditions are missing: agricultural use of the soil, temperature, soil parameters, details on analytics and on substance identification, sample storage conditions before analysis.

The study is therefore classified as reliable with restrictions (Category 2).

1. Information on the study

Data point:	KCA 7.1.3.1.1
Report author	Gómez Ortiz, A., et al.
Report year	2017
Report title	Sorption and desorption of glyphosate in mollisols and ultisols soils of Argentina
Document No	Environmental Toxicology and Chemistry, Vol. 36, No. 10, pp. 2587–2592, 2017
Guidelines followed in study	None
Deviations from current test guideline	None
GLP/Officially recognised testing facilities	No, not conducted under GLP/Officially recognised testing facilities (literature publication)
Acceptability/Reliability:	Reliable with restrictions (Soils were from outside EU (Argentina))

2. Full summary of the study according to OECD format

In Argentina, glyphosate use has increased exponentially in recent years as a result of the widespread adoption of no-till management combined with genetically modified glyphosate-resistant crops. This massive use of glyphosate has created concern about its potential environmental impact. Sorption–desorption of glyphosate was studied in 3 Argentinean soils with contrasting characteristics. Glyphosate sorption isotherms were modeled using the Freundlich equation to estimate the sorption coefficient (K_f). Glyphosate sorption was high, and the K_f varied from 115.6 to 1612 $mg^{1-1/n}L^{1/n}/kg$. Cerro Azul soil had the highest glyphosate sorption capacity as a result of a combination of factors such as higher clay content, cation exchange capacity, total iron, and aluminum oxides, and lower available phosphorus and pH. Desorption isotherms were also modeled using the Freundlich equation. In general, desorption was very low (<12%). The low values of hysteresis coefficient confirm that glyphosate strongly sorbs to the soils and that it is almost an irreversible process. Anguil soil had a significantly higher desorption coefficient (K_{fd}) than the other soils, associated with its lower clay content and higher pH and phosphorus. Glyphosate high sorption and low desorption to the studied soils may prevent groundwater contamination. However, it may also affect its bioavailability, increasing its persistence and favoring its accumulation in the environment. The results of the present study contribute to the knowledge and characterization of glyphosate retention in different soils.

Materials and Methods

Soils

Soil samples were taken from agricultural fields of Cerro, Tandil, and Anguil, The studied soils are located in areas of high agronomic land use and have different edaphoclimatic conditions. Four composite soil samples from the top 15 cm of topsoil were collected from each field. Samples were homogenized, air-dried, and sieved to a particle size of 2 mm. A subsample of each replicate was used for physicochemical analysis of the soils (see Table 1). Particle size distribution was measured using the pipette method; organic carbon content was measured according to the Walkley-Black method; CEC was determined by displacement with 1M ammonium acetate at pH 7; soil pH was measured by electrode in a soil:water ratio of 1:2.5; available phosphorus (P-Bray) was determined according to Bray and Kurtz; total iron (Fe) was determined by atomic absorption spectrophotometry; and exchangeable aluminum (Al) was measured according to the Al method.

Table 1. Main characteristics of the sampled locations and soil physicochemical properties

	Soil		
	Anguil	Cerro Azul	Tandil
Altitude (masl)	157	280	256
Annual average temperature (°C)	15.3	20.5	13.7
Mean annual precipitation (mm)	760	1844	993
Latitude	36°35′54″S	27°39′42″S	37°36′0.1″S
Longitude	63°58′31″W	55°26′25″W	59°04′29″W
Soil type	Mollisol	Ultisol	Mollisol
Main textural class	Loam	Clay	Loam
pH	6.3 A	4.9 C	5.4 B
Clay (%)	14.7 C	78.5 A	23.0 B
Silt (%)	45.6 A	15.4 C	40.9 B
Sand (%)	39.6 A	6.1 C	36.0 B
Organic carbon (%)	1.3 C	2.4 B	3.4 A
P-Bray (mg/kg)	29.6 A	7.6 C	17.1 B
CEC (meq/100 g)	17.4 C	20.6 B	25.2 A
Ca^{2+} (meq/100 g)	8.1 B	5.6 B	14.7 A
Mg^{2+} (meq/100 g)	2.9 B	3.2 B	5.1 A
K^{+} (meq/100 g)	3.2 A	1.2 A	2.8 A
Na^{+} (meq/100 g)	0.3 A	0.2 A	0.5 A
Al^{3+} (meq/100 g)[b]	0.15 B	0.69 A	0.11 B
Total Fe (%)[b]	1.08 B	8.40 A	0.81 B

[a]Different letters indicate differences among soils ($p < 0.05$).
[b]From Gianelli et al. [8].
CEC = cation exchange capacity; P-Bray = available phosphorus.

Chemicals

Stock solutions for the standard curves and the isotherm study solutions were prepared using analytical pure glyphosate (99.9%). For analytical procedures HPLC - grade methanol and HPLC - grade acetonitrile were purchased commercially. Nanopure water was obtained by purifying demineralized water.

Sorption isotherms

The sorption isotherms were performed according to the batch equilibrium method. First, 2 g of soil was shaken with 40 mL of a 0.01M $CaCl_2$ solution. After 24 h, glyphosate was spiked at different initial concentrations (C_0): 0, 0.5, 1, 5, 10, and 20 mg/L. The suspensions were shaken for another 24 h at constant temperature (20°C). Afterward, tubes were centrifuged, and an aliquot (3 mL) of the aqueous solution was analyzed for glyphosate concentration. Each initial concentration was tested by duplicate for each soil sample. These laboratory duplicates were averaged, finally obtaining data of 4 replicate isotherms per soil.

Desorption isotherms

The desorption isotherms were performed using the spiked soil with the C_0: 5 mg/L solution from the sorption isotherm studies. This concentration is equivalent to the commonly used dose in the field per year (6 L/ha/yr) considering 5 cm depth of soil. After the sorption study, the aqueous phase was carefully discarded to avoid any soil loss during manipulation. The volume of the solution that was removed was replaced with 0.01M $CaCl_2$, and the soil was re-suspended and shaken at a constant temperature for another 24 h. Then, samples were centrifuged and glyphosate was measured in the aqueous solution to quantify the glyphosate that desorbed from the soil matrix. This procedure was repeated at 48 and 72 h by removing the aqueous solution and adding again $CaCl_2$. The amount of adsorbed glyphosate at each desorption step was calculated as the difference between the initially adsorbed concentration and the desorbed amount.

Glyphosate analysis

To quantify the remaining glyphosate in the aqueous solution, an aliquot of 3 mL was transferred to a 15-mL polyethylene flask, and 0.5 mL of borate buffer solution (0.04 mM $Na_2B_4O_7 \cdot 10\ H_2O$, pH 9) and

0.5 mL of acetonitrile were added. Samples were shaken vigorously, then derivatized with 0.5 mL of 9-fluorenylmethylchloroformate dissolved in acetonitrile (6 g/L) and incubated overnight at room temperature. As a cleanup step, CH_2Cl_2 was added to the samples to remove any organic impurities and minimize matrix effects. The aqueous fraction was separated from the organic solvent by centrifuging. The supernatant was collected and filtered and then analyzed by liquid chromatography coupled to a tandem mass spectrometer (MS/MS).
Chromatographic analysis was carried out using a Waters ACQUITY1 ultra-performance liquid chromatography system. Target molecules were detected by a triple quadrupole MS/MS Quattro Premier XE (Waters). The equipment was operated with an electrospray ionization source in positive mode. To take into account the matrix effect of each soil, standard curves were prepared using a background solution of each soil obtained after shaking with $CaCl_2$ 0.01 M. After separating the solid phase from the aqueous phase, the solution was used to prepare each point of the standard curves by adding the corresponding glyphosate concentration. A sample without any glyphosate was also analyzed to check the concentration of presorbed glyphosate. In all cases, the background solution had non-detectable levels of glyphosate. The limit of detection was 0.1 µg/L, and the limit of quantification was 0.5 µg/L.

Sorption modeling
Following the experimental design proposed by the Organisation for Economic Co-operation and Development Guidelines for the Testing of Chemicals, Test No. 106, the measured glyphosate in the aqueous solution was used to estimate the remaining glyphosate sorbed to the soil (Cs).

$$C_s = M_s/M_{soil} = (C_0 - C_w)V_0/M_{soil} \qquad (1)$$

where C_s is the concentration of glyphosate adsorbed to the soil at equilibrium (mg/kg), M_s is the mass of glyphosate sorbed to the soil at sorption equilibrium (mg), M_{soil} is the dry mass of the soil sample (kg), C_0 is the initial tested concentration of glyphosate in contact with the soil sample (mg/L), C_w is the analytically measured mass concentration of glyphosate in the aqueous phase at sorption equilibrium (mg/L), and V_0 is the initial volume of the aqueous phase in contact with the soil sample (mL).

The Freundlich equation was used to describe sorption and desorption isotherms

$$C_s = K_f C_w^{1/n} \qquad (2)$$

where K_f ($mg^{1-1/n} L^{1/n}/kg$) is the Freundlich sorption coefficient and 1/n is the Freundlich exponent (K_f and 1/n will hereafter refer to sorption and K_{fd} and $1/n_d$ to desorption). The K_f coefficient indicates the affinity of the substance to the soil matrix, and 1/n indicates the degree of linearity between the amounts adsorbed and the concentration in the solution.

The hysteresis coefficient (H) for the sorption/desorption isotherms was calculated according to the equation

$$H = (1/n_d)/(1/n) \qquad (3)$$

where 1/n and $1/n_d$ are the Freundlich slopes obtained for the sorption and desorption isotherms, respectively.

Statistical analysis
For the isotherm sorption and desorption studies, each soil sample was analyzed in duplicate. Laboratory duplicate samples were averaged, and the isotherm curves were then modeled using the NLIN procedure of SAS software. Statistical analyses of the soil properties and of the estimated sorption and desorption parameters were performed using a completely randomized design with 4 replicates per soil. Analysis of variance was performed using the PROC GLM procedure to evaluate differences in the Freundlich parameters at a significance level of 5%.

Results and Discussion

Soil characteristics

Tandil and Anguil soils correspond to a loam texture, while Cerro Azul is classified as clay. Cerro Azul soil had a significantly higher clay content, followed by Tandil and then Anguil ($p<0.05$). On the other hand, the organic carbon content and CEC were significantly higher in Tandil, followed by Cerro Azul and Anguil soil ($p<0.05$). Anguil soil had significantly higher pH and P-Bray values than Tandil and Cerro Azul ($p<0.05$). Regarding the exchangeable cations, significant differences were observed only for Ca^{2+} and Mg^{2+}, following the order Tandil>Cerro Azul>Anguil ($p<0.05$). The highest Al^{3+} and Fe contents were found in Cerro Azul soil, denoting its Ultisol origin.

Sorption isotherms

Glyphosate sorption and desorption isotherms are shown in Figure 1. The K_f values for glyphosate were very high and ranged from 115.6 to 1612 (Table 2), being generally higher than those usually reported in the literature. Glyphosate K_f was significantly higher in Cerro Azul compared with Tandil and Anguil soil ($p<0.05$) (Table 2). The values of 1/n ranged from 0.4 to 0.8 (Table 2). Isotherms exhibited an L-type ($1/n<1$) curve according to the classification of Giles et al. This indicates that sorption is not constant as the concentration of the herbicide increases and that the sorption sites become saturated with increasing glyphosate concentration. In the case of Tandil and Anguil soils, glyphosate was almost completely sorbed to the soil at low initial concentrations; and as the concentration increased, sorption became less efficient (Figure 1). Isotherms of this type occur when the adsorbent has a high initial affinity for the herbicide until the sorption sites become saturated. In contrast, the Cerro Azul isotherm exhibits an almost linear relationship between the amount of sorbed glyphosate and its concentration at equilibrium in the solution (Figure 1), with 1/n values closer to 1 (Table 2). Therefore, it can be assumed that the number of sorption sites remains almost constant even at high concentrations. The reason glyphosate sorption was significantly higher in Cerro Azul soil can be explained by the soil's textural composition. At the soil's pH, the negatively charged glyphosate molecule can be complexed with cations released from the clays via a cation exchange reaction with solution protons. On the other hand, Fe and Al oxides also play an important role in glyphosate sorption because the phosphonate group of glyphosate establishes coordination links with the interchangeable surfaces of Fe^{3+} and Al^{3+} cations. In this sense, the lower soil pH of Cerro Azul could also be favoring sorption via Fe and Al oxides because as the pH decreases, these oxides become more protonated, increasing the affinity toward the negatively charged glyphosate molecule. Therefore, aside from cation exchange reactions, glyphosate may strongly bond through ligand exchange with the metal ions (Fe or Al) at the surface of the clay minerals. This mechanism has been proposed for other organic weak acids, and hence it can be applied to glyphosate.

Table 2. Glyphosate Freundlich sorption and desorption parameters for Anguil, Cerro Azul, and Tandil soils[a]

	Sorption			Desorption[b]							
							Percentage[c]				
Soil	K_f ($mg^{1-1/n}L^{1/n}/kg$)	$1/n$	r^2	K_{fd} ($mg^{1-1/n}L^{1/n}/kg$)	$1/n_d$	r^2	1°	2°	3°	Total[d]	H[e]
Cerro Azul	1612.0 (859.8) A	0.8 (0.5) A	0.97–0.99	101.2 (2.9) C	0.01 (0.0) C	0.99–0.99	0.7 (0.1)	0.6 (0.0)	0.5 (0.1)	1.6 (0.8)	0.01 (0.0) B
Tandil	412.6 (50.9) B	0.5 (0.07) AB	0.98–0.99	105.4 (1.7) B	0.02 (0.0) B	0.99–0.99	0.8 (0.1)	0.6 (0.0)	0.3 (0.0)	1.9 (0.5)	0.04 (0.0) B
Anguil	115.6 (12.9) B	0.4 (0.2) B	0.90–0.99	117.5 (0.6) A	0.20 (0.0) A	0.99–0.99	4.5 (0.3)	3.6 (0.1)	3.3 (0.3)	12.3 (4.1)	0.4 (0.2) A

[a]Mean values of 4 replicates; standard deviation in parentheses. Different letters indicate significant differences among soils ($p < 0.05$).
[b]Desorption from initial glyphosate aqueous concentration $C_0 = 5$ mg/L.
[c]Percentage of desorbed glyphosate in the 1°, 2°, and 3° desorption cycle.
[d]Total desorbed glyphosate after 3 successive desorption cycles.
[e]Hysteresis coefficient ($H = 1/n_d/1/n$).

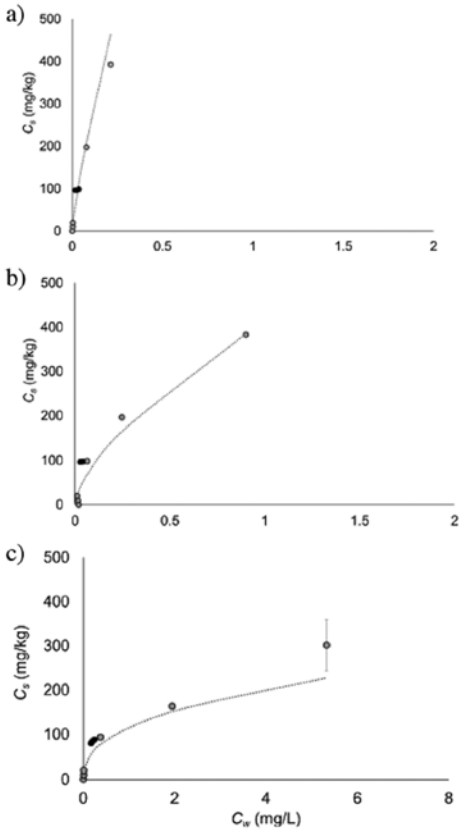

Figure 1. Adsorption (gray dots) and desorption (black dots) isotherms for (a) Cerro Azul, (b) Tandil, and (c) Anguil soils. Error bars represent standard deviation. Black dotted line represents the Freundlich model fit. Note different x axis scale for Anguil soil. C_s = concentration of glyphosate adsorbed to the soil at equilibrium; C_w = analytically measured mass concentration of glyphosate in the aqueous phase at sorption equilibrium.

Desorption isotherms

The K_{fd} values of the studied soils ranged from 101.2 to 117.5 $mg^{1-1/n}kg^{-1}L^{1/n}$ (Table 2). Anguil soil had the highest K_{fd}, while Cerro Azul had a significantly lower desorption coefficient than the rest ($p<0.05$). The total desorbed glyphosate at the end of the desorption study was 1.6 and 1.9% for Cerro Azul and Tandil, respectively, whereas in Anguil soil desorption reached 12% (Table 2). The values of $1/n_d$ ranged from 0.01 to 0.2 (Table 2). The irreversibility of glyphosate sorption was confirmed by the lower values of $1/n_d$ with respect to 1/n. The more pronounced curvature of the desorption isotherms suggests that more energy is required to desorb the molecules than that needed for the sorption process. In consequence, hysteresis coefficients were low, ranging from 0.01 to 0.4 (Table 2). When comparing the 3 soils, desorption and hysteresis coefficients were significantly higher in Anguil. This can be explained by the lower clay content and lower CEC, as well as the significantly higher pH and available phosphorus, which affect glyphosate sorption mechanisms in an inverse way, as explained before. Nevertheless, desorption hysteresis can be considered significant in all the studied soils because the hysteresis coefficient was <0.7, indicating that glyphosate sorption is nearly an irreversible process.

The fact that glyphosate binds strongly to the studied soils and that desorption was very low has a major implication for glyphosate bioavailability. Glyphosate's biological degradation is strongly limited in soils that have high glyphosate affinity and low desorption.

The results obtained in the present study indicate that sorption of glyphosate increases in soils with high contents of Al^{3+}, Fe, and clays as well as low pH and phosphorus content. This situation favors greater glyphosate retention and, therefore, lower desorption, which would reduce the likelihood of leaching and therefore the potential risk of groundwater contamination. However, glyphosate bioavailability can also be reduced, increasing its persistence and therefore contributing to its accumulation in the environment. These results contribute to the knowledge about glyphosate retention in soils and allow the identification of behavior patterns of this extensively applied herbicide in different edaphic scenarios.

This is of major importance for the development of decision-making tools and criteria to reduce the potential negative impacts on soil and groundwater resources.

3. Assessment and conclusion

Assessment and conclusion by applicant:
The study describes a adsorption / desorption experiment with glyphosate on three different agricultural soils from Argentina. The soils do not reflect current EU conditions. Furthermore, no labelled test item was used and no mass balances were provided.
The study is therefore classified as reliable with restrictions (Category 2).

1. Information on the study

Data point:	KCA 7.1.3.1.1
Report author	Jodeh S., et al. .
Report year	2014
Report title	Fate and Mobility of Glyphosate Leachate in Palestinian Soil Using Soil Column
Document No	Journal of Materials and Environmental Sciences (6) (2014) 2008–2016
Guidelines followed in study	None
Deviations from current test guideline	None
GLP/Officially recognised testing facilities	No, not conducted under GLP/Officially recognised testing facilities
Acceptability/Reliability:	Reliable with restrictions for the adsorption experiment Not reliable for the column leaching experiment (Used soil does not reflect EU conditions (soil, climate))

2. Full summary of the study according to OECD format

In recent years, pesticides were used heavily in Palestine, which led to the contamination of soil and water and causing many diseases. Many studies focused on the impact of pollutants such as pesticides and oil on soil, humans, animals, plants and the environment in general. Using column study the amount of glyphosate in soil decreases with increasing depth of soil, where it is for 0–30 cm (11 ppm) >30–60 cm (6 ppm) >60–100 cm (2 ppm) due to organic content and metal oxides founded in soil that can form stable complexes with glyphosate. When we increased the concentration of glyphosate, the amount of glyphosate (contaminant) in leachate where found to be 25 x (15.96 ppm) >15 x (3.91) >5 x (3 ppm) column. The behavior of glyphosate leachate fits the first order reaction and the isotherm is in according with the Freundlich adsorption equation with R^2 value 0.98, *k* value 6.4 and n value 1.07 which indicates good adsorption to soil.

Materials and Methods

Chemicals

Glyphosate (purity 98.5 %) was purchased commercially. Other chemicals like carbon disulfide, copper nitrate and chloroform were available at the university department of chemistry. All chemicals and solvents used in the experiment were of high performance liquid chromatography and high purity.

Acid digestion of soil

To find the metals in soil and $HClO_4$ (70 %) and HF (40 %) were added then heated to incipient (near dryness). HF were added again and heated to dryness then $HClO_4$ and distilled water were added and heated to incipient. The remaining residue was dissolved in HCl and water. Volume was made up to the 100 mL volume and stored in polyethylene bottle. Fe and Cu in the supernatant were determined by AAS. The physicochemical soil properties (Table 1) were determined using standard methods.

Sampling site and Collection

The soil was sampled in three layers; 0–30 cm, 30–60 cm and 60–100 cm from agricultural locations in Nablus, Mount Gerizim before herbicide treatment of the fields. The soil samples were mixed well separately. The soil used for chemical analysis was air dried, sieved to 2 mm stored in the dark at room temperature and protected from humidity. Basic physicochemical properties of soil were conducted on soil before any treatment with glyphosate**.**

Table. 1: Physico–chemical characteristics of the soil column.

Soil texture • Sand [%] • Silt [%] • Clay [%] •	35% 57.5% 7.5%
Moisture **%**	3.3%
Moisture correction factor (mcf)	1.033
pH	7.62
Organic Carbon %	2.11%
Organic Matter %	3.63%
Conductivity(µs)	530
N%	0.1934%
Ca CO_3 (mg)	0.795
Cu (mg/kg)	44
Fe (mg/kg)	1982.27
Available Phosphorous (P) (mg/kg)	62.41

Leachate extraction columns

Leachate extraction columns consist of four columns of polyvinyl chloride (PVC) pipe. A metal mesh screen was placed at the bottom end of each column and a plastic bottle was placed under each column to collect water. Soil column was washed with distilled water to remove air bubbles from soil and to ensure that the pH of leachate water from each column is neutral.

Glyphosate application to soil–column experiment

Glyphosate contains the monoisopropylamine salt of glyphosate (N–(phosphonomethyl)–glycine) (360 g/L) was applied to each column with concentrations; 5 X, 15 X and 25 X, where X equals amount of glyphosate applied to soil yearly (nearly 2 L/dunom), numbers (5, 15, 25) are the years of applying glyphosate to soil. Blank soil samples were used as controls without glyphosate addition. The concentrations of glyphosate added to soil columns are listed in Table 2.

Leachate

Leachate was collected from each column in plastic bottle at the end of every period. Leachate volumes were determined gravimetrically. Leachate water was centrifuged to remove solid particles and then the supernatant was filtered before analysis. Glyphosate extracted by the method described below and derivatized using the method shown below then measured by Spectrometer at 435 nm.

Procedure for Solid–Phase Extraction (SPE) of glyphosate from water samples

A cation exchange resin was used for the pre concentration and cleanup of glyphosate. A slurry of the Amberlite IR–120, Na–ion exchange resin (cationic) was made in 10 mL distilled water and packed into a narrow glass column, plugged with glass wool at the bottom. The resin was rinsed with distilled water and then with 1 M HCl at a flow rate of 2 mL/min several times before sample application. The pH of water sample spiked with glyphosate was adjusted to 2 and amine group of glyphosate was converted into its protonated form. The protonated sample (25 mL) was passed through the column at a flow rate of 0.5 mL/min in order to have maximum exchange of protonated sample. After the loading step, the sorbent was washed with 25 mL of 2 M NaCl solution (used as eluent) at the same flow rate. The eluted solution was evaporated to about 10 mL at 70ºC then evaluated by the proposed method.

Table. 2: Main characteristics of soil after application of glyphosate at different depths.

Column	Depth (cm)	PH	C %	O.M %	N %	Available P mg/kg	$CaCO_3$ mg/kg	Fe mg/kg	Cu mg/kg
Blank	0-30	7.45	1.56	2.69	0.145	7.91	0.211	1941	43
	3-60	7.78	1.53	2.64	0.082	5.3	0.245	1997	38
	60-100	7.7	1.36	2.33	0.024	5.27	0.292	2008	52
5x	0-30	7.55	2.08	3.58	0.321	66.62	0.147	1853	30
	30-60	7.86	2.05	3.53	0.270	48.49	0.161	1953	35
	60-100	7.72	2.03	3.49	0.250	45.71	0.199	2000	64
15x	0-30	7.68	2.08	3.58	0.373	72.57	0.194	1909	35
	30-60	7.75	2.02	3.48	0.356	66.1	0.197	2053	44
	60-100	7.88	1.99	3.42	0.305	53.26	0.208	2103	52
25x	0-30	7.49	2.21	3.80	0.425	95.04	0.178	1909	24
	30-60	7.56	2.05	3.53	0.375	88.31	0.206	1985	29
	60-100	7.66	2.01	3.46	0.319	74.13	0.200	2032	34

Derivatization procedure of glyphosate

Glyphosate was derivatized using carbon disulfide to convert the amine group into dithiocarbamic acid. The dithiocarbamate group was used as chelating group for reaction with transition metal ion Cu (II). The resultant yellow colored complex was measured at 435 nm using UV–Spectrophotometer. Carbon disulfide (1 % CS_2) solution was prepared and an aliquot of glyphosate were added to a series of 100 mL separating funnels followed by the addition of CS_2 solution. Then the mixture was shaken for 3 minutes for the formation of dithiocarbamic acid. An ammonical solution of Cu(II) (1000 mg/L) was added to the mixture, shaken again vigorously to form complex with dithiocarbamic acid and then kept for separation of two phases. The yellow colored chloroform layer containing the complex was separated in a 10 mL flask and diluted with ethanol. The absorbance of the complex was measured at 435 nm.

Soil columns after glyphosate application

At the end of the experiment, soil columns were cut into three parts. Three samples were taken from each part, air dried and stored in an air tight polythene bottle to analyze their parameters in soil lab at An Najah National University. Glyphosate were extracted from the three parts of soil columns, derivatized and measured spectrophotometrically.

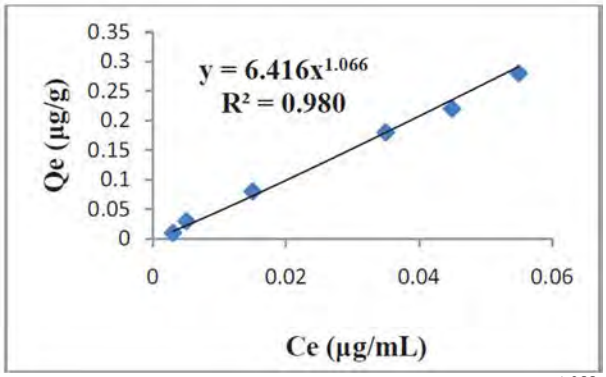

Figure 1: Adsorption isotherm of glyphosate for Palestenian soil ($Qe = 6.416C_e^{1.066}$, $r^2 = 0.9803$).

Batch sorption experiment

Sorption kinetics was analyzed by altering the contact time at a constant concentration of 20 and 30 ppm per vessel for determination of an appropriate equilibrium time at room temperature for the sorption isotherm experiments. They were shaken for 1, 2, 4, 6, 8, 24, 48 and 72 hours, respectively. Samples were equilibrated and processed.

Table. 3: Freundlich isotherm constants for glyphosate.

Coefficient	K	1/n	n	R^2
Glyphosate	6.41	0.93	1.07	0.98

Adsorption isotherm experiment

Soil samples were air–dried, sieved, stored in the dark at room temperature (23°C), and protected from humidity. Sorption experiments were carried out using the standard batch equilibration method. A series of five selected glyphosate concentrations were carried out to determine the adsorption isotherms of glyphosate on soil. The adsorption measuring steps were as follows:

- 200 mL of a PTFE vessels containing 25 g air dried weight soil.
- 100 mL aqueous solutions containing 0–50 mg/L glyphosate were equilibrated for 24 h at room temperature on a reciprocating shaker at low speed 120 excursions per minute.
- The supernatant equilibrium concentration is obtained after centrifuging at 3000 rpm (round per minute) for 20 minutes.
- Blank without glyphosate was also equilibrated. The equilibrium concentrations of each soil were measured spectrophotometrically after derivatization.

Consequently, the differences between the initial and equilibrium concentrations were assumed to be due to sorption onto soil. Sorption isotherms were obtained by plotting the amount of glyphosate sorbed per weight of soil at equilibrium (Qe, μg/g) versus the amount of glyphosate per volume of solution at equilibrium (Ce, μg/mL). The sorption data were described using the Freundlich equation:

$$Qe = K_f . C_e^{nf} \qquad \text{eq. 1}$$

where Qe is the concentration of glyphosate sorbed onto the solid phase (μg/g), Ce is the concentration of glyphosate in solution at equilibrium (μg m/L), and Kf (in $\mu g^{1-nf}\ mL^{nf}\ g^{-1}$) and nf are empirical constants which are related to the adsorption phenomenon and calculated by regression analysis. Kf can be considered as a characterisation of the intensity of sorption, modulated by the deviation from the unity of the nf exponent.

Glyphosate extraction from soil samples

Homogenized soil sample (10 g) was extracted for 60 min with 25 mL of 2 M NH_4OH solution. The extraction was repeated three times. The pH of eluted sample was re–adjusted to pH 5.4 and was evaluated by the proposed method. Each recovery was performed in triplicates.

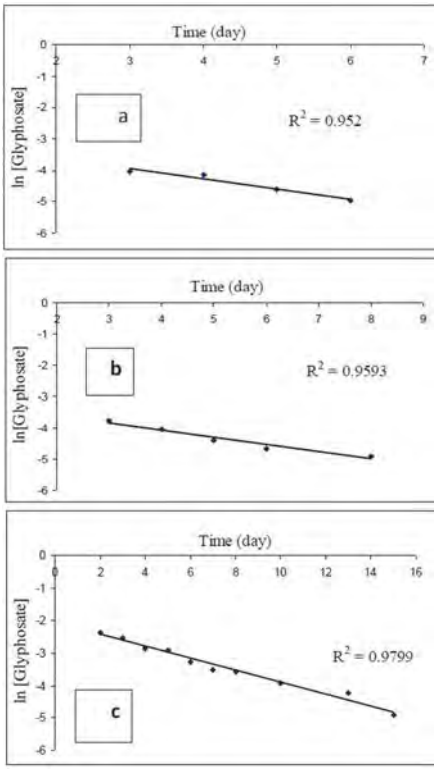

Figure. 2: Plot of time vs. Ln concentration for 5 X (a), for 10 X and (c) for 25 X times glyphosate

Results and Discussion

Batch sorption experiments

The sorption kinetics of the soil were studied to determine an appropriate shaking time for the sorption isotherm experiments. Readings were recorded until 72 hours, no changes in concentrations were observed after 24 hours for all samples, and therefore 24 hours were chosen as equilibrium time for the sorption isotherm experiment due to the quick degradation of glyphosate. The equilibrium adsorption data over the range of concentrations studied here were used to fit Freundlich adsorption equation (eq. 1). The values of n within the range of 2–10 represent good adsorption. Higher values of *k* indicate high adsorption capacity. The isotherm equilibrium results for the examined soil are shown in Figure 1. Freundlich isotherm constants (*k* & n) for glyphosate, the correlation coefficient "R" were obtained from Figure 1. and listed in Table 2. Glyphosate sorption at 25°C in the studied soils was evidenced to be a kinetics process, with a reasonable equilibration time of 24 hours. Literature usually reports Freundlich adsorption constants for glyphosate adsorption by soils which are consistent with that founded in our study. It is indicated from Table 3 and Figure 1. that "n" of glyphosate adsorption is higher than 1. The adsorption isotherms for the soil is of S–type, which indicates the easiness of the adsorption, mainly at higher concentrations.

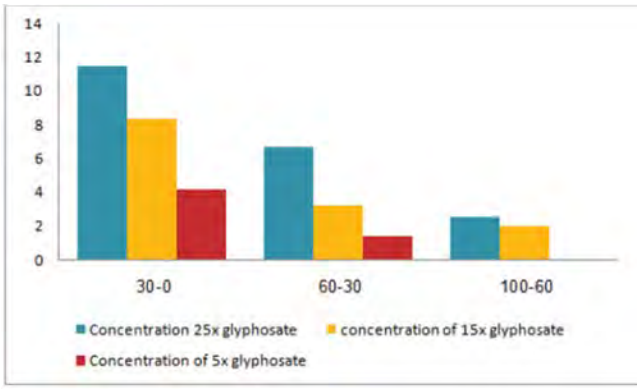

Figure 3: Concentration (mg/L) of glyphosate in soil column at different depths**.**

Glyphosate in leachate

It is indicated that the amount of glyphosate detected in leachate decreases with increasing time. It takes time for 25 x >15 x >5 x until the inability to detect glyphosate in leachate for concentrations less than 1 ppm. Doubling the concentration of glyphosate increases the amount glyphosate (contaminant) in leachate. The above resulting curves shows that the best fit of the glyphosate degradation data was obtained using a first–order reaction as shown in Figure 2. DT_{50} values of glyphosate was 2, 3 and 3.75 days for 5 x, 15 x & 25 x column respectively. This indicate relatively rapid degradation.

Glyphosate in column soil

The results indicated that the glyphosate mobility in the soil columns increased with application rate. With more glyphosate applied, more glyphosate in the soil columns was capable of moving out of the columns. Amount of glyphosate detected in soil columns was increased in the order : 25 x >15 x >5 x. The amount of glyphosate was decreased with depth increasing due to decreasing organic content. It means that the adsorption tendency decreases as the depth increases. No glyphosate detected in 60–100 cm depth as shown in Figure 3. This due to low concentration of glyphosate less than 1 ppm that couldn't be measured by the method used here. Lowest concentration was used also most of glyphosate adsorbed on the upper layer of soil (0–30 cm). This study indicates that glyphosate can be extensively mobile in soil environment if it is applied on soils unable to retain the molecule long enough for its microbial degradation. This may also lead to herbicide leaching to lower soil layers where a limited biological activity occurs.

The effect of organic matter

Soil organic matter consists of a variety of components. These include, in varying proportions and many intermediate stages:

- Raw plant residues and microorganisms (1 to 10 %).
- "Active" organic traction (10 to 40 %).
- Resistant or stable organic matter (40 to 60 %) also referred to as humus.

Table 2 shows that organic matter content of the soil at different depths ranges between 2–3.8 % which is considered as a moderate organic matter soil. Organic matter content of the soil at different depths for each column nearly the same as shown in Figure 4. It is indicated that organic matter only may not affect the adsorption of glyphosate at different depths and it could affect sorption in two ways:

- Reducing glyphosate sorption by blocking sorption sites.
- Increasing glyphosate sorption because poorly ordered aluminium and iron oxides with high sorption capacity are favored at higher soil organic matter content.

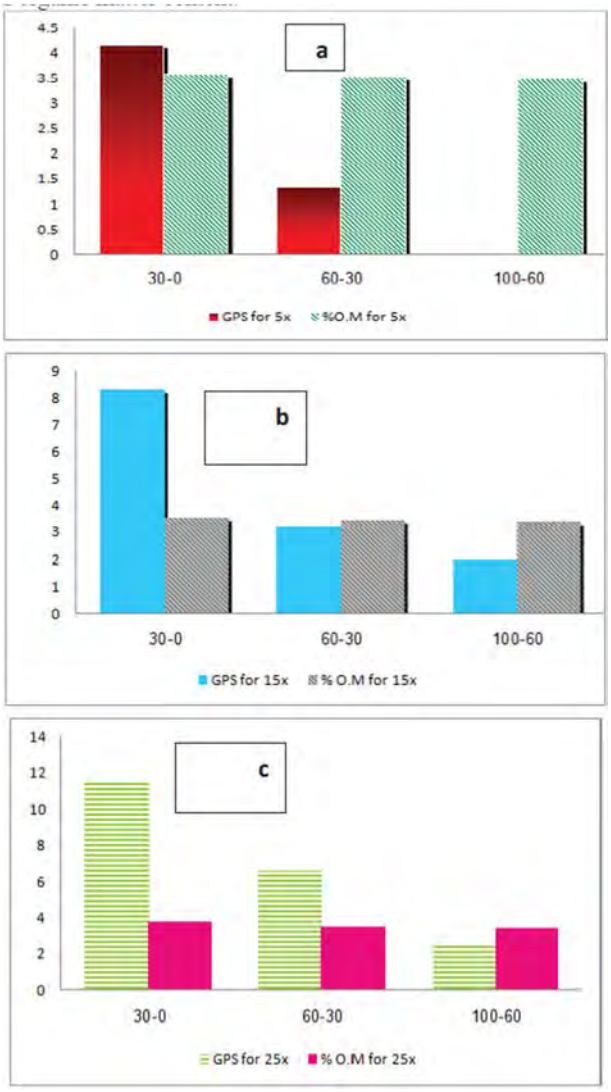

Figure 4: Organic matter content in 5 X (a), 15 X (b) and 25 X (c) column and concentrations of glyphosate at certain depths.

The effect of soil metals

The high sorption values for glyphosate can be in part due to the pH values of soils and to the presence of iron oxides, copper and other metals that can form stable complexes with glyphosate. Glyphosate coordinates strongly to Cu, and Cu–glyphosate complexes formed seem to have higher ability to be adsorbed on the soil than free glyphosate. Copper acts as a bridge between the soil and glyphosate. At these pH values glyphosate is a di–anion and both the carboxylate and the phosphonate functional groups in its molecule are deprotonated, being able to compete for the surface adsorption sites on the metal oxides.

Available phosphorous after glyphosate application

Figure 5 shows that the amount of phosphorous in soil columns after application of glyphosate increased this indicates degradation of glyphosate to its components where phosphorous is one of the degradation products. Glyphosate could be source of phosphorous, nitrogen and carbon in soil as it is shown in Figure 5 and Table 1. The nitrogen content of soil has been increased after glyphosate application to soil columns due to biodegradation of glyphosate.

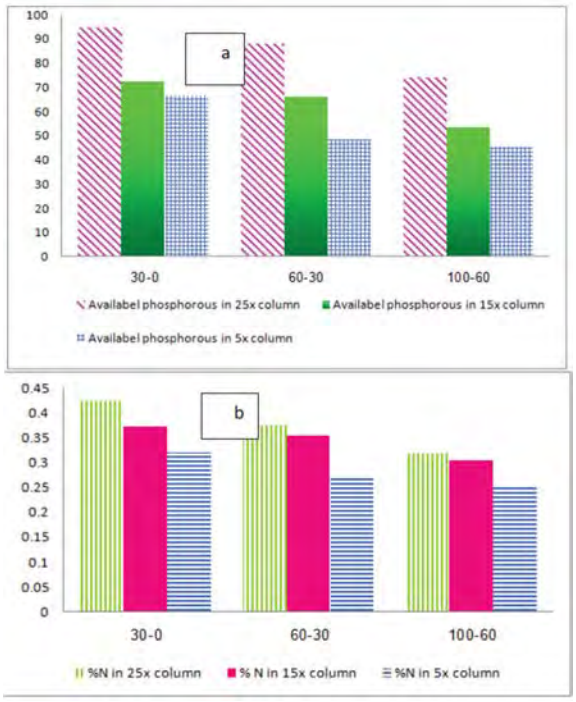

Figure 5: Phosphorous content (a) and nitrogen content (b) in soil columns after application of glyphosate.

Conclusion

Adsorption is an important process in determining the fate of glyphosate in soil. The texture for soil used has been found to be silty clay and the total organic matter (TOM) close to 4 %. Batch equilibrium technique was used to evaluate the extent of glyphosate adsorption on soil as adsorbent. Isotherm is in accord with the Freundlich adsorption equation with R^2 value 0.98; the parameters of this isotherm have been calculated. The adsorption isotherm was fit the S–type isotherm according to Giles. The values of "n" in Freundlich equitation was more than one indicating good adsorption for glyphosate with the soil used. Freundlich constant "*k*" indicates the tendency of glyphosate in this study to be adsorbed on soil particles. *k* increases with increasing the soil minerals and decreases with increasing the depth of soil where the main binding mechanism for glyphosate is the covalent bond between the herbicide and the metals from soil oxides, and so the adsorption decreasing due to decreasing the organic matter content as depth increases. Many factors affect the adsorption of glyphosate as phosphorous content, pH, and temperature. The high sorption values for glyphosate can be in part due to the presence of metal oxides that can form stable complexes with glyphosate.

3. Assessment and conclusion

Assessment and conclusion by applicant:

The article describes both a column leaching experiment and an adsorption experiment with non-labelled glyphosate with a Palestinian agricultural soil. Due to analytical method insensitivity, the lowest rate examined in the column leaching experiment was 5 times the yearly application rate. In addition, some essential information necessary for assessment of validity of both experiments is not reported (e.g. mass balances).

The article is classified as not reliable (Category 3) for the column leaching experiment and as reliable with restrictions for the adsorption experiment (Category 2).

1. Information on the study

Data point:	KCA 7.1.2.1.1; KCA 7.1.2.1.3; KCA 7.1.3.1.1
Report author	Kanissery, R. G. et al.
Report year	2015
Report title	Effect of Soil Aeration and Phosphate Addition on the Microbial Bioavailability of Carbon-14-Glyphosate
Document No	Journal of Environmental Quality
Guidelines followed in study	USEPA guidelines for adsorption studies (USEPA, 2008)
Deviations from current test guideline	None
GLP/Officially recognised testing facilities	No, not conducted under GLP/Officially recognised testing facilities
Acceptability/Reliability:	Reliable with restrictions (slight differences to EU guidelines, no EU soils; soil deg: insufficient reporting of results for kinetic evaluation accord. current guidelines; ads/des: no single measurements for each concentration reported)

2. Full summary of the study according to OECD format

The adsorption, desorption, degradation, and mineralization of ^{14}C-glyphosate [*N*-(phosphonomethyl)glycine] were examined in Catlin (a fine-silty, mixed, superactive, mesic Oxyaquic Argiudoll), Flanagan (a fine, smectitic, mesic Aquic Argiudoll), and Drummer (a fine-silty, mixed, superactive, mesic Typic Endoaquoll) soils under oxic and anoxic soil conditions. With the exception of the Drummer soil, soil aeration did not significantly alter the adsorption pattern of ^{14}C-glyphosate to soils. Herbicide desorption was generally enhanced with anaerobiosis in all the soil types. Anoxic soils demonstrated slower microbial degradation and mineralization kinetics of ^{14}C-glyphosate than oxic soils in all the soil types studied. Phosphate additions significantly reduced the adsorption of ^{14}C-glyphosate to soils irrespective of soil aeration and confirmed the well-established competitive adsorption theory. The addition of soil phosphate stimulated degradation only in anoxic soils. The results from this research highlight the importance of soil redox conditions as an important factor affecting the bioavailability and mobility of glyphosate in soils.

Materials and Methods

Chemicals

Carbon-14-glyphosate (phosphonomethyl-^{14}C) (specifc activity: 1.85 × 109 Bq/mmol) was obtained from American Radiolabeled Chemicals. Unlabeled glyphosate (chemical purity: 99 %) was procured from Sigma Chemical Company. Organic solvents and water were of Optima grade from Fisher Scientifc and used without further purification.

Soils

The soils used were a Drummer silty clay loam, a Flanagan silt loam, and a Catlin silt loam. The moderately well drained Catlin, the somewhat poorly drained Flanagan, and the poorly drained Drummer soils occur in proximity in landscapes and form a soil catena; they thus have similar parent materials but vary in organic matter content, landscape position, and soil drainage class. The soils were collected (to a depth of 15 cm) from a field with no previous glyphosate application history at the University of Illinois Crop Sciences Research and Education Center in Urbana. All soil samples were sieved through a 2-mm screen and stored at 4°C for 4 weeks. Relevant physical and chemical properties of the three soil types used in this study were analyzed at the A&L Great Lake Laboratories and are listed in Table 1. Each soil type had three replicates for each treatment in the subsequent experiments.

Table 1. Selected properties of the soils used in the experiment (analysis by A&L Great Lakes Laboratories, Inc.).

Soil	pH	Texture†			WHC‡	CEC§	Organic matter¶	P
		Sand	Silt	Clay				
		%				$cmol_c\ kg^{-1}$	%	$mg\ kg^{-1}$
Catlin	7.6	10	58	32	31.4	13.9	3.3	69
Flanagan	6.5	12	56	32	32.0	17.5	3.7	154
Drummer	7.1	14	46	40	33.0	23.8	4.9	81

† Determined by hydrometer method.

‡ Water holding capacity at 33 1/3 kPa (determined by porous plate/pressure apparatus).

§ Cation exchange capacity.

¶ Determined by loss-on-ignition.

Adsorption-Desorption Study

Adsorption isotherms of ^{14}C-glyphosate were determined using the batch equilibrium method for the three soil types. The initial concentrations of ^{14}C-glyphosate (0.1, 1, 5, and 10 mg/L) were prepared in 0.1 mol/L KCl solution and the adsorption experiment followed USEPA guidelines for adsorption studies. Two grams of air-dried soil was equilibrated with 10 mL of ^{14}C-glyphosate in 20-mL Teflon centrifuge tubes in a horizontal shaker (150 rpm) for 24 h (sufficient for apparent equilibrium in a preliminary study) at room temperature (25 ± 1°C). For the anaerobic treatments, 2-g portions of the soil samples contained in the Teflon centrifuge tubes were flooded with sterile, deoxygenated water. Preliminary studies revealed that <5 % of added glyphosate was degraded during 24 h of contact with any of the soils used (data not shown). The tubes were flushed with N_2 gas, sealed, and incubated in an anaerobic chamber from Coy Laboratory Products containing a primary headspace of $N_{2(g)}$ with 5 % $CO_{2(g)}$ and <2 % $H_{2(g)}$ at room temperature (25°C) for 2 wk to allow reduction. To study anaerobic adsorption, ^{14}C-glyphosate was added, using a concentrated O_2-free stock solution, to the reduced (anoxic) soil to attain final concentrations of 0.1, 1, 5, and 10 mg/L. Sealed tubes were equilibrated on a shaker inside the anaerobic chamber for 24 h, where the O_2 was maintained at zero concentration. The effect of phosphate addition on glyphosate adsorption in oxic and anoxic soils was examined by incorporating $CaHPO_4$ into the Catlin, Flanagan, and Drummer soils at an overwhelming concentration (500 mg/kg soil), followed by thorough mixing of the soils before the addition of the herbicide.

At the end of the equilibration period, the soil suspension was centrifuged (15 min, 12,000 × g) and aliquots removed from each tube for a radioactivity assay using a Packard Tri-Carb (1900TR) scintillation counter. Controls (treatment without herbicide) were included for calibration and background correction purposes. The amount of ^{14}C-glyphosate adsorbed to the soil was calculated based on the difference between the initial and final concentrations of herbicide in the solution.

Following equilibration and removal of 5 mL of the initial 10 mL of supernatant, herbicide desorption from the soil was estimated by adding equal amounts of fresh 0.1 mol/L KCl solution to the centrifuge tubes, dispersing the soil aggregates by vibration, and shaking for 24 h. Sampling from the anaerobic soil treatments was handled inside the anaerobic chamber. Soil samples were centrifuged (15 min, 12,000 × g), and an aliquot of the supernatant was removed and analyzed utilizing the radioactivity assay. The desorption process was repeated four times. Desorption was estimated by determining the amount of herbicide (described below) in the soil solution following equilibration and calculated by subtracting the amount of herbicide remaining on the soil surface.

Degradation Study

Microcosm Preparation

Soil incubations were performed for 56 d under reduced (anoxic) or oxidized (oxic) conditions using serum bottle microcosms to determine the degradation kinetics of ^{14}C-glyphosate. No degradation was detected in aqueous or organic stock solutions of glyphosate during the experiment.

Anaerobic incubations: Microcosms consisting of serum bottles (60 mL) were amended with soil (10 g) and were spiked with phosphonomethyl-C-labeled ^{14}C-glyphosate (specifc activity of 3.33 x 103 Bq/mmol, diluted with unlabeled glyphosate) in 50 mL of methanol to produce a final concentration of 2 mg/kg of soil that corresponded to the recommended agricultural application rate. The glyphosate-spiked soils were agitated on a reciprocating shaker for 24 h at room temperature to ensure thorough mixing and to evaporate the solvent. To determine the effect of soil phosphate on glyphosate degradation, $CaHPO_4$ was uniformly mixed into the soils at a concentration of 500 mg/kg soil before the addition of the herbicide. The soil was then flooded with 20 mL of sterile (autoclaved), deoxygenated water to mimic soil saturation by rainfall. The microcosm headspace was flushed with N_2 gas and immediately crimp sealed with a butyl stopper fitted with a vial containing 1 mL of 0.5 mol/L NaOH to trap the mineralized $^{14}CO_2$. These microcosms were incubated in a dark, temperature-controlled chamber at 25°C. Sterilized soil microcosms were included as controls for each soil type. Sterilization was achieved by autoclaving the soils twice at 121°C for 1 h on successive days.

Aerobic incubations: Soil microcosms were built from serum bottles as described above. Sterile, distilled water was added to the glyphosate-spiked soils to adjust the moisture content to about 60 % of the field water-holding capacity. The serum bottles were lightly capped (no crimp seal) with a butyl stopper fitted with a NaOH trap and stored in the dark at 25°C. At 1-wk intervals, the microcosms were aerated by equilibrating the headspace with the atmosphere, and the soil moisture content was adjusted by returning each vessel to its initial weight with sterile, distilled water.

Sample Extraction and Analysis

Anaerobic and aerobic microcosms were destructively sampled at consecutive intervals (0.5, 3, 7, 14, 28, 42, and 56 d) by removing the NaOH trap, followed by agitating the microcosm for 1 min and transferring the contents to a 50-mL Teflon centrifuge tube. Quantification of $^{14}CO_2$ in the NaOH traps was accomplished by direct liquid scintillation spectrometry (LSS) using a Packard Tri-Carb (1900TR) scintillation counter. The solid and liquid phases of the soil slurry were then separated by centrifugation (15 min, 12,000 × g). Aqueous samples were removed and filtered (0.2 µm), and the total aqueous radioactivity was estimated using LSS. The soil was extracted with 20 mL of NaOH (0.1 mol/L) in a Teflon centrifuge tube with horizontal shaking following the method described by Druart et al. (2011). Extracts were centrifuged at 12,000 rpm for 15 min, an aliquot was removed for LSS (to quantify extractable radioactivity), and the supernatant was retained for analysis of the herbicide. The recovery values of glyphosate from oxic soils were 73 to 78 % and 74 to 76 % from anoxic soils. The recovery efficiencies obtained were taken into consideration in the calculations of the results. Soil extract samples containing ^{14}C-glyphosate were analyzed using high-performance liquid chromatography with a Packard Radiomatic Flo-one Beta scintillation detector. Separation was achieved with an isocratic elution of the mobile phase composed of acetonitrile/water (10:90 v/v) through a 4.6 × 150 mm, 5-µm particle size, C_{18} column from Prontosil. Glyphosate had a reproducible retention time of 4.1 min at a flow rate of 1 mL/min.

Data Analysis

The adsorption and desorption parameters of glyphosate under oxic and anoxic conditions for each soil type were calculated using the transformed Freundlich equation; equation: $\log C_s = \log K + 1/n \log C_e$, where C_s is the amount of glyphosate adsorbed to the soil (mg/kg), C_e is the equilibrium concentration in the soil solution (mg/L), and K and $1/n$ are empirical constants that reflect the affinity of the soil for the herbicide and the degree of linearity between the amount adsorbed and the solution concentration, respectively. Regression analysis was performed on adsorption and desorption isotherms to calculate K (intercept) and $1/n$ (slope) values of glyphosate in oxic and anoxic soils. Hereafter, K_{ads} and $1/n_{ads}$ will indicate Freundlich parameters for adsorption, and K_{des} and $1/n_{des}$ will refer to desorption parameters. The data on the degradation of glyphosate in soils were fitted into the first-order kinetics model $C_t = C_0 \exp(-kt)$, where C_0 is the initial concentration (mg/kg soil) of the herbicide in the soil, C_t is the herbicide concentration (mg/kg soil) detected in the soil at time t, and k is the first-order rate constant. Degradation rate constants were calculated by linear regression of the natural logarithm of the percentage of herbicide remaining against the time. The aerobic and anaerobic degradation half-lives ($T_{1/2}$) for each soil type

were calculated using the equation $T_{1/2}$ = ln2/k. The statistical program SAS Version 9.3 from SAS Institute was used to calculate the treatment means and standard errors (n = 3). The experiments were set up as a completely randomized design, and the differences between treatments were evaluated using one-way analysis of variance followed by a least significant difference test at p <0.05.

Results

Adsorption-Desorption

Adsorption data from the experiment were very well fitted by the Freundlich equation (R^2 = 1) for the range of herbicide concentrations (0.1-10 mg/L) and soils tested regardless of the soil redox conditions (Table 2). Among the different soils and treatments, the slope ($1/n_{ads}$) values ranged from 0.76 to 0.93 and the Freundlich adsorption coefficient (K_{ads}) from 62.21 to 103.46. Soil redox conditions did not alter glyphosate adsorption to the Catlin and Flanagan soils, as evident from their nearly equal K_{ads} values. However, the herbicide exhibited a noticeably lower K_{ads} value in the anaerobically treated Drummer soil vs. the aerobic Drummer soil incubations. Further, K_{ads} was observed to be lowest for Catlin and highest for Drummer regardless of the soil redox conditions. A higher K_{ads} indicates a higher adsorption affinity of the herbicide to the soils. Desorption isotherms for glyphosate in all the soils fit well into the Freundlich model (R^2 >0.92). The calculated desorption parameters of glyphosate in the oxic and anoxic soils are presented in Table 3. Freundlich desorption coefficient (K_{des}) values of glyphosate were considerably lower in the anoxic soils than the oxic soils. Among the three soils tested, the highest K_{des} was observed in the Catlin soil irrespective of the soil redox conditions. A higher K_{des} indicates a greater retention of glyphosate on the soil surface.

Table 2. Adsorption (Freundlich model) of ^{14}C-glyphosate in different soil types under oxic and anoxic environmental conditions.

Soil	K_{ads}†		$1/n_{ads}$‡		R^2§	
	Oxic	Anoxic	Oxic	Anoxic	Oxic	Anoxic
Catlin	62.21 (±1.71)¶	72.38 (±5.80)	0.92 (±0.02)	0.76 (±0.05)	0.999	0.999
Flanagan	78.14 (±2.05)	69.64 (±4.02)	0.90 (±0.02)	0.78 (±0.04)	0.999	1.000
Drummer	103.46 (±5.11)	84.82 (±4.36)	0.93 (±0.03)	0.88 (±0.03)	0.998	0.998

† Freundlich adsorption coefficient.

‡ Adsorption isotherm slope.

§ Goodness of fit for Freundlich model.

¶ 95% confidence intervals in parentheses.

Table 3. Desorption (Freundlich model) of ^{14}C-glyphosate in different soil types under oxic and anoxic environmental conditions

Soil	K_{des}†		$1/n_{des}$‡		R^2§	
	Oxic	Anoxic	Oxic	Anoxic	Oxic	Anoxic
Catlin	46.52 (±0.03)¶	42.85 (±0.20)	0.02 (±0.002)	0.28 (±0.003)	0.94	0.94
Flanagan	17.08 (±0.03)	5.81 (±0.02)	0.09 (±0.002)	0.25 (±0.005)	0.92	0.92
Drummer	17.95 (±0.04)	7.75 (±0.05)	0.02 (±0.003)	0.25 (±0.005)	0.92	0.92

† Freundlich desorption coefficient.

‡ Desorption isotherm slope.

§ Goodness of fit for Freundlich model.

¶ 95% confidence intervals in parentheses.

Degradation and Mineralization

Figures 1a to 1c depict the degradation pattern of ^{14}C-glyphosate in the Catlin, Flanagan, and Drummer soils incubated under oxic and anoxic conditions. The first-order parameters including the rate constant (k) and degradation half-life ($T_{1/2}$) of the ^{14}C-glyphosate in the different soil types and redox conditions are presented in Table 4. The ^{14}C-glyphosate degradation followed first-order kinetics in all the nonsterile oxic and anoxic soils, as obvious from their R^2 values (0.83 -1.00). The loss of herbicide from the sterile soil control microcosms was not substantial in either aerobic or anaerobic incubations (Figure 1a -1c). In all three soil types studied, the aerobic $T_{1/2}$ values (15 – 18 d) calculated for glyphosate were

significantly lower than the corresponding anaerobic values (42 -51 d). The $T_{1/2}$ of the herbicide in the Catlin, Flanagan, and Drummer soils were comparable in the aerobic incubations. On the other hand, compared with the other soils, glyphosate degradation was relatively slow in the Flanagan soil in the anaerobic incubations. Figures 1d to 1f illustrate the comparative microbial mineralization trends of glyphosate amendments observed as the amount of $^{14}CO_2$ measured from the alkali trap from aerobic and anaerobic soil microcosms. More than half (53 – 63 %) of the radioactivity in the applied ^{14}C-glyphosate was mineralized as $^{14}CO_2$ from the oxic soils, and only 38 to 41 % of the applied ^{14}C-glyphosate was mineralized in the anaerobic microcosms by the end of incubation. Conversely, aerobically or anaerobically incubated sterilized microcosms had little or no mineralization of the herbicide in all the soil types considered. Another interesting observation from the study is the absence of a lag phase before the evolution of $^{14}CO_2$ from the soils. The evolution of $^{14}CO_2$ from soils was evident immediately after Day Zero of the incubation in both oxic and anoxic soils. Glyphosate mineralization in oxic soils was initially rapid, followed by a gradually decreasing rate. However, in anoxic soils, mineralization of the glyphosate started out slowly and steadily increased toward the end of incubation.

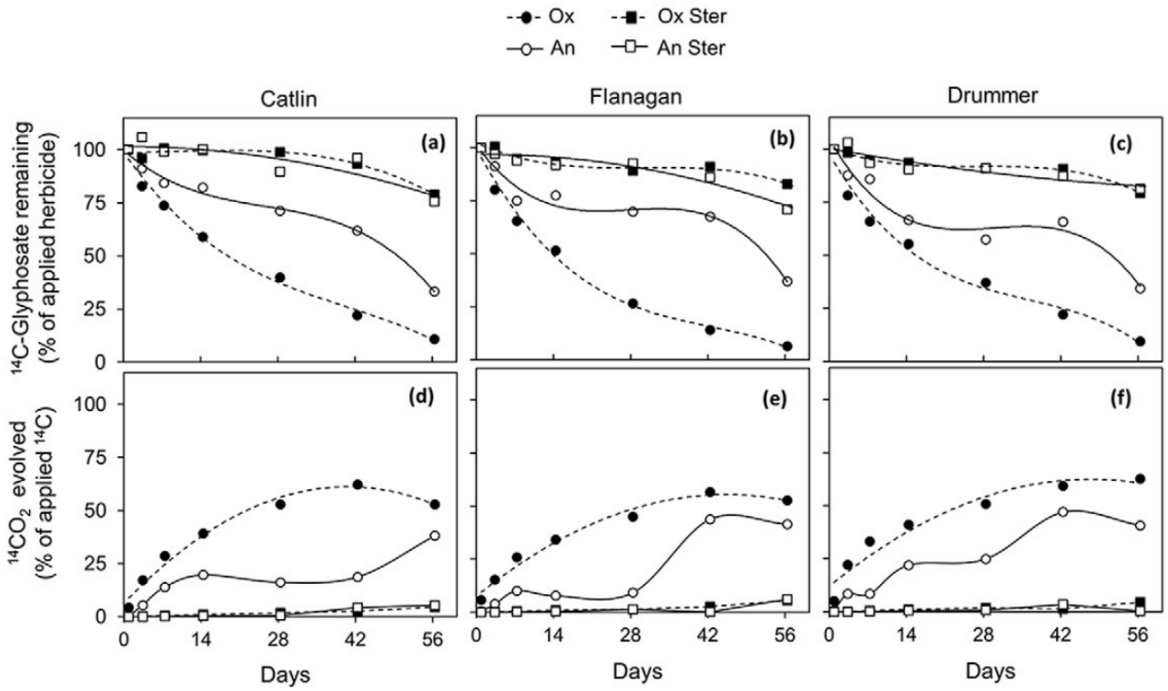

Figure 1. **(a,b,c) Degradation kinetics and (d,e,f) mineralization patterns of ^{14}C-glyphosate under oxic (Ox) and anoxic (An) soil conditions in Catlin, Flanagan, and Drummer soils. Data from oxic (Ox Ster) and anoxic (An Ster) sterilized control soils are also shown.**

Table 4. Degradation (first-order kinetics) parameters of ^{14}C-glyphosate in different soil types under oxic and anoxic environmental conditions.

Soil	k†		$T_{1/2}$‡		R^2§	
	Oxic	Anoxic	Oxic	Anoxic	Oxic	Anoxic
	d^{-1}		d			
Catlin	0.038 (0.003)¶	0.016 (0.005)	18 c# (209)	42 b (154)	0.99 (0.73)	0.88 (0.68)
Flanagan	0.048 (0.003)	0.014 (0.005)	15 c (228)	51 a (140)	1.00 (0.84)	0.81 (0.85)
Drummer	0.038 (0.003)	0.015 (0.004)	18 c (210)	45 b (200)	1.00 (0.85)	0.83 (0.86)

† Rate constant.

‡ Degradation half-life.

§ Goodness of fit for first-order degradation model.

¶ Corresponding values for the sterilized soil control in parentheses.

Means followed by the same letter are not significantly different ($p < 0.05$).

Effect of Phosphate Addition on Adsorption and Degradation

The addition of phosphate to the Catlin, Drummer, and Flanagan soils significantly reduced the ^{14}C-glyphosate adsorption to oxic and anoxic soils (Figure 2a - 2c). Moreover, the extent of the reduction in herbicide adsorption was more pronounced in the oxic soils. Phosphate additions did not improve or had no effect on the degradation of ^{14}C-glyphosate in the oxic soils, as observed from the degradation half-life values ($T_{1/2}$) of the herbicide in the respective soils (Figure 2b). Conversely, the presence of soil phosphate significantly enhanced the anaerobic degradation of ^{14}C-glyphosate in all three soil types studied (Figure 2d).

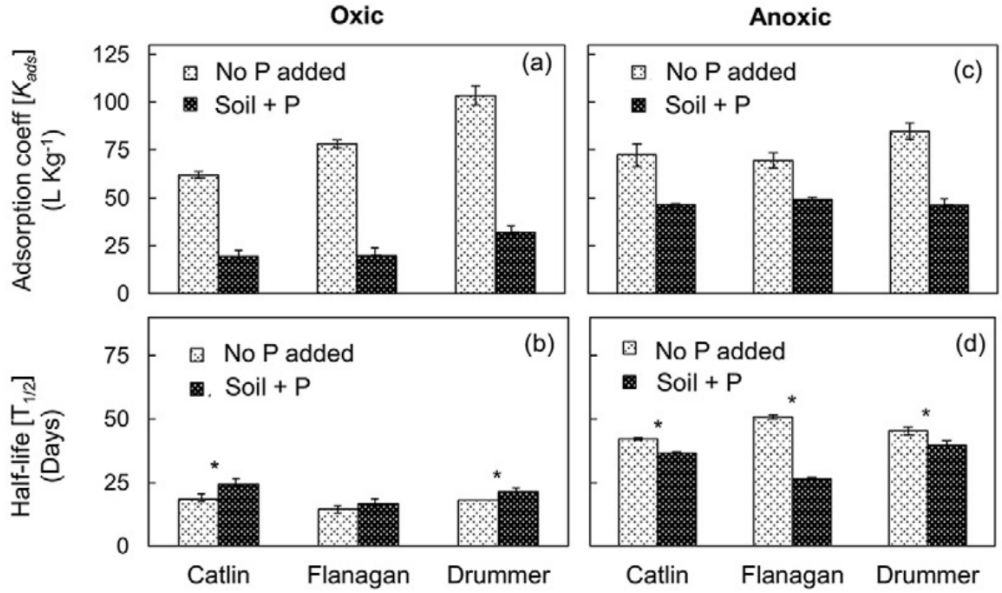

Figure 2. **Effect of phosphate addition (500 mg/kg soil) on the adsorption and degradation of ^{14}C-glyphosate in oxic and anoxic soils: comparison of (a,c) the adsorption coefficient and (b,d) the degradation half-life of glyphosate in oxic and anoxic soils without (No P added) and with (Soil + P) phosphate amendment.**
***Signifcantly different at p <0.05. Error bars represent standard errors (n = 3).**

Discussion

Adsorption-Desorption

High K_{ads} values of ^{14}C-glyphosate from the present study (62.21-103.46) clearly indicate a strong adsorption affinity of the herbicide to the soils (Table 2). The results obtained from this study were comparable to reported K_{ads} values (33-152.9) for glyphosate. The greatest extent of ^{14}C-glyphosate desorption was observed in the soils having the least adsorption (Table 3). Relatively lower K_{des} values in the anaerobic treatments than the corresponding aerobic treatments in all the tested soils indicate that desorption of the herbicide was enhanced in the anoxic, reduced soils. Increased desorption of the herbicide under anoxic conditions may result in an enhanced bioavailability of glyphosate, increasing the risk of movement or crop damage and possibly enhancing degradation of the herbicide under anoxic soil conditions.

Degradation and Mineralization

Degradation of ^{14}C-glyphosate occurred more rapidly in the aerobically incubated Catlin, Flanagan, and Drummer soils than in the corresponding anaerobic incubations, as evident from the significantly lower aerobic $T_{1/2}$ values (Table 4). This concurs with previous studies. Glyphosate degradation could be inferred to be a purely microbially mediated process because practically no degradation or mineralization occurred in the sterile control soils in any soil type or redox condition. The slow start in the anaerobic mineralization may be ascribed to the acclimation of specialized herbicide degrading microbial populations in the anoxic soil.

Impact of Soil Phosphate

Suppression of glyphosate adsorption in both oxic and anoxic soils with phosphate addition explicitly demonstrated the competition for adsorption sites between glyphosate and phosphate despite differences in redox conditions (Figure 2). Several studies have confirmed similar competitive adsorption of glyphosate and phosphate on Al^{3+} and Fe^{3+} surface sites in soil. The effect of phosphate addition on the enhanced microbial bioavailability of glyphosate was found only in the anoxic soils, where the $T_{1/2}$ of glyphosate was noticeably reduced in all the soil types treated anaerobically with phosphate (Figure 2). Phosphate addition did not stimulate glyphosate degradation in oxic soils.

Implications

This study examined the significance of oxic and anoxic soil conditions on the microbial bioavailability of glyphosate in soils. Although ^{14}C-glyphosate was highly adsorbed to the soils regardless of the soil type and redox conditions, desorption or release of the adsorbed herbicide was enhanced in anoxic soils. The degradation and mineralization of ^{14}C-glyphosate exhibited slower kinetics in anoxic soils than oxic soils in all the soil types investigated. The addition of phosphate to the soil suppressed the adsorption of glyphosate in both oxic and anoxic soils and improved the degradation rate in anoxic soils. The effects of anaerobiosis on the observed K_{ads} and K_{des} suggest greater glyphosate bioavailability in saturated soils. Significant decreases in degradation kinetics observed under anaerobiosis across soils could confer a greater potential for transport in water and subsequent environmental impacts. These findings are based on soils in corn (*Zea mays* L.) - soybean [*Glycine max* (L.) Merr.] rotations from the Upper Midwest and may not reflect outcomes in soils in warmer climates or situations involving frequent flooding cycles, such as in wetland rice (*Oryza sativa* L.) production or crop areas in river floodplains. The conflicting observations between oxic and anoxic soil conditions on the environmental fate of glyphosate in the presence of soil phosphate requires additional research attention.

3. Assessment and conclusion

Assessment and conclusion by applicant:

The article describes the sorption and degradation behavior of glyphosate in three different US soils under consideration of aerobic and anaerobic conditions and the addition of phosphates. The sorption experiment is well described according to the USEPA guidelines, however not sufficient results are reported (ads/des results at each concentration not available numerically) to check the validity of the article.

The degradation experiment was conducted in a microcosm with insufficient description of results for calculating degradation or dissipation endpoints according current guidelines.

The article is therefore classified as reliable with restrictions (Category 2).

E-Fate: Reliability criteria for the detailed assessment of full-text documents

Data requirements (indicated by the corresponding EU data point)	Criteria for "Reliable" articles	Criteria met? Yes / No / Uncertain
General criteria for reliability considered for all data requirements indicated by the corresponding EU data points as specified in EC Regulation (EU) No 283/2013	1. For guideline-compliant studies (GLP studies): OECD, OPPTS, ISO, and others. The validity/quality criteria listed in the corresponding guidelines met.	No
	2. Previous exposure to other chemicals is documented (where relevant).	No
	3. The test substance is dissolved in water or non-toxic solvent	Yes
	4. Glyphosate, when the test substance, is sufficiently documented - identity of the test material reported (i.e. purity, source, content, storage conditions)	Yes

E-Fate: Reliability criteria for the detailed assessment of full-text documents

Data requirements (indicated by the corresponding EU data point)	Criteria for "Reliable" articles	Criteria met? Yes / No / Uncertain
	5. Only glyphosate is the tested substance (excluding mixture), and information on application of glyphosate is described	Yes
	6. The endpoint measured can be considered a consequence of glyphosate (or a glyphosate metabolite)	Yes
	7. Study design / test system is well described, including when relevant: concentration in exposure media (dose rates, volume applied, etc.), dilution/mixture of test item (solvent, vehicle) where relevant.	Yes
	8. Analytical verifications performed in test media (concentration)/ collected samples, stability of glyphosate in test media documented	No
	9. An endpoint can be derived. Findings do deliver a regulatory endpoint, and/or is useful as supporting information	Yes
	10. Assessment of the statistical power of the assay is possible with reported data.	Yes
	11. If statistical methodology was applied for findings reported, then the data analysis applied is clearly reported (e.g., checking the plots and confidence intervals)	Yes
	12. Field locations relevant/comparable to European conditions. Soils not completely matching the OECD criteria but from Europe or to some extent representative for the European Agriculture.	Yes
	13. Characterization of soil: texture (sandy loam, silty loam, loam, loamy sand), pH (5.5-8.0), cation exchange capacity, organic carbon (0.5-2-5 %), bulk density, water retention, microbial biomass (~1 % of organic carbon)	Yes
	14. Other soils where information on characterization by the parameters: pH, texture, CEC, organic carbon, bulk density, water holding capacity, microbial biomass	No
	15. For tests including agricultural soils, they should not have been treated with test substance or similar substances for a minimum of 1 year	Yes
	16. For soil samples, sampling from A-horizon, top 20 cm layers; soils freshly from field preferred (storage max 3 months at 4 +/- 2°C).	Yes
	17. Data on precipitation is recorded	No
	18. The temperature was in the range between 20-25°C and the moisture was reported	Yes
	19. The presence of glyphosate identified in samples collected from groundwater, soil, surface waters, sediments or air from European areas	No
	20. Analytical results present residues measurements which can be correlated with the existing residues definition of glyphosate	Yes
	21. Analytical methods clearly described and adequate Statement of specificity and sensitivity of the analytical methods is included	Yes
	22. Radiolabel characterization: purity, specific activity, location of label	Yes
	23. If degradation kinetics are included: expect to see data tables provided, model description. Statistical parameters for kinetic fit.	No

E-Fate: Reliability criteria for the detailed assessment of full-text documents

Data requirements (indicated by the corresponding EU data point)	Criteria for "Reliable" articles	Criteria met? Yes / No / Uncertain
	24. Glyphosate monitoring data: description of matrix analysed, and analytical methods fully described as above.	No
	25. For environmental fate studies: clear description of application rate and relevance to approved uses.	No